A rapid review exploring the effectiveness of artificial intelligence for cancer diagnosis

Authors: Alesha Wale[1], Hannah Shaw[1], Toby Ayres[1], Chukwudi Okolie[1], Helen Morgan[1], Jordan Everitt[1], Kirsty Little[1], Rhiannon Tudor Edwards[2], Jacob Davies[2], Ruth Lewis[3], Alison Cooper[4], Adrian Edwards[4]

1. Public Health Wales Evidence Service, Wales, United Kingdom
2. Centre for Health Economics & Medicines Evaluation, Bangor University, United Kingdom
3. Health and Care Research Wales Evidence Centre, Bangor University, United Kingdom
4. Health and Care Research Wales Evidence Centre, Cardiff University, United Kingdom,

There is growing demand for diagnostic services in the UK. This rapid review aimed to assess the effectiveness of artificial intelligence (AI) in diagnostic radiology with a focus on cancer diagnosis. A range of AI models including machine learning, deep learning and ensemble models, were assessed in this review.

The review included an initial broad mapping exercise and a more in-depth synthesis of a specific sub-set of the evidence. The review included evidence available from 2018 until June 2023.
A total of 92 comparative primary studies were included in the evidence map. The evidence map identified 52 studies in which the AI models were in the early stages of development and validation, and highlighted breast, lung and prostate cancers as the type of cancers most frequently reported on. 28 studies evaluating an established model and focusing on the diagnosis of breast, lung, and prostate cancer were included in the in-depth synthesis. All studies included in the in-depth synthesis were classified as diagnostic accuracy studies. Only one study evaluated an AI model that was commercially available in the UK.

Most studies reported results in favour of the AI models, however, these improvements were not always statistically significant. The studies also varied considerably in terms of AI models studied, type of cancer, images used, and comparison made; and were limited in terms of their methodology. When used as a standalone diagnostic tool, there is evidence to suggest that AI can improve diagnostic accuracy or is comparable to experienced radiologists, however this may be dependent on the AI model being used. There is evidence to suggest that AI may be beneficial when used as a support tool for clinicians/radiologists with less experience. The impact of AI on the timeline involved in diagnosis appeared inconsistent. AI may speed up the diagnostic timeline when the level of cancer suspicion is low but may increase diagnostic timelines when the level of cancer suspicion is high. The evidence suggests that clinicians are accepting of AI-based assistance for cancer diagnosis.

Policy and practice implications: The overall evidence for effectiveness appeared in favour of AI and several factors were identified that impact the effectiveness of the AI models. AI may improve diagnostic accuracy in clinicians/radiologists with less experience of interpreting radiological images. However, further well-designed high-quality research is needed from the UK and similar countries to better understand the effectiveness of AI in cancer diagnosis.

Economic considerations: There is little evidence on the cost-effectiveness of using AI for cancer diagnosis. In theory, it might be possible for AI to assist with earlier diagnosis of cancer with both health and economic benefits.

Health and Care Research Wales Evidence Centre

Canolfan Dystiolaeth Ymchwil Iechyd a Gofal Cymru

A rapid review exploring the effectiveness of artificial intelligence for cancer diagnosis

November 2023

Ariennir gan Lywodraeth Cymru
Funded by Welsh Government

GIG CYMRU NHS WALES | Iechyd Cyhoeddus Cymru Public Health Wales

Review conducted by Public Health Wales Evidence Service

Report Contributors

Review Team
Alesha Wale, Hannah Shaw, Toby Ayres, Chukwudi Okolie, Helen Morgan, Jordan Everitt, Kirsty Little

Stakeholders
Gareth Ashman, James Triscott, Rebecca Andrews, Delyth James, Christopher Rolls

Economic Considerations
Rhiannon Tudor Edwards and Jacob Davies

Methodological Advice
Ruth Lewis

Evidence Centre Team
Ruth Lewis, Adrian Edwards, Alison Cooper, Micaela Gal and Natalie Joseph-Williams involved in stakeholder engagement, review of report and editing

Public Partners
Anthony Cope and Robert Hall

Evidence need submitted to the Evidence Centre: May 2023

Initial Stakeholder Consultation Meeting: May 2023

Final report issued: November 2023

This review should be cited as: Health and Care Research Wales Evidence Centre. A rapid review exploring the effectiveness of artificial intelligence for cancer diagnosis (0008). November 2023.

Disclaimer: The views expressed in this publication are those of the authors, not necessarily Health and Care Research Wales. The Health and Care Research Wales Evidence Centre and authors of this work declare that they have no conflict of interest.

A rapid review exploring the effectiveness of artificial intelligence for cancer diagnosis

EXECUTIVE SUMMARY

What is a Rapid Review?

Our rapid reviews (RR) use a variation of the systematic review approach, abbreviating or omitting some components to generate the evidence to inform stakeholders promptly whilst maintaining attention to bias.

Who is this Rapid Review for?

The review question was suggested by the Health Sciences Directorate (Policy).

Background / Aim of Rapid Review

There is growing demand for diagnostic services in the UK. The use of artificial intelligence in diagnosis is part of the Welsh Government's programme for transforming and modernising planned care and reducing waiting lists in Wales. This rapid review aimed to assess the effectiveness of artificial intelligence (AI) in diagnostic radiology with a focus on cancer diagnosis. A range of AI models including machine learning, deep learning and ensemble models, were assessed in this review. The term 'AI models' was therefore used to encompass these different types of AI models described in the literature. The review included an initial broad mapping exercise and a more in-depth synthesis of a specific sub-set of the evidence. The focus of the in-depth synthesis was informed by the review's stakeholders based on the findings of the mapping exercise.

Results

Recency of the evidence base

- The review included evidence available from 2018 until June 2023.

Extent of the evidence base

- A total of 92 comparative primary studies were included in the evidence map.
- The evidence map identified 52 studies in which the AI models were in the early stages of development and validation, and highlighted breast, lung and prostate cancers as the type of cancers most frequently reported on.
- **28 studies evaluating an established model and focusing on the diagnosis of breast (n=14), lung (n=7) and prostate (n=7) cancer were included** in the in-depth synthesis.
- Studies included in the in-depth synthesis were conducted in the USA (n=8), Japan (n=5), UK (n=2), Italy (n=2), Turkey (n=2), Germany (n=2), Netherlands (n=2), Portugal (n=1), Greece (n=1) and Norway (n=1). Two studies were conducted across multiple countries.
- All studies included in the in-depth synthesis were classified as **diagnostic accuracy studies**.
- Only one study evaluated an AI model that was commercially available in the UK.
- A total of 14 studies compared AI models to human readers or to other diagnostic methods used in practice, 13 studies compared the impact of AI on human interpretation of radiologic images when diagnosing cancer, four studies compared multiple AI models, and one study compared an inexperienced AI-assisted reader with an experienced reader without AI.
- **Five studies reported on the impact of AI on diagnostic timelines (time to diagnosis, assessment time, evaluation times, and reading time).**

- **Four studies** also reported on **the impact of AI on inter/intra-reader variability, reliability, and agreement.**
- **One study** reported on **clinicians' acceptance and receptiveness** of the use of AI for cancer diagnosis.

Key findings and certainty of the evidence

- Most studies reported results in favour of the AI models, however, these improvements were not always statistically significant. The studies also varied considerably in terms of AI models studied, type of cancer, images used, and comparison made; and were limited in terms of their methodology (unclear level of certainty).
- When used as a standalone diagnostic tool, there is evidence to suggest that AI can improve diagnostic accuracy or is comparable to experienced radiologists, however this may be dependent on the AI model being used (unclear level of certainty).
- There is evidence to suggest that AI may be beneficial when used as a support tool for clinicians/radiologists with less experience (unclear level of certainty).
- The impact of AI on the timeline involved in diagnosis appeared inconsistent. AI may speed up the diagnostic timeline when the level of cancer suspicion is low but may increase diagnostic timelines when the level of cancer suspicion is high (low level of certainty).
- The evidence suggests that clinicians are accepting of AI-based assistance for cancer diagnosis (low level of certainty).

Research Implications and Evidence Gaps

- No study reported on any patient outcomes, including patient harms.
- No study reported on any economic outcomes.
- No study reported on equity outcomes, including equity of access.
- Further research in a real-world setting is needed to better understand the cost implications and impact on patient safety of AI for cancer diagnosis.

Policy and Practice Implications

- The overall evidence for effectiveness appeared in favour of AI and several factors were identified that impact the effectiveness of the AI models.
- AI may improve diagnostic accuracy in clinicians/radiologists with less experience of interpreting radiological images.
- AI models are continually being developed and updated and findings are likely to vary between different AI models.
- Further well-designed high-quality research is needed from the UK and similar countries to better understand the effectiveness of AI in cancer diagnosis.

Economic considerations

- In theory it might be possible for AI to assist with earlier diagnosis of cancer with both health and economic benefits.
- There is little evidence on the cost-effectiveness of using AI for cancer diagnosis. One modelling paper from the United States (US) suggests using AI in lung cancer screening using low-dose computerised tomography (CT) scans can be cost-effective, up to a cost of $1,240 per patient screened.
- The UK (and its constituent countries) perform consistently poorly against European and international comparators in terms of cancer survival rates. Cancer screening was suspended and routine diagnostic work deferred in the UK during the COVID-19 pandemic.
- The cost of cancer to the UK economy in 2019 was estimated to be least £1.4 billion a year in lost wages and benefits alone. When widening the perspective to include mortality, this figure rises to £7.6 billion a year. Pro-rating both figures to the Welsh economy and adjusting for inflation gives figures of £79 million and £429 million per annum respectively.

TABLE OF CONTENTS

TABLE OF CONTENTS 6
1. BACKGROUND 10
1.1 Who is this review for? 10
1.2 Background and purpose of this review 10
2. Mapping the wider evidence base 11
3. Results of the in-depth synthesis 13
3.1 Overview of the evidence base 13
3.2 Impact of AI on diagnostic accuracy 16
3.2.1 Bottom line results for the impact of AI on diagnostic accuracy 22
3.3 Impact of AI on inter and intra-reader variability, reliability, agreement 23
3.3.1 Bottom line results for the impact of AI on inter and intra-reader variability, reliability, agreement 24
3.4 Impact of AI on cancer diagnostic time intervals 24
3.4.1 Bottom line results for the impact of AI on cancer diagnostic time intervals 25
3.5 Clinicians' acceptance and receptiveness of the use of AI for cancer diagnosis 25
3.5.1 Bottom line results for clinicians' acceptance and receptiveness of the use of AI for cancer diagnosis 25
4. DISCUSSION 31
4.1 Summary of the findings 31
4.2 Strengths and limitations of the available evidence 32
4.3 Strengths and limitations of this rapid review 33
4.4 Implications for policy and practice 33
4.5 Implications for future research 34
4.6 Economic considerations* 35
5. REFERENCES 36
6. METHODS 38
6.1 Mapping exercise methods 38
6.1.1 Eligibility criteria 38
6.1.2 Literature search 39
6.1.3 Study selection process 39
6.1.4 Study design classification 39
6.1.5 Classification of studies for map 39
6.2 In-depth synthesis methods 39
6.2.1 Study selection process 39
6.2.2 Eligibility criteria for the in-depth synthesis 40
6.2.3 Data extraction 41
6.2.4 Quality appraisal 41
6.2.5 Synthesis 41
6.2.6 Assessment of body of evidence 41

7. EVIDENCE 42
7.1 Search results and study selection 42
7.2 Data extraction 43
7.3 Quality appraisal 73
7.4 Information available on request 75
8. ADDITIONAL INFORMATION 75
8.1 Conflicts of interest 75
8.2 Acknowledgements 75
9. APPENDIX 76
APPENDIX 1: Reference list for studies included in the map 76
APPENDIX 2: Titles and weblinks for ongoing or recently completed trials 86
APPENDIX 3: Summary of Artificial intelligence (AI) models investigated as interventions 88
APPENDIX 4: MEDLINE search strategy 96

Abbreviations

Acronym	Full Description
AI	Artificial intelligence
AIS	Artificially Intelligent Systems
AUC	Area Under The Curve
BI-RADS	Breast Imaging Reporting and Data System
bpMRI	Biparametric Magnetic Resonance Imaging
BPN	Back Propagation Neural Networks
CAD	Computer Aided Diagnosis
CANARY	Computer-Aided Nodule Assessment and Risk Yield
CBCT	Cone-beam Computed Tomography
CE	The Conformité Européene
CI	Confidence Interval
CL-bpMRI	Conventional Biparametric Magnetic Resonance Imaging
CNN	Convolutional Neural Network
CQC	Care Quality Commission
CsPCa	Clinically significant prostate cancer
CT	Computed Tomography
DBT	Digital Breast Tomosynthesis
DCE MRI	Dynamic Contrast Material–Enhanced Magnetic Resonance Imaging
DCNN	Deep Convolutional Neural Network
DL	Deep learning
DLCAD	Deep Learning Computer Aided Diagnosis Software
DLCNN	Deep Learning Convolutional Neural Network
DL-bpMRI	Deep Learning-Accelerated Biparametric Magnetic Resonance Imaging
DNN	Deep Neural Network
DRE	Digital Rectal Examination
FDA	The United States Food and Drug Administration
GAN	Generative Adversarial Networks
kNN	k-Nearest Neighbour
LCP-CNN	Lung Cancer Prediction Convolutional Neural Network
ML	Machine Learning
MRI	Magnetic Resonance Imaging
mpMRI	Multiparametric Magnetic Resonance Imaging
mRMR	Minimum Redundancy Maximum Relevance
NHS	National Health Service
NICE	The National Institute for Health and Care Excellence
NPV	Negative Predictive Value
PCa	Prostate cancer
PI-QUAL	Prostate Imaging Quality
PI-RADS	Prostate Imaging Reporting & Data System
PPV	Positive Predictive Value
PSA	Prostate-Specific Antigen
ROC	Receiver Operating Characteristics
ROC AUC	Area Under The Receiver Operating Characteristic curve
ROI	Region of Interest
RR	Rapid Review
SD	Standard Deviation
SVM	Support Vector Machine

UK	United Kingdom
USA	United States of America

1. BACKGROUND

1.1 Who is this review for?

This Rapid Review was conducted as part of the Health and Care Research Wales Evidence Centre Work Programme. The above question was suggested by the Health Sciences Directorate (Policy).

1.2 Background and purpose of this review

There has been a growing demand across multiple aspects of diagnostic services in the UK. This has impacted on waiting times for both diagnostics and treatment. Data from March 2023 showed that over 116,000 patients were waiting eight weeks or more for diagnostic services, of which approximately 68,000 were waiting specifically for radiology tests (Stats Wales, 2023). As part of the 'Programme for transforming and modernising planned care and reducing waiting lists in Wales', the Welsh Government recommended the use of Artificial Intelligence (AI) technologies to help transform diagnostic services and reduce waiting lists (Welsh Government, 2022). A range of techniques can be used to create Artificially Intelligent Systems (AIS) that are capable of carrying out health and care tasks that until now have only been able to be completed by humans (NHS, 2022). For the purposes of this rapid review, the term 'AI model' will encorporate any computer algorithm described within the literature that is programmed to detect cancer from a range of radiologic images.

The NHS Artificial Intelligence Laboratory (NHS AI lab) aims to incorporate AI into the health and care sector, with the goal of reducing waiting times, improving diagnosis and saving healthcare professionals' time (NHS England, 2022). To support this the 'AI in Health and Care Award' was created (Department of Health and Social Care, 2021). Over three rounds of funding, the NHS AI lab have invested £123m in 86 AI technologies, including some which process images to detect cancers allowing for faster, more accurate diagnosis (Department of Health and Social Care, 2023).

With growing investment in the use of AI in diagnostic radiology, and the rapid rate of development of AI models available that could potentially be utilised by the NHS in Wales, it is important to determine if AI is effective. The puropse of this rapid review is to assess the effectiveness of AI in diagnostic radiology with a focus on cancer diagnosis. Stakeholders were interested in the following sub-questions (listed in order of priority):

- Is there any documented **harm** from use of the AI models /applications /approaches in radiology for cancer diagnosis?
- To what extent does the use of AI models /applications /approaches in radiology for cancer diagnosis improve **patient outcomes**?
- Are the AI models /applications /approaches effective in **diagnosing cancer in a real-world setting?**
- Is there evidence of the **adoption** of AI models /applications /approaches in diagnosing cancer **within the UK?**
- Are the AI models /applications /approaches described in the primary literature, **licensed for use in the UK**?
- To what extent do the AI models /applications /approaches used in radiology for the diagnosis of cancer reduce **time for completion of diagnostic testing, review, reporting** within a given clinical workflow?

- Does the evidence suggest the AI models /applications /approaches used in radiology for the diagnosis of cancer are able to be **replicated in Wales?**
- What is the **cost-effectiveness** of the AI models /applications /approaches used in radiology for the diagnosis of cancer?
- To what extent do the use of AI models /applications /approaches in radiology for cancer diagnosis reduce overall **clinician time**, reduce need for follow up, and reduce need for further intervention?
- What are the **perceptions of clinicians** with the AI models /applications /approaches used in radiology for the diagnosis of cancer?

This rapid review was conducted in two parts. Firstly, a broad mapping exercise of the existing literature on the use of AI in cancer diagnostics was conducted in order to identify and classify the available evidence. Secondly, the findings of this mapping exercise were then used to identify a focus for an in-depth synthesis of the evidence relating to the effectiveness of AI in breast, lung and prostate cancer diagnosis.

2. Mapping the wider evidence base

Our literature searches identified 21,403 records. This was narrowed to a total of 92 published comparative primary studies included in the mapping exercise and 21 ongoing trials. The mapping exercise sought to outline the outcome measures reported in the literature pertaining to cancer diagnostic radiology and provide details on the types of AI models assessed and the datasets utilised in the evidence base. The eligibility criteria used to select studies for the mapping exercise are outlined in Section 6.1. A reference list of all the studies included in the map can be found in appendix 1. A list containing the titles and weblinks of the 21 ongoing trials identified can be found in appendix 2.

As outlined in the evidence map presented in Table 1, 40 studies focussed on the diagnosis of breast cancer, 14 on lung cancer, 12 on prostate cancer, while 26 focussed on a range of other cancers (including gynaecological n=7, renal n=4, brain n=2, bone n=2, liposarcoma n=2, pancreatic n=1, salivary gland n=1, thyroid n=1, liver n=1, colon n=1, bowel n=1, peripheral nerve sheath n=1, soft tissue n=1, oesophageal n=1). Only diagnostic accuracy outcome measures were consistently reported across all included studies. Some studies reported 'other' outcomes as can be seen in the map. These included: clinician perceptions, image quality, and the impact of different manufacturers on the ability of AI to read the images. The number of images used to test the various AI models varied greatly, but generally ranged from between 101 to 500 images. The AI models identified also varied considerably. Studies were categorised in the map by those that were reporting on commercially available AI models (as stated by the publication's study authors), those that evaluated models that had been developed previously for use in other research work, and those that included the development and validation of new models. The evidence map also sought to differentiate between studies that compered AI models with human reader comparators, and those that made comparisons between different AI models.

The evidence map was presented to stakeholders in order to aid their selection of a substantive focus for a more in-depth review of the research, given the short time frame allocated for completion of this review.

Table 1. Map showing the outcome measures, stage of development of AI model and size of the overall datasets used of the evidence base (n=92).

Key:

Breast Total number of studies that have a human comparator **(**number of studies that have a non-human comparator**)**	**Prostate** Total number of studies that have a human comparator **(**number of studies that have a non-human comparator**)**
Lung Total number of studies that have a human comparator **(**number of studies that have a non-human comparator**)**	**Other** Total number of studies that have a human comparator **(**number of studies that have a non-human comparator**)**

Commercially available AI model	**Outcomes Images**	**Safety/harm outcomes**		**Patient care outcomes**		**Performance outcomes**		**Diagnostic accuracy outcomes**		**Economic outcomes**		**Equity**		**Other**	
	Over 1000														
	501-1000														
								1							
	101-500						1	3	3						
						1		2							
	0- 100														
	Total						1	3	3						
						1		3							
Previously developed AI model	**Outcomes Images**	**Safety/harm outcomes**		**Patient care outcomes**		**Performance outcomes**		**Diagnostic accuracy outcomes**		**Economic outcomes**		**Equity**		**Other**	
	Over 1000					1		2(1)	(1)					1	
								(1)	3						
	501-1000							1							
	101-500					2	1	6(1)	3					1	1
								2(1)	5(2)						1
	0- 100							2							
								(1)	4(2)						
	Total					3	1	11(2)	4(1)					2	1
								4(2)	12(4)						1
AI model developed for the study	**Outcomes Images**	**Safety/harm outcomes**		**Patient care outcomes**		**Performance outcomes**		**Diagnostic accuracy outcomes**		**Economic outcomes**		**Equity**		**Other**	
	Over 1000							8(1)	2						
								(2)	1						
	501-1000					2(1)		6(3)							
								3(2)	3						
	101-500							10(2)	3(1)					1	
							(1)	2(1)	6(1)						(1)
	0- 100							2(1)							
									4						
	Total					2(1)		26(7)	5(1)					1	
							(1)	7(5)	14(1)						(1)
Total						5(1)	2	40(9)	12(2)					3	1
						1	(1)	14(8)	26(5)						2(1)

3. Results of the in-depth synthesis

3.1 Overview of the evidence base

As part of the prioritisation process, stakeholders agreed that the in-depth evidence synthesis should focus on previously developed or commercially available AI models[1] (see Table 2). Similarly, a focus on breast, lung and prostate cancers was agreed, as these were the most prevalent cancers in Wales requiring urgent action. The detailed eligibility criteria used for selecting studies for the in-depth synthesis is presented in Section 6.2 and a full summary of the included studies can be seen in Section 7.2.

The in-depth synthesis included a total of 28 studies (breast cancer n=14, prostate cancer n=7 and lung cancer n=7). Included studies were conducted in a range of countries including USA (n=8), Japan (n=5), UK (n=2), Italy (n=2), Turkey (n=2), Germany (n=2), Netherlands (n=2), Portugal (n=1), Greece (n=1), and Norway (n=1). Two studies were conducted across multiple countries. Study designs were poorly reported across all 28 studies; however, the majority were retrospective in nature (n = 25), and most were observational. Fourteen studies explored the effectiveness of AI as an alternative method to radiologists or other conventional methods for cancer diagnosis (two of which were prospective). Thirteen studies explored the impact of AI on human interpretation of radiological images for cancer diagnosis, one of which was prospective (a total of four studies explored the effectiveness of AI as an alternative method and when assisting human interpretation). Four studies compared multiple AI models to determine the most effective models for diagnosing cancer and one study compared an inexperienced AI-assisted reader with an experienced reader without AI. All studies examined the diagnostic accuracy of AI models. Seven studies (two of which were prospective) investigated the effectiveness of commercially available AI tools while 21 studies (one of which was prospective) investigated the effectiveness of a previously developed tool.

The majority of studies relied on either existing databases of patients or datasets of images for evaluating the effectiveness of AI. Participants/images were selected from institutional databases (n=17), multiple sources (n=6), open-source datasets (n=4) and from previous studies (n=1). Most often institutional datasets were utilised for breast cancer and prostate cancer studies. The datasets used did not always originate from the country in which the study was conducted (See appendix 3). Usually, most participants or images used were those that had been flagged as having abnormal images or were confirmed as having lesions or nodules identified previously by a gold standard (often biopsy). However, the information on study population was often poorly reported, and as such it was not always clear how included patients or images were selected into the included studies.

The retrospective studies generally obtained images from historic datasets that are publicly available. The three studies that self-identified as prospective investigated the use of AI in the diagnosis of breast cancer (O'Connell et al, 2022 and Uhlig et al, 2018) and prostate cancer (Forookhi et al, 2023). The two breast cancer studies identified their populations from patients who were found to have abnormalities initially identified from ultrasound or mammography during screening or from a prior study (O'Connell et al, 2022 and Uhlig et al, 2018), the final diagnosis was already known at the time of the study, as this was used as the reference standard. However, the prostate cancer study was a truly prospective study as

[1] For the purposes of this review, an AI model was classed as commercially available if it was stated as such in the primary study. An AI model was classed as previously developed if it was stated as such in the primary study or if it was made clear that the model had not been developed for use in the study.

consecutive patients were prospectively enrolled from a cohort undergoing MRI examination for clinical suspicion of prostate cancer due to either an increase from baseline prostate-specific antigen (PSA) levels or positive digital rectal examination (DRE) findings. This study used an expert radiologist as the reference standard. Population numbers in the prospective studies tended to be small, between 35 and 299 participants and between 80 and 299 images. It should be noted that participants had already begun the diagnostic pathway and it was the initial images that were utilised in these prospective studies. Also, important to note is that study authors excluded patients on active surveillance (Forookhi et al, 2023), those with a prior diagnosis (Forookhi et al, 2023 and O'Connell et al, 2022) and in one study those who were unable to read or understand English (O'Connell et al, 2022), or those participating in a breast screening program (Uhlig et al, 2018).

Patient characteristics generally included clinical and pathological rather than demographic information. Those that did report demographic characteristics (n=23), age was the most commonly reported. This was reported in all prostate cancer studies. Six of the seven lung cancer studies also reported sex. All, but one breast cancer study (O'Connell et al, 2022) were conducted in women only. The majority of breast cancer studies included participants with lesions, although these could be normal, benign or malignant in nature. One of these (van Zelst et al, 2020) included only women with dense breasts and one study (Pacilè et al, 2020) included women with no clinical symptoms. In addition, one study (Uhlig et al, 2018) identified participants who were pre- and post-menopausal. Lastly, one breast cancer study (Lo Gullo et al, 2020) included only BRCA 1 or BRCA 2 mutation carriers. Two studies (O'Connell et al, 2022 and Maldonado et al, 2021) included ethnicity, of which Caucasians predominated. Only one lung cancer study (Maldonado et al, 2021) reported participant smoking status. Generally, participants with a prior history of or those under active surveillance or treatment for the specific cancer of interest were excluded from studies.

The included studies utilised a range of diagnostic imaging techniques including MRI (n=12), CT scans (n=6), ultrasound (n=4), X-rays (n=2), mammograms (n=2), and digital breast tomosynthesis (DBT)(n=1). One study included a combination of mammograms, ultrasound and MRI. Outcome measures reported included: the impact of AI on diagnostic accuracy, inter/intra-variability/agreement, time to diagnosis, assessment time, evaluation time, reading time, and clinicians' acceptance and receptiveness of the use of AI for cancer diagnosis.

The type of AI models used within the studies were not always clearly described. The studies included deep learning (DL) models (n=16), machine learning (ML) models (n=5), 'AI software' n=2, ensemble learning models (n=1), Generative Adversarial Networks (GAN) (n=1), convolutional neural networks (CNN) (n=1), Computer aided diagnosis software (CAD) (n=1), and Computer-Aided Nodule Assessment and Risk Yield (CANARY) (n=1). Within the studies using a DL model, nine were reported to be deep learning convolutional neural networks (DLCNNs), three were deep learning computer aided diagnosis software (DLCADs) and four were just described as DL models).

The AI models evaluated in the included studies were at different stages of development. Seven studies explored the use of commercially available AI models. It should be noted that the commercially available models were licenced for use in different countries, however, this was not always clearly stated in the studies. Only one AI model was commercially available within the UK (Red Dot, Behold.ai). The remaining 21 studies explored the use of previously developed AI models. The majority of AI models that were included in this in-depth synthesis were specifically named as shown in Table 2. However, some AI models were only given descriptors rather than a specific name, with the descriptors outlining details about the type of AI model used (e.g. radiomics, prediction CNN, CAD system). Full details about the AI models used in each study can be seen in section 7.2.

Table 2. Name or descriptor of the artificial intelligence (AI) models utilised in the included studies

Commercially available AI models	Previously developed AI models
Quantib® - AI software	BreastScreening-AI –DNN
The Koios DS – DL	Xception – DLCNN
Prostate AI, Version Syngo.Via VB60,	InceptionV3, Inception, -DLCNN
Prostate AI, version 1.3.2, - DLCAD	DenseNet121, DenseNet161, - DLCNN
EIRL Chest X-ray Lung nodule (LPIXEL Inc) – CAD	NASNetMobile – DLCNN
QVCAD Qview Medical Inc,	ResNetV2, ResNet50, ResNet101, ResNet 152, - CNN
Red Dot, Behold.ai, -DNN	QuantX – CAD
	Koios DS – DL
	S-Detect – CNN
	MammoScreen V1 – DCNN
	Transpara. version 1.6.0 – CAD
	AlexNet, - DCNN
	VGG, VGG-16 – DCNN
	LeNet DCNN
	GoogLeNet/Inception, - CNN
	Residual Networks (ResNets) – DL
	AdaBoost, GBoost, XGBoost, LightGBM – Ensemble model
	f-AnoGAN, HealhtyGAN, StarGAN, StarGAN-v2, FP-GAN, DeScarGAN - GAN
	Grt123 – DL
	JWDH- DL
	Aidence – DL
	CANARY*
	Radiomics + Machine learning model* - ML
	Random forests, back propagation neural networks (BPN), extreme learning machines, support vector machines, and K-nearest neighbors* - ML
	Convolutional neural network (CNN)*
	Lung Cancer Prediction CNN (LCP-CNN)*
	CAD system*

* Only the description of type of AI model used provided

The methodological quality of included studies was assessed using the QUADAS-2 (Whiting et al, 2011) and QUADAS-C (Yang et al, 2021) tools. Quality appraisal identified three studies to be at low risk of bias (Lo Gullo et al, 2020, Maldonado et al, 2021, Tong et al, 2023), while the remaining studies had methodological limitations and were therefore judged to be at high or unclear risk of bias. Common methodological limitations across studies included poor reporting of patient/image selection. Studies also often failed to adequately describe how images were distributed among the intervention and control groups. In addition, several studies excluded images that were considered of poor quality or images containing several or complex lesions which could have limited the generalisability of the findings. Two of the three prospective studies were determined to have an unclear risk of bias due to missing details around how the comparators were conducted (Uhlig et al 2018, and Forookhi et al 2023) and one was determined to have a high risk of bias due to some participants being removed from the analysis (O'Connell et al 2022).

A clear description of how the index test was conducted and interpreted was lacking among some studies. Many studies utilised the diagnosis reported in the database from where the images were taken as the final diagnosis. Other studies did interpret images independently,

or in the case of images collected at local hospitals, used the final diagnosis as the reference standard. However, in the case of AI being compared against human readers, the timing of the index test and reference standard was unclear, which could have introduced bias. Further details of the quality appraisal can be found in section 7.3.

3.2 Impact of AI on diagnostic accuracy

All studies reported on the impact of AI on diagnostic accuracy, the findings of which are summarised in Table 3.

When assessing the diagnostic accuracy of a test, multiple measurements can be reported, which include but are not limited to: sensitivity and specificity, positive and negative predictive values (PPV, NPV), and the area under the receiver operating characteristic curve (ROC AUC, often reported as AUC) (Šimundić 2009). The sensitivity of a diagnostic test measures the proportion of true positives identified by the test, whereas the specificity of a diagnostic test represents the proportion of true negatives identified (Wong and Lim 2011). PPV represents the likelihood that a patient with a positive test actually has the disease and the NPV represents the likelihood that a patient with a negative test does not have the disease (Safari et al 2015). The AUC represents how well the diagnostic test can discriminate, in this case between cancer and non-cancer, an AUC of 1 would be a perfect diagnostic test whereas a non-discriminative test would give an AUC of 0.5 (Eusebi 2013).

The results for diagnostic accuracy are grouped according to the comparisons made into the following categories:

- AI compared to human readers/usual methods
- AI assisting human interpretation
- Comparison of different AI models

(individual studies may have multiple aims and are therefore reported under more than one category).

As the AI models, comparators and datasets varied widely across studies, each study has been narratively reported separately. It was not always appropriate to combine findings. Where this has been done, it should be highlighted that the studies may have used different imaging techniques for the diagnosis of different types of cancer.

Effectiveness of AI compared to human readers/conventional methods

A total of 14 studies assessed the effectiveness of AI models in detecting cancer compared to human readers (radiologists/clinicians) or other conventional diagnostic methods (e.g., the Brock model, a lung cancer probability calculator). The findings were inconsistent.

Four studies (breast n=2, lung n=2) found evidence that the use of AI may improve cancer diagnosis (Uhlig et al, 2018, Lo Gullo et al, 2020, Baldwin et al, 2020, Maldonado et al, 2021). Three studies used CT images and one study used MRI scans.

Uhlig et al (2018) compared the diagnostic performance of five machine learning techniques (random forests, back propagation neural networks [BPNs], extreme learning machines, support vector machines, and K-nearest neighbours) with that of two independent human readers (radiologists) for the diagnosis of breast cancer from Cone-beam Computed Tomography (CBCT) images. BPNs were found to be the highest performing model and also **performed better than the human readers** (0.91 AUC, 0.85 sensitivity, 0.82 specificity for the BPNs vs 0.72 to 0.84 AUC, 0.71 to 0.89 sensitivity, 0.67 to 0.72 specificity for human readers). **The AUC was statistically significantly higher for BPNs when compared with both human reader 1 ($p = 0.01$) and human reader 2 ($p < 0.001$)**.

Lo Gullo et al (2020) investigated the diagnostic accuracy of radiomic analysis and ML in differentiating between benign and malignant breast lesions from MRIs compared to independent assessments by two human readers (radiologists). The findings showed **an improved diagnostic performance by the machine learning model compared to the radiologists** (diagnostic accuracy 81.5% vs 53.4%, sensitivity 63.2% vs 75%, specificity 91.4% vs 42.1%, PPV 80% vs 40.5%, NPV 82.1% vs 76.2%; respectively).

Baldwin et al (2020) compared the effectiveness of an AI model (LCP-CNN) to the Brock model for the diagnosis of lung cancer from CT scans. This study found that **the AI model was statistically significantly better at predicting the risk of malignancy compared to the Brock model**. The AUC for the AI model was 89.6% (95% CI: 87.6% to 1.5%), compared with 86.8% (95% CI: 84.3% to 89.1%) for the Brock model ($p \leq 0.005$).

Maldonado et al (2021) assessed the effectiveness of the BRODERS radiomic predictive model in predicting the probability of malignancy in an independent dataset of incidentally detected indeterminate pulmonary nodules by comparing its performance to that of the Brock model on CT scans. The findings showed **a significantly greater AUC for the BRODERS model compared to the Brock model at all pre-test malignancy probabilities** 0.90 (95% CI:0.85% to 0.94%) vs 0.87 (95% CI:0.81% to 0.92%) ($p<0.001$).

Eight studies (breast n=3, lung n=2, and prostate n=3) found evidence to suggest the use of AI led to no significant difference between groups or reported similar outcomes when compared to human readers (Fujioka et al, 2021, O'Connell et al, 2022, Goto et al, 2023, Tam et al, 2021, Jacobs et al, 2021, Akatsuka et al, 2019, Arslan et al, 2023, Zhang et al, 2022). However, two of these studies found that the level of experience of radiologists impacted whether the use of AI improved accuracy of diagnosis (O'Connell et al, 2022, Goto et al, 2023). These studies used CT (n= 1), MRI (n= 5) and ultrasound (n= 1) and X-rays (n=1).

Fujioka et al (2021) evaluated the effectiveness of six CNN models in discriminating between benign and malignant breast lesions on MRI by comparing their performance with that of two human readers (a breast surgeon and a radiologist). **The findings showed no significant differences between the CNN models** (DenseNet121, DenseNet169, InceptionResNetV2, InceptionV3, NasNetMobile, and Xception) **and the human readers**. The mean AUC of all AI models was 0.83 (range 0.75 to 0.90). The best performing AI model was InceptionResNetV2, however no statistically significant differences were reported when compared with the two human readers (AUC 0.90 vs 0.82, and 0.85; sensitivity 74.5% vs 72.3%, and 78.7%; and specificities of 96.0%, 88.0%, and 80.0%, respectively [$p > 0.125$]).

O'Connell et al (2022) studied the performance of an AI model (S-Detect™) in the diagnosis of breast cancer in ultrasound images by comparing this model to manual readings by 10 human readers (radiologists) with varying levels of experience. **The AI model was found to have similar levels of accuracy, sensitivity and specificity compared to the experienced radiologists** (accuracy 0.82 vs 0.72, sensitivity 0.81 vs 0.79, specificity 0.83 vs 0.67, respectively).

Goto et al (2023) compared an AI model (ResNet50) to three human readers (radiologists with varying levels of experience) when determining malignancy from breast MRI. **When precise segmentation was conducted the AI model achieved similar levels of accuracy compared to a highly experienced radiologist** (AUC =0.91, 95% CI:0.90% to 0.93% vs AUC =0.89, 95% CI:0.81% to 0.96%; p=0.45, respectively). When rough segmentation was conducted, the AI model showed similar levels of accuracy to a board-certified radiologist (AUC 0.80, 95% CI:0.78% to 0.82% vs. AUC 0.79, 95% CI:0.70% to 0.89%, respectively).

However, regardless of segmentation method, the AI model was found to be significantly more accurate than a radiology resident (AUC =0.64,95% CI: 0.52% to 0.76%; p=0.01).

Tam et al (2021) evaluated the use of a commercially available AI model (Red Dot, Behold.ai) for the diagnosis of lung cancer from X-rays compared to three human readers (radiologists) and in combination with the readers. **The average accuracy and sensitivity for the three human readers alone was 87%** (range 84 to 90%) and 78% (range 69 to 86%); respectively, **which was similar to when the AI model was used alone** (accuracy 0.87%, sensitivity 0.8).

Jacobs et al (2021) compared the performance of three top-performing AI algorithms (grt123, JWDH, and Aidence) to that of 11 human readers (radiologists) in their ability to identify lung cancer from low-dose CT scans. The AUC values were 0.88 (95% CI: 0.84% to 0.91%) for grt123 algorithm, 0.90 (95% CI: 0.87% to 0.93%) for Aidence algorithm, and 0.90 (95% CI: 0.87% to 0.93%) for JWDH algorithm. For the radiologists, the AUCs ranged from 0.841 (95% CI: 0.80% to 0.88%) to 0.94 (95% CI: 0.92% to 0.96%), with an average AUC of 0.92 (95% CI: 0.89% to 0.95%). **The grt123 AI algorithm performed statistically significantly better compared to radiologists** (p = 0.02) **but no differences were found between the other models and radiologists** (JWDH, p = 0.29; and Aidence, p = 0.26).

Akatsuka et al (2019) assessed whether a DeepCNN AI model (Xception) could correctly locate prostate cancer on MRIs compared to human readers (radiologists and pathologists). **The AI model overlapped the reader-identified targets in a statistically significant similar number of the MRI images** (70.5% p < 0.001) and was found to focus on a statistically significant number of genuine cancer locations (72.1% p<0.001).

Arslan et al (2023) compared the diagnostic performance of four human readers (radiologists with different levels of experience), with and without the use of a commercially available deep learning AI model (Prostate AI, Version Syngo.Via VB60) for the diagnosis of prostate cancer using bi-parametric MRI images. **The AUCs of the experienced radiologist and one of the less-experienced radiologists were statistically significantly higher than the AI model on its own** (AUC 0.92; 95% CI:0.88% to 0.96% and 0.85; 95% CI: 0.79% to 0.91% vs 0.76; 95% CI:0.67% to 0.84%; p< 0.0001 and p= 0.04; respectively). **However, no significant differences were reported for the other less-experienced radiologists** (p = 0.63 and p = 0.23 respectively).

Zhang et al (2022) assessed the effectiveness of 12 human readers (radiology residents) when using a deep learning CNN AI model for the diagnosis of prostate cancer from MRIs. **The AUC of the AI model alone was 0.77 (95% CI: 0.70% to 0.85%), which was similar to clinical assessment 0.78; (95% CI: 0.72% to 0.84%). The AUC for the human readers was also similar** 0.74; (95% CI: 0.67% to 0.81%) with no statistically significant differences reported.

One study evaluated the impact of different image types on the diagnostic performance of readers and an AI model in diagnosing prostate cancer.

Tong et al (2023) assessed the impact of using conventional Biparametric MRI (CL-bpMRI) and deep learning accelerated Biparametric MRI (DL-bpMRI) images in both a human reader study (three radiologists) and a study using a commercially available deep learning-based computer-assisted detection (DL-CAD) AI model. When using the AI model to assess CL-bpMRI and DL-bpMRI images no differences were reported between sensitivity (0.71 vs 0.71), PPV (0.23 vs 0.24), or NPV (0.88 vs 0.88). However, a statistically significant reduction in specificity when using DL-bpMRI compared to CL-bpMRI was found (0.59 vs 0.44; p = 0.05). **No statistically significant differences were reported between the human readers for the different image types.** The AUC of the human readers ranged from

0.57 to 0.77, sensitivity 0.29 to 0.65, specificity 0.5 to0.87, PPV 0.23 to0.41 and NPV 0.81 to 0.87.

One study evaluated the impact of AI on diagnostic accuracy when looking at lesion shape and found mixed results.

Heller et al (2020) assessed the effects of a commercially available deep learning AI support system (Koios DS) for the diagnosis of breast cancer from ultrasound images. The AI model was statistically significantly more accurate than human readers for irregular shaped masses (74.1% vs 57.4%, p = 0.002) and significantly less accurate for round shaped masses (26.5% vs 50.0%, p = 0.049).

Effectiveness of AI plus human interpretation of radiological images

A total of 13 studies assessed the effect of AI assisted human interpretation of images when diagnosing cancer.

Seven studies (breast n=5, lung n=2) reported a positive effect of using AI plus human interpretation on diagnostic accuracy (Jiang et al, 2021, Mango et al, 2020, Pacilè et al, 2020, Pinto et al, 2021, Calisto et al, 2022, Ueda et al, 2021, Tam et al, 2021). These studies used MRI (n=1), ultrasound (n=1), mammograms (n=1), DBT (n=1), CT (n=1), X-ray (n=1), and one study used mammograms, ultrasounds and MRIs (n=1).

Jiang et al 2021 compared the diagnostic performance of 19 human readers (radiologists) with and without the use of an AI model (QuantX) for the diagnosis of breast cancer from dynamic contrast material–enhanced (DCE) MRI**. The average AUC of the human readers significantly improved when using the AI system** (0.71 to 0.76 p = 0.04). Sensitivity improved when BI-RADS category 3 was used as the cut-off point (90% to 94%; 95% CI: 0.8% to 7.4%) but not when using BI-RADS category 4a (80% to 85%; 95% CI: 20.9% to 11%). Specificity showed no difference with either BI-RADS category 4a or category 3 (from 52% to 52%;(95% CI: 27.3% to 6.0%), and from 29% to 28%; (95% CI: 26.4% to 4.3%), respectively, no p value reported).

Mango et al (2020) assessed the effects of a deep learning AI support system (Koios DS) for the diagnosis of breast cancer from ultrasound images in 15 human readers (physicians). **The mean AUC for the human readers statistically significantly improved from 0.83 (95% CI: 0.78% to 0.89%) to 0.87 (95% CI: 0.84% to 0.90%) when using the AI model** (p<0.0001) compared to human readers alone.

Pacilè et al (2020) assessed the effects of an AI model (MammoScreen V1) for the diagnosis of breast cancer from mammograms. **The average AUC across the 14 included human readers (radiologists) significantly improved when using the AI model** from 0.77 (95% CI: 0.72% to 0.81%), to 0.80 (95% CI: 0.75% to 0.84%); average difference 0.03 (95% CI:0.00% to 0.06%; p = 0.035). Sensitivity was also found to significantly improved when using the AI model (average increase of 0.03; p=0.21).

Pinto et al (2021) compared the use of an AI model (Transpara. V1.6.0) for the diagnosis of breast cancer from DBT images with 14 human readers (radiologists). **The average AUC for the 14 human readers was statistically significantly higher when interpreting results with AI** (0.88;95% CI: 0.84% to 0.92% vs 0.85;95% CI: 0.80% to 0.89%, respectively; p = 0.01). The average sensitivity also significantly increased with the use of AI from 81% (95% CI: 74% to 88%) to 86% (95% CI: 80% to 92%) p= 0.006), whereas no differences were found in the specificity (71.6%; 95% CI: 65% to 78%; vs 73.3%; 95% CI: 65% to 81%; p = 0.48).

Calisto et al (2022) assessed the use of a deep neural network (DNN) AI model (DenseNet) for the diagnosis of breast cancer from mammograms, ultrasound and MRIs. **Diagnostic accuracy was higher when the 45 human readers (clinicians) used the AI model** (mean =19.20 and SD =12.81) compared to human reader alone (mean =3.60, SD =4.03). The mean and standard deviation for precision and recall with and without using the AI model was similar, (M = 0.66, SD = 0.34 and M = 0.62, SD = 0.27, respectively). However, it was unclear if these differences were statistically significant.

Ueda et al (2021) compared the diagnostic performance of 18 human readers (nine GPs and nine radiologists with different levels of experience), with and without the use of a commercially available deep learning AI model (EIRL) for the diagnosis of lung cancer using CT images. **All human readers significantly improved accuracy, sensitivity, PPV and NPV when using the AI model** ($p<0.001$, $p<0.001$, $p=0.002$, $p<0.001$ respectively). The overall increases for sensitivity were 1.22 (95% CI:1.14% to 1.30%), specificity 1.00 (95% CI:1.00% to 1.01%), accuracy 1.03 (95% CI:1.02% to 1.04%), PPV 1.07 (95% CI:1.03% to 1.11%), and NPV 1.02 (95% CI:1.01% to 1.03%).

Tam et al (2021) evaluated the use of a commercially available AI model (Red Dot, Behold.ai) for the diagnosis of lung cancer from X-rays compared to three human readers (radiologists) and in combination with the readers. **The overall accuracy and sensitivity was significantly increased when human readers used the AI model, improving average scores by 3.67% and 13.33%, respectively, $p<0.05$).**

Three studies (lung n=1, prostate n=2) found that the benefits of using different AI models to assist human readers were impacted by the level of experience of the reader themselves (Wataya et al, 2023, Forookhi et al, 2023, Arslan et al, 2023). These studies used MRI (n=2) and CT images (n=1).

Wataya et al (2023) compared the performance of 15 human readers (radiologists with varying levels of experience) with and without the use of a deep learning AI model (CAD) for the diagnosis of lung cancer from CT images. For all radiologists, significant improvements were found when using the AI model for lesions with an ill-defined boundary (AUC from 0.83 to 0.85 $p=0.02$), irregular margin (AUC from 0.95 to 0.97 $p=0.01$), irregular shape (AUC from 0.86 to 0.91 $p<0.01$), as well as calcification (AUC from 0.89 to 0.91 $p=0.03$), plural contact (AUC from 0.92 to 0.94 $p=0.02$) and malignancy (AUC from 0.80 to 0.82 $p=0.02$). **However, no significant differences were reported in the group of radiologists with more than five years' experience before and after using the AI model.**

Forookhi et al (2023) compared the diagnostic accuracy of four human readers (radiologists with different levels of experience), with and without the use of a commercially available AI model (Quantib®) for the diagnosis of prostate cancer using mpMRI images. **For less experienced human readers, the AI model improved diagnostic accuracy,** AUC ranges rose when using the AI model (from 0.73-0.81 to 0.75-0.86). However, **more experienced human readers performed better without the use of the AI model** (AUC 0.86; 95% CI:0.81% to 0.91%, sensitivity 77.2%, specificity 94.3% and AUC 0.92; 95% CI:0.89% to 0.96%, sensitivity 86.9, specificity 97.7 to AUC 0.81[95% CI:0.76% to 0.86%, sensitivity 75.4, specificity 86.8 and AUC 0.82 95% CI:0.76% to 0.87%, sensitivity 71.1, specificity 92.0; respectively).

Arslan et al (2023) compared the diagnostic performance of four human readers (radiologists with different levels of experience), with and without the use of a commercially available deep learning AI model (Prostate AI, Version Syngo.Via VB60) for the diagnosis of prostate cancer using bi-parametric MRI images. **The AUCs of radiologists with and without the AI model did not differ overall** (AUC ranged from 0.78 to 0.92 without AI to AUC 0.78 to 0.92 with AI $p > 0.05$).

Three studies (breast n=2, prostate n=1) found the use of AI made no statistically significant difference to the diagnostic performance of the human readers (Van Zelst et al, 2020, Heller et al, 2020, Zhang et al, 2022). These studies used ultrasound (n=2) and MRIs (n=1).

Van Zelst et al (2020) assessed the effectiveness of eight human readers (radiologists) when using a commercially available AI model (QVCAD) for the diagnosis of breast cancer from ultrasounds**. The overall difference in AUC was not statistically significant before 0.82 (95% CI: 0.73% to 0.92%) and after 0.83 (95% CI: 0.75% to 0.92%) using the AI model (p= 0.74).** However partial AUC improved significantly from 0.13 (95% CI:0.10 to 0.15) to 0.14 (95% CI: 0.12% to 0.17%) (p=0.04) after the AI model was used.

Heller et al (2020) assessed the effects of a commercially available deep learning AI support system (Koios DS) for the diagnosis of breast cancer from ultrasound images. **No statistically significant differences were found in accuracy (69.8% vs 73%) NPV (98.5% vs 100%), PPV (42.4% vs 45.5%), sensitivity (96.7% vs 100%), and specificity (61.9% vs 65.2%; p= 0.12–0.41) before and after two human readers (with breast imaging experience) used the AI model.** The AI model also significantly improved diagnostic accuracy for human reader-rated low-confidence lesions with increased PPV (24.7% AI vs 19.3%, p = 0.004) and specificity (57.8% vs 44.6%, p = 0.008).

Zhang et al (2022) assessed the effectiveness of 12 human readers (radiology residents) when using a deep learning CNN AI model for the diagnosis of prostate cancer from MRIs. Overall **radiology residents achieved similar sensitivity and specificity before and after using the AI model** (83.3% and 57.8% vs 81.8% and 59.3%; p=1.0. The AUC for the human readers was also similar 0.74; (95% CI: pre, 0.67% to 0.81%; post, 0.68% to 0.81%) with no statistically significant differences reported.

Effectiveness of AI as a support tool for inexperienced readers compared to expert readers' interpretation alone

While the above studies compared the diagnostic accuracy of readers before and after being assisted by an AI model, only one study assessed the impact of AI on less experienced readers compared to expert readers without the use of AI.

Faiella et al (2022) evaluated the clinical utility of an AI model (Quantib Prostate) for prostate cancer detection on Multiparametric MRI (mpMRIs) by comparing its diagnostic performance when used by human readers with differing levels of experience (an inexperienced radiologist using the AI model and an expert radiologist not aided by the AI model). **The AI-assisted radiologist had a sensitivity of 100% in both zones and a PPV of 93.1% in the peripheral zone and 85.7% in the transitional zone. Whereas the expert radiologist had a sensitivity of 78.5% in the peripheral zone and 76.9% in the transitional zone and a PPV of 92.7% in the peripheral zone and 73.2% in the transitional zone.** However, it was unclear if these differences were statistically significant.

Effectiveness of different AI models

A total of four studies (breast n=2, lung n=1, prostate n=1) compared the diagnostic accuracy of a range of AI models (Tsochatzidis et al, 2019, Vamvakas et al, 2022, Toğaçar et al, 2019, Patsanis et al, 2023). Findings identified factors that could potentially improve diagnosis when using AI. These studies used MRI (n=2), mammograms (n=1), and CT images (n=1).

Tsochatzidis et al (2019) compared the diagnostic accuracy of eight CNN AI models (AlexNet, VGG-16, VGG-19, ResNet-50, ResNet-101, ResNet-152, GoogLeNet and Inception-BN (V2)) either trained from scratch or pre-trained and fine-tuned for the diagnosis

of breast cancer using mammograms obtained from two datasets. The highest performing models were the fine-tuned ResNet-50 and ResNet-101 models in both datasets (AUC 0.86 and 0.80 vs 0.86 and 0.79; accuracy 0.74 and 0.75 vs 0.79 and 0.75, respectively). Fine-tuning a pre-trained network improved accuracy compared to training from scratch (AUC ranged from 0.77 to 0.86, accuracy ranged from 0.63 to 0.79 for pre-trained networks compared to AUC 0.58 to 0.72 and accuracy 0.54 to 0.66; respectively). **However, it was unclear if these differences were statistically significant.**

Vamvakas et al (2022) evaluated the use of ensemble classification AI models for the diagnosis of breast cancer utilising mpMRI. AI models (XGboost, LGBM, Adaboost and GB) were compared to a support vector machine (SVM). **XGboost achieved the highest accuracy and overall performance** (accuracy 0.88; 95% CI: 0.84% to 0.92%, AUC 0.95; 95% CI: 0.91% to 0.99%), followed by LGBM (accuracy 0.87; 95% CI: 0.83% to 0.91%, AUC 0.94; 95% CI: 0.90% to 0.98%). XGBoost also achieved the highest sensitivity (0.91; 95% CI: 0.85% to 0.97%) and specificity (0.90; 95% CI: 0.82% to 0.98%) compared to the other models. The SVM had a statistically significantly lower performance (accuracy 0.84; 95% CI: 0.80% to 0.88%, AUC 0.88; 95% CI: 0.84% to 0.92%) than XGBoost and LGBM but was found to be statistically comparable with the performances demonstrated by AdaBoost and GB.

Toğaçar et al (2019) compared the effectiveness of multiple AI models (LeNet, AlexNet and VGG-16) for lung cancer diagnosis using CT images and found the AlexNet(SGD-Drop(0,5) was the best performing model (accuracy 89.14%). However, using a combination of the AlexNet model and a k -nearest neighbour (kNN) classifier improved the accuracy of the model by 98.74%. Finally, when **adding a minimum redundancy maximum relevance (mRMR) feature selection method to the model along with the kNN classifier the accuracy increased further** (99.51%, sensitivity 99.32% and specificity 99.71%).

Patsanis et al (2023) assessed six previously developed deep learning GANs for the diagnosis of prostate cancer from MRIs. Six GANs (f-AnoGAN, HealthyGAN, StarGAN, StarGAN-v2, Fixed-Point-GAN and DeScarGAN) were evaluated using a validation data set. Fixed-Point-GAN performed significantly better (AUC 0.76; 95% CI: 0.65% to 0.84%) than f-AnoGAN and StarGAN-v2 (AUC 0.54; 95% CI: 0.43% to 0.66%, vs AUC 0.49; 95% CI: 0.37% to 0.60%; respectively) but not compared to HealthyGAN, StarGAN, and DeScarGAN (AUC 0.69; 95% CI: 0.58% to 0.78%, AUC 0.70; 95% CI: 0.60% to 0.80%, AUC 0.68; 95% CI: 0.56% to 0.77% respectively).

3.2.1 Bottom line results for the impact of AI on diagnostic accuracy

The use of AI for the diagnosis of cancer shows inconsistent findings. There is evidence to suggest that AI alone may be used to improve the accuracy of cancer diagnosis, but that this is dependent on the specific AI model being used. There is also evidence to show that the use of AI models to support the accuracy of cancer diagnosis using different radiological techniques may be more beneficial to less experienced human readers, and less helpful to more experienced human readers. There is very limited evidence to indicate the beneficial use of AI when interpreting irregular shaped lesions.

The evidence suggests that pre-training the AI model may improve its diagnostic performance. Ensemble models (a combination of multiple AI models) may be more effective and additional classifiers can be added to further increase the diagnostic performance of an AI model. However, these outcomes were only reported by individual studies and as such firm conclusions cannot be made.

3.3 Impact of AI on inter and intra-reader variability, reliability, agreement

Four studies (breast n=3, prostate n=1) reported on inter/intra-variability or agreement before and after readers used AI (Calisto et al, 2022, Pacilè et al, 2020, Mango et al, 2020, Forookhi, et al 2023). These studies used mammograms (n=1), ultrasounds (n=1) and MRIs (n=1), with one study using mammograms, ultrasounds and MRIs (n=1). Inter reliability/variability or agreement is the agreement or differences in diagnosis between the individual human readers and intra reliability/variability or agreement assesses the differences reported by the same reader e.g. if the diagnosis would differ after the reader used AI. All studies reported some improvement in accuracy when using AI for cancer diagnosis.

Calisto et al (2022) assessed the use of a DNN AI model (DenseNet) for the diagnosis of breast cancer from mammograms, ultrasound and MRIs. It was found that the **inter-variability of the diagnosis made by the 45 human readers (clinicians) improved when using the AI model** on patients with low, medium and high severities (depending on BI-RAD classification) (11%, 3.28%, 34.1% respectively). When looking at **the intra-variability, all human readers also improved** their results with the introduction of AI, those with little experience improved by 6.65%, those with 6 to 10yrs experience improved by 23.66%, those with 11 to 30yrs experience improved by 14.58% and those with 31 to 40 yrs improved by 19.64%. **However, it was unclear if these differences were statistically significant.**

Pacilè et al (2020) assessed the effects of an AI model (MammoScreen V1) for the diagnosis of breast cancer from mammograms and reported that the inter reader reliability among the 14 human readers (radiologists) appeared to increase when using AI. A moderate inter-rater reliability was found in both reading conditions. **For the unaided reading condition, the inter-rater agreement between the human readers was 0.59 (95% CI: 0.53% to 0.64%), while for the reading with AI inter-rater agreement increased to 0.68 (95% CI: 0.62% to 0.73%). However, it was unclear if these differences were statistically significant.**

Mango et al (2020) assessed the effects of a deep learning AI support system (Koios DS) for the diagnosis of breast cancer from ultrasound images on 15 human readers (physicians). Inter-reader variability without AI was 0.54 (95% CI: 0.53% to 0.55%; compared to 0.68 (95% CI: 0.67% to 0.69%) with the AI. **Intra-reader variability improved with AI, showing a statistically significant difference** ($\alpha = 0.05$). Intra-reader variability resulted in less class switching (e.g. from lower than BI-RADS 4A to BI-RADS 4A or higher) with AI than without overall. Although a statistically significant trend toward lower intra reader variability with AI was reported. The class switching rate without AI was 13.6%, and with AI was 10.8% ($p = 0.04$). Nine readers showed decreased class switching with AI, one reader showed equivalent class switching and five showed more class switching with AI. **The findings indicate that the overall improvement in intra reader variability did not extend to all readers.**

Forookhi et al (2023) compared the diagnostic accuracy of four human readers (radiologists with different levels of experience), with and without the use of a commercially available AI model (Quantib®) for the diagnosis of prostate cancer using mpMRI images. The results showed that the inter-reader agreements at different PI-QUAL scores were higher with the use of the AI model, particularly for less experienced human readers, showing a moderate to slight agreement. **However, it was unclear if the differences were statistically significant.**

3.3.1 Bottom line results for the impact of AI on inter and intra-reader variability, reliability, agreement

There is some evidence to suggest that using an AI model as a support tool may increase agreement between human readers and inter/intra variability. There is also evidence to suggest that agreement between readers may be improved more in those with less experience. However, as a limited number of studies reported this outcome firm conclusions cannot be made.

3.4 Impact of AI on cancer diagnostic time intervals

A total of five studies (breast n=3, lung n=1, prostate n=1) reported the impact of AI on cancer diagnostic time intervals, all of which explored the impact of AI on human reader interpretation of different radiological images (Calisto et al, 2022, Wataya et al, 2023, Forookhi et al, 2023, Pinto et al, 2021, Pacilè et al, 2020). These time intervals included time to diagnosis, assessment time, evaluation times, and reading time. The different time intervals were not clearly defined in most studies and as such are reported individually below. The findings appear to be inconsistent.

Time to diagnosis

One study reported the impact of AI models on diagnostic time. Calisto et al (2022) assessed the use of a DNN AI model (DenseNet) for the diagnosis of breast cancer from mammograms, ultrasound and MRIs. The findings showed that **when the 45 human readers (clinicians) used the AI model, the time to diagnosis was reduced** by 31% with an average of 308 seconds (s) (SD = 57.03s) when using the AI model in comparison with no assistance in which the average was 377s (SD = 44.56s). However, it is unclear if this difference was statistically significant.

Assessment time

One study reported the impact of the AI on assessment time. Wataya et al (2023) compared the performance of 15 human readers (radiologists with varying levels of experience) with and without the use of a deep learning AI model (CAD) for the diagnosis of lung cancer from CT images**. A statistically significant reduction in median assessment time was found when the readers used the AI model** (83.6s without AI to 69.9s with AI; p= 0.01). However, this difference was not seen for all radiologists, with the assessment time actually being prolonged when using the AI model for three of the 15 radiologists included, no reasons were provided for this difference.

Reading time

Two studies (breast n=2) reported on the impact of AI specifically on human reading times (Pinto et al, 2021, Pacilè et al, 2020). These studies used DBT images (n=1) and mammograms (n=1). Both of which found that the reading times changed depending on the level of suspicion/likelihood of malignancy.

Pinto et al (2021) assessed the use of an AI model (Transpara. V1.6.0) for the diagnosis of breast cancer from DBT images. **Reading times of the 14 human readers (radiologists) were shown to decrease when using AI for low suspicion examinations (by 8%) but increase when using AI for high suspicion** examinations (by 28%), however no significant differences were found (p=0.35).

Similarly, Pacilè et al (2020) assessed the effects of an AI model (MammoScreen V1) for the diagnosis of breast cancer from mammograms in 14 human readers (radiologists). Reading

time was considered from the opening of a new case until a BI-RADS score was provided. **For images with a low likelihood of malignancy the time was similar** in the first reading session and slightly decreased in the second reading session. However, **for images with a higher likelihood of malignancy, the reading time was on average increased with the use of AI.**

Time for entire process of image interpretation

One study reported the impact of AI on a range of time outcomes. Forookhi et al (2023) compared the diagnostic accuracy of four human readers (radiologists with different levels of experience), with and without the use of a commercially available AI model (Quantib®) for the diagnosis of prostate cancer using mpMRI images. Reporting time included four different time intervals (mean uploading time, mean time taken for segmentation and contouring, mean time taken for lesion identification, mean report generation time). **The use of the AI model led to a statistically significant increase in reporting time** which ranged from 123.81s (+/- 51.25s) to 189.14s (+/- 67.08s) without Quantib®, and from 697.44s (+/- 98.88s) to 792.47s (+/- 122.37) with Quantib®. ($p < 0.001$). The uploading time was reported to be the most time-consuming step, followed by the time for segmentation and time for lesion identification.

3.4.1 Bottom line results for the impact of AI on cancer diagnostic time intervals

The evidence regarding the impact of AI on cancer diagnostic time intervals appears to be inconsistent. Time to diagnosis and assessment times were reported to decrease, however these findings were only reported by individual studies meaning firm conclusions cannot be made. The evidence for reading times appears to show that the use of AI could increase or decrease reader time compared to reader only, depending on the suspicion level or likelihood of malignancy. Further research would be needed to better understand the impact of using AI on the workflow of cancer diagnosis.

3.5 Clinicians' acceptance and receptiveness of the use of AI for cancer diagnosis

One study (Calisto et al, 2022) assessed the use of a DNN AI model (DenseNet) for the diagnosis of breast cancer from mammograms, ultrasound and MRIs and explored the acceptance and receptiveness of the human readers (clinicians) who utilised the AI model using a questionnaire**. A total of 98% of the 45 clinicians questioned suggested that they understood what the system was thinking, 93% trusted the AI models capabilities, and 91% were accepting of and preferred the AI approach**.

3.5.1 Bottom line results for clinicians' acceptance and receptiveness of the use of AI for cancer diagnosis

There is evidence to suggest that human readers (clinicians) may understand and trust the use of AI and in general may be accepting of using AI when diagnosing cancer in practice. However, the evidence was reported by one study only and as such firm conclusions cannot be made. Further research would be needed to better understand the acceptability of clinicians when using AI for cancer diagnosis.

Table 3: Summary of the findings for the impact of artificial intelligence (AI) on diagnostic accuracy

Study	Cancer	Comparison	Type of diagnostic test	Direction of effect[2]	Findings (AI vs control) Statistically significant effects highlighted in green	Comments
Effectiveness of AI compared to human readers/usual methods						
Uhlig et al (2018)	BC	5 AI models (machine learning techniques) vs 2 radiologist	CT	Favours intervention	AUC: 0.91 vs 0.72-0.84 Sensitivity 0.85 vs 0.71-0.89 specificity 0.82 vs 0.67-0.72	
Lo Gullo et al (2020) ~	BC	AI model vs 2 radiologists	MRI	Favours intervention	Diagnostic accuracy: 81.5% vs 53.4% Sensitivity: 63.2% vs 75%, Specificity: 91.4% vs 42.1% PPV: 80% vs 40.5% NPV: 82.1% vs 76.2%	
Baldwin et al (2020)	LC	AI model vs Brock model**	CT	Favours intervention	AUC: 89.6% (95% CI: 87.6% to 1.5%) vs 86.8% (95% CI: 84.3% to 89.1%)	
Maldonado et al (2021) ~	LC	AI model vs Brock model**	CT	Favours intervention	AUC : 0.90 (95% CI:0.85% to 0.94%) vs 0.87 (95% CI:0.81% to 0.92%)	
Fujioka et al (2021)	BC	6 AI models vs 1 breast surgeon and 1 radiologist	MRI	No change	AUC: 0.90 vs 0.82, and 0.85 Sensitivity: 74.5% vs 72.3%, and 78.7% Specificity: of 96.0%, 88.0%, and 80.0%	
O'Connell et al (2022)	BC	AI model vs 10 radiologists	Ultrasound	No change	Accuracy: 0.82 vs 0.72 Sensitivity: 0.81 vs 0.78 Specificity: 0.83 vs 0.66	Results were impacted by the level of experience of the reader
Goto et al (2023)	BC	AI model vs 3 radiologists	MRI	No change	AUC: 0.91, (95% CI:0.90% to 0.93%) vs 0.89, (95% CI:0.81% to 0.96%)	Results were impacted by the level of experience of the reader
Tam et al (2021)	LC	AI vs 3 radiologists	X-ray	No change	Accuracy for AI: 87%, Sensitivity for AI: 80% Accuracy for humans: 87% (range 84-90%) Sensitivity for humans: 78% (range 69-86%);	

[2] The direction of effect was determined based on whether the results were statistically significant.

Study	Cancer	Comparison	Type of diagnostic test	Direction of effect[2]	Findings (AI vs control) Statistically significant effects highlighted in green	Comments
Jacobs et al (2021)	LC	3 AI models vs 11 radiologists	CT	No change	AUC for AI models: 0.88 (95% CI: 0.842% to 0.910%), 0.90 (95% CI: 0.87% to 0.93%) and 0.90 (95% CI: 0.87% to 0.93%). AUC for radiologists: 0.92 (95% CI: 0.89% to 0.95%).	Results were impacted by the individual AI model used
Akatsuka et al (2019)	PC	AI model vs radiologists and pathologists	MRI	No change	Overlap of targets: 70.5% Genuine cancer locations 72.1%	
Arslan et al (2023)	PC	AI vs 4 radiologists	MRI	Mixed effects	AUC for AI: 0.76 (95% CI 0.67–0.84) AUC for experienced radiologist: 0.92 (95% CI 0.88–0.96), AUC for less-experienced radiologist 1: 0.85 (95% CI 0.79–0.91), AUC for less-experienced radiologist 2: 0.81 (95% CI 0.73–0.88), AUC for less-experienced radiologist 3: 0.78 (95% CI 0.70–0.86).	Results were impacted by the experience of the radiologists
Zhang et al (2022)	PC	AI vs 12 radiology residents	MRI	No change	AUC for AI: 0.77 (95% CI: 0.70% to 0.85%), AUC for clinical assessment: 0.78; (95% CI: 0.72% to 0.84%). AUC for the humans: 0.74; (95% CI: 0.67% to 0.81%)	
Tong et al (2023) ~	PC	AI model vs 3 radiologists	MRI	No change	Sensitivity of AI for different image types: 0.71 vs 0.71 PPV of AI for different image types: 0.23 vs 0.24 NPV of AI for different image types: 0.88 vs 0.88 specificity of AI for different image types: 0.59 vs 0.44; p = 0.05. Radiologist AUC: 0.57-0.77 sensitivity: 0.29-0.65 specificity 0.5-0.87 PPV: 0.23-0.41 NPV: 0.81-0.87	Specificity was reduced when using the DL-bpMRI images with the AI model.
Heller et al (2020)	BC	AI model vs 2 human readers	Ultrasound	Mixed effects	Accuracy for irregular shaped masses (AI vs human): 74.1% vs 57.4%, p = 0.002 Accuracy for round shaped masses (AI vs human): 26.5% vs 50.0%, p = 0.049	Results were impacted by the shape of the breast lesions
Impact of AI on human interpretation of different radiological images						

Study	Cancer	Comparison	Type of diagnostic test	Direction of effect[2]	Findings (AI vs control) Statistically significant effects highlighted in green	Comments
Jiang et al 2021	BC	19 radiologists without vs with AI	MRI	Favours intervention	AUC: 0.71 VS 0.76 Sensitivity with BI-RADS 4a cut-off: 80% vs 85%; (95% CI: 20.9%-11%) Sensitivity with BI-RADS 3 cut-off: 90% vs 94%; (95%CI: 0.8% -7.4%) Specificity with BI-RADS 4a cut-off: 52% to 52%;(95% CI: 27.3%t to 6.0%) Specificity with BI-RADS 3 cut-off: 29% to 28%; (95% CI: 26.4% to 4.3%)	
Mango et al (2020)	BC	15 physicians without vs with AI	Ultrasound	Favours intervention	AUC: 0.83 (95% CI: 0.78% to 0.89%) vs 0.87 (95% CI: 0.84% to 0.90%)	
Pacilè et al (2020)	BC	14 radiologists without vs with AI	Mammogram	Favours intervention	AUC: 0.77; (95% CI: 0.72% to 0.81%) vs 0.80;(95% CI: 0.75%-0.84%) Sensitivity: Average increase of 0.03	
Pinto et al (2021)	BC	14 radiologists without vs with AI	DBT	Favours intervention	AUC: 0.85;(95% CI: 0.80% to 0.89%) vs 0.88;(95% CI: 0.84% to 0.92% Sensitivity: 81%; (95% CI: 74% to 88%) vs 86%;(95% CI: 80% to 92%) Specificity: 71.6%;(95% CI: 65% to 78%) vs 73.3%;(95% CI: 65% to 81)	Change in specificity not significantly different
Calisto et al (2022)	BC	45 clinicians without vs with Ai	Mammogram	Favours intervention	Accuracy: mean =3.6, SD =4.03 vs mean =19.2 and SD =12.81	
Ueda et al (2021)	LC	9 GPs and 9 radiologists without vs with AI	CT	Favours intervention	Accuracy increase: 1.03 (95% CI:1.02% to 1.04%) Sensitivity increase: 1.22 (95% CI:1.14% to 1.30%) Specificity increase: 1.00 (95% CI:1.00% to 1.01%) PPV increase: 1.07 (95% CI:1.03% to 1.11%) NPV increase: 1.02 (95% CI:1.01% to 1.03%)	
Tam et al (2021)	LC	3 radiologists without vs with AI	X-ray	Favours intervention	Accuracy increased: 3.67% Sensitivity increased: 13.33%	
Wataya et al (2023)	LC	15 radiologists without vs with AI	CT	Mixed effects	AUC for ill-defined boundary: 0.83-0.85 p=0.02 AUC for irregular margin: 0.94-0.96 p=0.01 AUC for irregular shape: 0.86-0.90 p<0.01 AUC for calcification: 0.89-0.91 p=0.03	Results were impacted by the level of experience of the reader

Study	Cancer	Comparison	Type of diagnostic test	Direction of effect[2]	Findings (AI vs control) Statistically significant effects highlighted in green	Comments
					AUC for plural contact: 0.92-0.94 p=0.02 AUC for malignancy: 0.80-0.82 p=0.02 However, no significant differences were reported for radiologists with more than five years' experience	
Forookhi et al (2023)	PC	4 radiologists without vs with AI	MRI	Mixed effects	Low experience AUC: 0.73-0.81 vs 0.75-0.86 High experience AUC: 0.86-.0.92 vs 0.81-0.82 High experience sensitivity: 77.2-86.9 vs 75.4-71.1 High experience specificity 94.3-97.7 vs 86.8-92.0	Results were impacted by the level of experience of the reader
Arslan et al 2023	PC	4 radiologists without vs with AI	MRI	Mixed effects	AUC: 0.78-0.92 vs 0.78-0.92	Results were impacted by the level of experience of the reader
Van zelst et al (2020	BC	8 radiologists without vs with AI	Ultrasound	No change	AUC: 0.82 (95% CI:0.73% to 0.92%) vs 0.83 (95% CI:0.75% to 0.92%)	
Heller et al (2020)	BC	2 human readers without vs with AI	Ultrasound	No change	Accuracy: 69.8% vs 73% Sensitivity: 96.7% vs 100% Specificity: 61.9% vs 65.2% PPV: 42.4% vs 45.5% NPV: 98.5% vs 100%	
Zhang et al 2022	PC	12 radiology residents without vs with AI	MRI	No change	AUC: 0.74; (95% CI:0.67% to 0.81%) vs 0.74; (95%CI: 0.68% to 0.81%) Sensitivity: 83.3% vs 81.8% Specificity: 57.8% vs 59.3%	
Effectiveness of AI as a support tool for inexperienced readers compared to expert readers' interpretation alone						
Faiella et al (2022)	PC	Inexperienced radiologist using AI vs expert radiologist unaided by AI	MRI	Favours intervention	Sensitivity: 100% vs 78.5% in the peripheral zone; 100% vs 76.9% in the transitional zone PPV: 93.1% vs 92.7% in the peripheral zone and 85.7% vs 73.2% in the transitional zone	
Effectiveness of different AI models						
Tsochatzidis et al (2019)	BC	8 AI models	Mammogram	N/A	Pre-trained network AUC: 0.77-0.86, Pre-trained network accuracy: 0.63-0.79 Trained from scratch network AUC: 0.58-0.72	

Study	Cancer	Comparison	Type of diagnostic test	Direction of effect[2]	Findings (AI vs control) Statistically significant effects highlighted in green	Comments
					Trained from scratch network accuracy: 0.54-0.66	
Vamvakas et al (2022)	BC	5 AI models	MRI	N/A	Accuracy of best performing model: 0.88; (95%;CI:0.84%-0.92%) AUC of best performing model: 0.95; (95%CI:0.91% to 0.99%)	
Toğaçar et al (2019)	LC	3 AI models	CT	N/A	Accuracy of best performing model: 89.14% Accuracy of model with and added kNN classifier: 98.74% Accuracy of model with Knn classifier and feature selection method:99.51% Sensitivity of model with Knn classifier and feature selection method: 99.32% Specificity of model with Knn classifier and feature selection method: 99.71%	
Patsanis et al (2023)	PC	6 AI models	MRI	N/A	Fixed-Point-GAN AUC: 0.76;(95% CI:0.65% to 0.84%) f-AnoGAN AUC: 0.54;(95% CI:0.43% to 0.66%) StarGAN-v2 AUC: 0.49;(95% CI:0.37% to 0.60%) HealthyGAN AUC: 0.69;(95% CI:0.58% to 0.78%) StarGAN AUC: 0.70;(95% CI:0.60% to 0.80%) DeScarGAN AUC: 0.68;(95% CI:0.56% to 0.77%)	

** Brock model is a lung cancer probability calculator. ~ Identified as low risk of bias using the QUADAS-2 and QUADAS-C tools .

Abbreviations: Breast cancer (BC), Lung cancer (LC), Prostate cancer (PC), Not applicable (N/A), Area under the curve (AUC), Confidence interval (CI), Negative predictive value(NPV), Positive predictive value (PPV), k-Nearest Neighbour (KNN) Generative Adversarial Networks (GAN).

4. DISCUSSION

4.1 Summary of the findings

The mapping exercise showed that there is a large volume of early stage (developmental and validation) research studies of AI models in cancer diagnosis, covering a wide range of cancers, but none of these studies evaluated the implementation of the AI models in clinical practice. There are a number of studies that have evaluated previously developed or commercially available AI tools, which may be useful to inform practice.

There is evidence to suggest that AI models may be effective at improving cancer diagnosis accuracy however, the evidence appears to be limited and the findings were not always statistically significant. No study reported findings that showed an overall greater degree of diagnostic accuracy in the control group compared to the AI. All studies that were identified showed significant improvements or no significant differences when compared to human readers or other conventional methods, and when the AI assisted human readers. Regardless of how the AI model was used (i.e., compared to readers or used to assist readers) or the cancer type being diagnosed, studies were identified that demonstrated the benefit of using AI in cancer diagnosis was dependent on the level of experience of the human reader. Evidence suggests that AI models may have a similar level of diagnostic accuracy compared to experienced human readers (clinicians or radiologists) but may increase the accuracy of less experienced human readers when used as a support tool. However, the criteria for being classed as a more or less experienced reader varied between studies so it is unclear how strong this impact is overall.

When comparing a range of AI models several factors were reported to improve diagnostic accuracy. This included pre-training the AI model, adding additional classifiers or combining models to build ensemble models. However, these findings were reported by individual studies and as such further evidence would be needed to confirm this.

Inter and intra-reader variability, reliability, agreement, was reported by a limited number of studies (n= 4). While all studies reported overall improvements, it was noted in one study that improvements were not reported for each human reader although no exploration as to why this occurred was provided. Another study again highlighted the effectiveness of an AI model to improve agreement was dependent on the level of experience of the human reader.

The evidence regarding the use of AI as a time saving measure in cancer diagnosis was also inconsistent. A limited number of studies (n=5) reported on the impact of AI on time and the specific time outcome reported varied between studies. While diagnostic time and assessment time were reported to be reduced overall when using an AI model, the overall image interpretation time was found to be increased when using AI. However, these outcomes were only reported by individual studies, so findings should be interpreted with caution. Two studies identified the impact of AI on reading times was dependent on the level of suspicion or likelihood of malignancy. However, this is based on very limited evidence and as such firm conclusions cannot be made. There was also very limited evidence to suggest that clinicians may be accepting of AI when used as a support tool in cancer diagnosis.

While the results of the quality appraisal showed minimal concern regarding applicability to the review question, the majority of studies had some methodological limitations which led to an increased risk of bias (see Table 7, Fig.1). This was primarily related to the patient image selection process, which was often poorly described within the included studies and how the index tests (comparators) were conducted. In some cases, the same images were used for

the human readers to interpret first without the use of the AI model and then with the AI model (with a short time gap between them) which could have introduced bias as the human reader plus AI group would have already seen all of the images being studied when the AI tool was introduced. The reference standard used also varied across studies and in one study the reference standard was not clearly stated.

The considerable variation in the individual AI models studied, type of cancer being diagnosed, and types of images being used (e.g. MRI CT, X-ray etc.), as well as the methodological limitations of included studies could limit the applicability of these findings and the results should be interpreted with caution. It should also be noted that some studies did acknowledge potential conflicts of interest as the authors worked for the company that developed the AI model. However, this may be expected, as not all AI models included in the in-depth synthesis were commercially available. The overall findings may also be subject to publication bias, were studies that have identified AI to be less effective than a control are not submitted for publication and therefore not included here.

The National Institute for Health and Care Excellence (NICE) (2019) have created the Evidence Standards Framework For Digital Health Technologies which outlines the standards a health technology, such as AI would need to meet in order to show its effectiveness for use in the UK. However further standards are to be developed for AI models using adaptive algorithms that continually update. It was unclear from the included studies whether the AI models assessed were fixed or adaptive, however only one study described the use of an AI model, Red Dot Behold.ai, that was commercially available in the UK (Tam et al, 2021). This model has been suggested to be able to diagnose multiple conditions including lung cancer and stroke using CT or X-ray images, further details about this model and its potential uses can be found online (behold.ai). While this model has been FDA and CE approved and CQC registered, it is unclear if it has received approval from NICE. However, the model was included in a recent early value assessment published by NICE exploring the use of AI in analysing chest X-rays for suspected lung cancer, further details on the findings of the assessment can be found online (NICE 2023).

4.2 Strengths and limitations of the available evidence

All included studies in the in-depth synthesis were comparative in design and as such were best suited to explore effectiveness of AI models in cancer diagnosis in a real-world setting. The evidence included was published within five years of this rapid review being conducted which should increase the relevancy of the findings. Despite some methodological limitations, all included studies were published in peer-reviewed journals.

The majority of the included studies (n=25) were retrospective and gained the images being studied through historical datasets, as such the data used may not reflect the real-world impact of incorporating AI into the healthcare sector.

The findings also highlighted several evidence gaps. As can be seen in Table 1, none of the studies that met the inclusion criteria reported any findings related to patient outcomes (including harms), economic outcomes or any outcomes related to equity. As the majority of studies were retrospective or utilised images from patients who had already been diagnosed with or without cancer no evidence was found to show AI may be effective in diagnosing cancer in a genuine real-world setting. While two studies were conducted in the UK only one of these described using an AI model that was commercially available in the UK. It was unclear if the AI models used for cancer diagnosis are able to be replicated in Wales.

There was limited evidence to suggest the use of AI could reduce the time to diagnosis and the perceptions of clinicians. Due to the heterogeneity of included studies, caution should be applied when interpreting the findings of the review.

The included studies explored the use of a range of AI models, which may explain the inconsistent findings, and is likely to limit the generalisability of the findings to all AI models.

Key details pertaining to the dataset used, and type of AI model were often lacking or not clearly reported within the included studies. Study designs were also poorly reported across included studies and the cancer type and imaging technique varied across studies, which could limit the generalisability of the findings to specific contexts.

4.3 Strengths and limitations of this rapid review

The studies included in this rapid review were identified through a comprehensive search of electronic databases. Despite making every effort to capture all relevant publications and reduce the risk of bias in our review process, it is possible that additional eligible publications may have been missed. To ensure the usefulness of our findings, only comparative studies were included in the review, as these are better placed to determine the presence of cause-and-effect relationships when exploring effectiveness.

AI is a complex and fast developing field. Multiple AI models have been assessed within the literature over time, and AI models that have shown promising results are also continually developed, adding for example additional classifiers etc to improve performance. As such, it is challenging to collate the evidence as even within a few months or years the technology evaluated within this rapid review is likely to be outdated compared to the newly developed advanced AI models. This development in technology also makes it difficult to directly compare different AI tools. The reference standard used across studies also varied including histopathologic examinations, decisions made by expert radiologists or follow-up and in one study the reference standard was not clearly stated further limiting the generalisability across studies.

It is also important to note that although the QUADAS-2 tool and its extension QUADAS-C are designed to assess the methodological quality of diagnostic and comparative study designs included in this rapid review, they are not designed to assess any methodological issues related to the use of the AI models. The review team is aware of a further adapted extension to the QUADAS tool (QUADAS-AI) that is due to be published in future, which would better assess specific methodological considerations relating to AI models. However, this extension was unavailable at the time this rapid review was conducted. Sounderajah et al (2021) highlighted potential biases that could occur when using AI. This included the use of open source datasets as these datasets may include duplications, may contain images that are not labelled correctly and may have incomplete data. As such, the results of the quality appraisal should be interpreted with caution. Furthermore, QUADAS-2 may not have been sufficient to assess the quality of the studies for evaluating outcomes other than diagnostic accuracy.

4.4 Implications for policy and practice

This rapid review has provided an insight into the effectiveness of AI in cancer diagnosis, and factors that can impact the accuracy of AI models, such as the level of experience of the individual interpreting the AI results. This information may be useful when planning how best to incorporate AI into the health and care sector. Further well-designed high-quality research is needed from the UK and similar countries to better understand the effectiveness of AI in

cancer diagnosis. However, given the pace of development in this field, it is difficult to make recommendations on one specific AI tool for use in radiology diagnostics for cancer.

Although the focus of the in-depth synthesis was on the use of AI for interpreting radiological images in breast, lung and prostate cancer diagnosis, other important areas in which AI could provide benefit were also identified during screening and during the mapping exercise. These included the use of AI for radiological image quality improvement, differentiating between different types of cancers (e.g. between glioblastoma and primary central nervous system lymphoma), or in the detection of metastases. These areas should be considered when planning for AI incorporation into the health and care sector.

4.5 Implications for future research

- Further research is needed to explore the effectiveness of AI models for cancer diagnosis in a real world setting and to evaluate the ongoing use of AI in cancer diagnosis.
- Further research is needed to validate the use of specific AI models.
- Further research is needed to determine in which context the use of AI would be most effective (e.g. as a support tool for less experienced clinicians/radiologists)
- Further research is needed to explore the impact of cancer diagnosis using AI on patient harm, costs, and equity.

4.6 Economic considerations*

- In theory it might be possible for AI to assist with earlier diagnosis of cancer with both health and economic benefits. However, there are currently no minimum requirement guidelines in terms of effectiveness or cost-effectiveness of AI use in cancer screening in the UK. Work from Vargas-Palacios (2023) and colleagues aims to develop such guidelines.
- There is little evidence on the cost-effectiveness of using AI for cancer diagnosis. One modelling paper from the United States (US) suggests using AI in lung cancer screening low-dose computerised tomography (CT) scans can be cost-effective, up to a cost of $1,240 per patient screened, giving a willingness-to-pay of $100,000 per quality-adjusted life year (QALY) gained (Ziegelmayer et al, 2022). This is high in comparison to US and UK payer thresholds.
- The UK (and its constituent countries) perform consistently poorly against European and international comparators in terms of cancer survival rates (Arnold et al, 2019). Cancer screening was suspended and routine diagnostic work deferred in the UK as a result of the COVID-19 pandemic. Modelling suggests up to 3,620 avoidable additional deaths will occur between 2020 and 2025 due to the impact of the pandemic on cancer services (Maringe et al 2021).
- Later stage diagnoses (3 & 4) incur greater costs to the healthcare system across most colorectal, pancreatic, lung and kidney cancers (White 2023). Almost half (46%) of all cancer cases were diagnosed at stage 3 and 4 (out of those with a known stage at diagnosis) in England in 2018 (Cancer research UK, 2023).
- The cost of cancer to the UK economy in 2019 was estimated to be least £1.4 billion a year in lost wages and benefits alone (Hilhorst and Lockey, 2023). When widening the perspective to include mortality, this figure rises to £7.6 billion a year. Pro-rating both figures to the Welsh economy and adjusting for inflation gives figures of £79 million and £429 million per annum respectively (Bank of England, 2023).

**This section has been completed by the Centre for Health Economics & Medicines Evaluation (CHEME), Bangor University*

5. REFERENCES

Arnold M, Rutherford MJ, Bardot A, et al. (2019) Progress in cancer survival, mortality, and incidence in seven high-income countries 1995-2014 (ICBP SURVMARK-2): a population-based study. Lancet Oncol.;20(11):1493-1505. doi:10.1016/S1470-2045(19)30456-5

Bank of England Inflation Calculator (2023). Available at: https://www.bankofengland.co.uk/monetary-policy/inflation/inflation-calculator , Accessed 16/10/2023.

Cancer Research UK. (2023) Available at: https://www.cancerresearchuk.org/health-professional/cancer-statistics-for-the-uk#heading-Three Accessed 16/10/2023.

Department of Health and Social care (2021) £36 million boost for AI technologies to revolutionise NHS care. Available at: £36 million boost for AI technologies to revolutionise NHS care - GOV.UK (www.gov.uk) [Accessed 19th May 2023].

Department of Health and Social care (2023) Thousands of patients to benefit from quicker diagnosis and more accurate tests from ground-breaking AI research. Available at: Thousands of patients to benefit from quicker diagnosis and more accurate tests from ground-breaking AI research - GOV.UK (www.gov.uk) [Accessed 19th May 2023].

Eusebi P. (2013) Diagnostic accuracy measures. *Cerebrovascular Diseases*, *36*(4), pp.267-272.

Hilhorst S, Lockey A. (2023) A 'ripple effect' analysis of cancer's wider impact. DEMOS cancer costs. Available at: https://demos.co.uk/wp-content/uploads/2023/02/Cancer-Costs-FINAL-Jan-2020-1.pdf Accessed 16/10/2023.

Maringe C, Spicer J, Morris M, et al. (2020) The impact of the COVID-19 pandemic on cancer deaths due to delays in diagnosis in England, UK: a national, population-based, modelling study [published correction appears in Lancet Oncol. 2021 Jan;22(1):e5]. Lancet Oncol.;21(8):1023-1034. doi:10.1016/S1470-2045(20)30388-0

NHS England (2022) The Artificial Intelligence in Health and Care Award. Available at: The Artificial Intelligence in Health and Care Award - NHS AI Lab programmes - NHS Transformation Directorate (england.nhs.uk) [Accessed 22nd May 2023].

NHS (2022) Artificial Intelligence: How to get it right. Available at: https://transform.england.nhs.uk/ai-lab/explore-all-resources/understand-ai/artificial-intelligence-how-get-it-right/artificial-intelligence-how-to-get-it-right/

NICE (2019) Evidence standards framework for digital health technologies. Available at: https://www.nice.org.uk/Media/Default/About/what-we-do/our-programmes/evidence-standards-framework/digital-evidence-standards-framework.pdf

NICE (2023) Artificial intelligence-derived software to analyse chest X-rays for suspected lung cancer in primary care referrals: early value assessment. Available at: https://www.nice.org.uk/guidance/hte12

Safari S, Baratloo A, Elfil M, et al. (2015) Evidence based emergency medicine part 2: positive and negative predictive values of diagnostic tests. *Emergency Journal,* 3(3): 87-88

Šimundić A.M. (2009) Measures of diagnostic accuracy: basic definitions. *ejifcc*, *19*(4), p.203.

Sounderajah V, Ashrafian H, Rose S, et al (2021) A quality assessment tool for artificial intelligence-centered diagnostic test accuracy studies: QUADAS-AI. *Nature medicine*, *27*(10), pp.1663-1665.

StatsWales (2023) Waiting times by month. Available at: Waiting times by month (gov.wales) [Accessed 24th May 2023].

Vargas-Palacios A, Sharma N, & Sagoo G.S. (2023). Cost-effectiveness requirements for implementing artificial intelligence technology in the Women's UK Breast Cancer Screening service. Nat Commun 14, 6110. Available at: https://doi.org/10.1038/s41467-023-41754-0

Welsh Government (2022) Our programme for transforming and modernising planned care and reducing waiting lists in Wales. Available at: https://www.gov.wales/sites/default/files/publications/2022-04/our-programme-for-transforming--and-modernising-planned-care-and-reducing-waiting-lists-in-wales.pdf [Accessed 19th May 2023].

Welsh Parliament (2023) Reducing the NHS waiting list backlog. Available at: Reducing the NHS waiting list backlog (senedd.wales) [Accessed 22nd May 2023].
Wong, H.B. and Lim, G.H., 2011. Measures of diagnostic accuracy: sensitivity, specificity, PPV and NPV. *Proceedings of Singapore healthcare*, *20*(4), pp.316-318.

White R, (2023). Macmillan Cancer Support, Exploring the healthcare implications of cancer stage. Available at: Exploring the healthcare cost implications of cancer stage (macmillan.org.uk) Accessed 16/10/2023.

Whiting P, Rutjes A, Westwood M, et al. (2011) QUADAS-2 Group. QUADAS-2: a revised tool for the quality assessment of diagnostic accuracy studies. Ann Intern Med. Oct 18;155(8):529-36. doi: 10.7326/0003-4819-155-8-201110180-00009. PMID: 22007046.

Yang B, Mallett S, Takwoingi Y, et al. (2021) QUADAS-C: A Tool for Assessing Risk of Bias in Comparative Diagnostic Accuracy Studies. Ann Intern Med. 2021 Nov;174(11):1592-1599. doi: 10.7326/M21-2234. Epub Oct 26. PMID: 34698503.

Ziegelmayer S, Graf M, Makowski M, et al. (2022) Cost-Effectiveness of Artificial Intelligence Support in Computed Tomography-Based Lung Cancer Screening. Cancers (Basel). Mar 29;14(7):1729. doi: 10.3390/cancers14071729. PMID: 35406501; PMCID: PMC8997030.

6. METHODS

The rapid review was conducted in two stages, which included an initial mapping exercise followed by a more in-depth review of a sub-set of study types that stakeholders considered to be the most relevant to inform practice.

6.1 Mapping exercise methods

6.1.1 Eligibility criteria

We searched for primary sources to answer the review questions: 'What is the effectiveness of artificial intelligence in radiology for cancer diagnosis?' The following eligibility criteria were used to identify studies for inclusion in the rapid review.

Table 4: Eligibility criteria for mapping exercise

	Inclusion criteria	Exclusion criteria
Participants	Patients of all ages (children and adults) referred to radiology with suspected cancer	
Intervention / exposure	The use of AI within the clinical workflow of medical imaging for diagnosis and screening of cancer (e.g. X-ray, CT, MRI, PET, CBCT, ultrasound)	
Comparison	Usual care (no AI) Alternative AI models /applications /approaches	
Outcomes	Primary outcomes(s): • Safety/harm outcomes • Patient care/outcomes (e.g. recovery time, need for further intervention) • Performance outcomes (e.g. time to diagnosis, time to treatment, time to discharge) • Clinical outcomes (e.g. diagnostic performance /classification /accuracy) • Economic outcomes • Equity (e.g. bias)	
Study design	Primary (comparative) studies, full economic evaluations, modelling studies with real world data	Secondary/tertiary research, partial economic evaluations, case reports
Countries	OECD countries pre-1974	Non-OECD countries or post 1974 membership
Language of publication	English	

Publication type	Published and preprint	Excluded letters and conference abstracts, commentaries and editorials
Publication date	Papers published since 2018	

6.1.2 Literature search

A search of Medline (Ovid), Embase (Ovid), Cochrane Central Register of Controlled Trials (CENTRAL) and ScanMedicine (NIHR) was conducted on the 20th June 2023. Terms to describe the key concepts of artificial intelligence, radiological imaging and cancer were utilised. Search concepts and keywords included artificial intelligence, deep learning, machine learning, neural networks, cancer, medical imaging (X-ray, CT, MRI, PET, CBCT, ultrasound). The searches included free text words and subject headings. The NICE OECD countries geographic search filter was used for the searches in Medline and Embase. Searches were limited to English language publications that were published since 2018 and to primary studies. A total of 21,403 records were retrieved which were managed in Endnote 20. Following deduplication, 20,043 records remained. The search strategy used to search MEDLINE is available in Appendix 4.

6.1.3 Study selection process

All studies were uploaded to the systematic reviewing platform Rayyan for title and abstract screening. All studies were screened by a single reviewer and to ensure consistency a proportion (5%) of studies were screened by two independent reviewers. Any conflicts were resolved within the team. A total of 640 articles were screened at full text by two independent reviewers, and any conflicts were discussed and resolved by a third reviewer. A visual representation of the flow of studies throughout the review can be found in Figure 6.1.

6.1.4 Study design classification

The included studies were classified as diagnostic test accuracy studies.

6.1.5 Classification of studies for map

All included studies were coded into the following categories:

- Type of cancer
- AI model development stage (commercially available, previously developed or developed specifically for the purposes of the study)
- The number of images used in the dataset
- Outcome measures reported in primary study
- The comparator (human or AI)

Once coding was complete, the map was constructed and presented to stakeholders to enable them to identify a focus for the rapid review.

6.2 In-depth synthesis methods

6.2.1 Study selection process

Once a focus for the in-depth synthesis had been agreed with stakeholders, the 92 studies included in the map were rescreened for eligibility in the in-depth synthesis. A visual representation of the flow of studies throughout the review can be found in section 7.1.

6.2.2 Eligibility criteria for the in-depth synthesis

Table 5. Eligibility criteria for inclusion in the in-depth synthesis

	Inclusion criteria	Exclusion criteria
Participants	Patients of all ages (children and adults) referred to radiology with suspected **breast, prostate or lung cancer**	Focus on other cancer types
Intervention / exposure	The use of AI within the clinical workflow of medical imaging for diagnosis of cancer (e.g. X-ray, CT, MRI, PET, CBCT, ultrasound)	
Comparison	Usual care (no AI) Alternative AI models /applications /approaches	No comparator
Outcomes	Primary outcomes(s): • Safety/harm outcomes • Patient care/outcomes (e.g. recovery time, need for further intervention) • Performance outcomes (e.g. time to diagnosis, time to treatment, time to discharge) • Clinical outcomes (e.g. diagnostic performance /classification /accuracy) • Economic outcomes • Equity (e.g. bias)	
Study design	Primary (comparative) studies, full economic evaluations, modelling studies with real world data	Secondary/tertiary research, Commentaries, Editorials, partial economic evaluations, case reports
Countries	OECD countries pre-1974	Non-OECD countries or post 1974 membership
Language of publication	English	
Publication date	Papers published since 2018	
Publication type	Published and preprint	
Other considerations	**Commercially available AI models and those that had previously been developed**	AI models specifically for the study

6.2.3 Data extraction

Data extracted was conducted by a single reviewer and was consistency checked by a second reviewer. Information extracted includes:

- Citation
- Study design
- Intervention (AI model)
- Comparator
- Study aim
- Data collection methods and dates
- Outcomes reported
- Sample size
- Participants
- Dataset details
- Cancer type
- Imaging technique
- Key findings
- Notes

6.2.4 Quality appraisal

The QUADAS-2 tool and the QUADAS-C extension tool were used to assess the methodological quality of each included study. The QUADAS-2 tool is used to assess the quality of diagnostic accuracy studies, however it is not well suited to studies that have multiple index tests (comparators), as such, the QUADAS-C tool was also used in order to account for the comparative nature of the included studies.

Quality assessment was undertaken by a single reviewer, with verification of all judgements by a second reviewer. Any discrepancies were discussed and resolved amongst the review team. The results of quality appraisals for individual studies can be seen in section 7.3. Although some studies were rated as having a low risk of bias, the majority of included studies had some methodological limitations.

6.2.5 Synthesis

A narrative synthesis was conducted reporting results from all included studies in the in-depth synthesis.

6.2.6 Assessment of body of evidence

An assessment of the overall body of evidence was made based on the relevance of the available evidence in addressing the review question and sub-questions, the amount and quality of the evidence, the magnitude and direction of effects and consistency in the findings, and clinical heterogeneity.

7. EVIDENCE

7.1 Search results and study selection

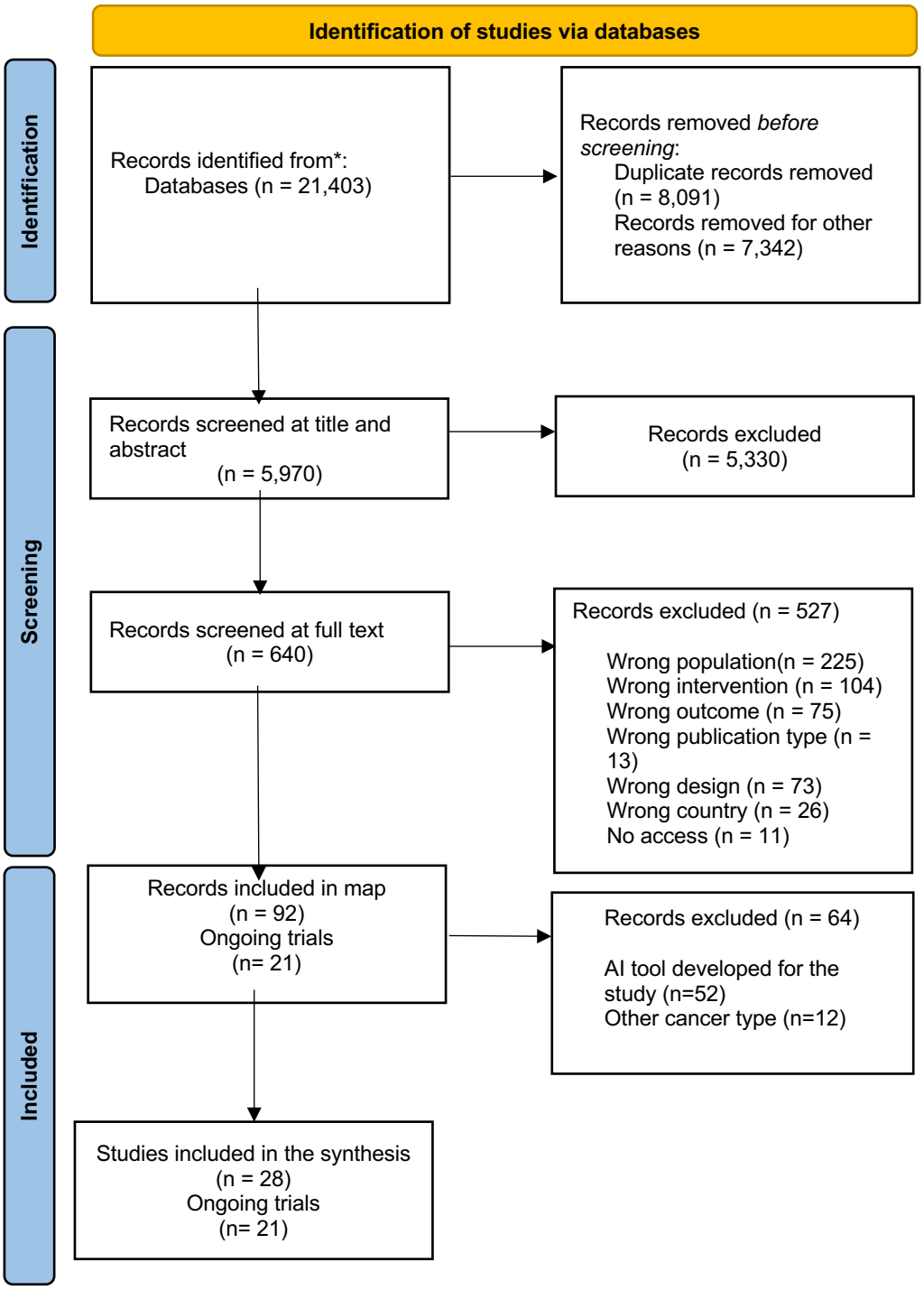

7.2 Data extraction

Table 6: Summary of included studies

Citation (Country)	Study Details	Participants & setting	Key findings	Observations/notes
Breast Cancer				
Calisto et al (2022). BreastScreening-AI: Evaluating medical intelligent agents for human-AI interactions. Artificial Intelligence in Medicine, 127, 102285. (Portugal)	**Study Design:** Mixed method (Retrospective) **Intervention:** BreastScreening-AI. A DenseNet model (Deep neural network) (previously developed) + clinician **Comparator:** Human (clinician) only **Study aim:** To quantitatively and qualitatively assess the proposed design principles that the BreastScreening-AI system embodies and to understand how these principles would fare in practice **Data collection methods and dates:** data retrieved from database containing 338 multi-modal image cases. Qualitative data collected using questionnaire. No dates stated **Outcomes reported:** - Performance accuracy (number of false-positives and false-negatives) - Diagnostic accuracy (precision and recall) - Time performance (diagnostic time) - User expectations (qualitative)	**Sample size:** 289 patients **Participants:** 45 clinicians recruited on a volunteer basis **Dataset details:** BreastScreening was fixed to operate on a limited subset of 289 classified patients from the collected dataset at Hospital Prof. Doutor Fernando Fonseca (HFF). The dataset were divided into three distinct patient types: P1 with low severity, i.e., BI-RADS ≤ 1; P2 with medium severity, i.e., 1 < BI-RADS ≤ 3; and P3 with high severity, i.e., BI-RADS > 3. **Cancer type:** Breast cancer **Imaging technique:** Mammography, ultrasound, and MRI	**Primary Findings:** ***Performance accuracy*** with the proposed AI integration was found to be superior in comparison with the performance without integration. With AI: The classification accuracy of clinicians with AI recommendations was 71% for the number of True-Positives. On the other hand, the number of False-Negatives was 2% and the number of False-Positives was 27%, only. The Provided value was most accurate in classifying low (BI-RADS < 2) and high (BIRADS ≥ 4) severity cases. Without AI: The classification accuracy of clinicians was just 40% for the number of True-Positives. On the other hand, the number of False-Negatives was 6% and the number of False-Positives was 54%. The Provided value was most accurate in classifying high (BI-RADS ≥ 4) severity cases. ***Diagnostic accuracy*** was found to be higher with the AI assistant compared to without the assistant: mean values of (M = 19.2, SD = 12.81) vs (M = 3.6, SD = 4.03). Mean and standard deviation with and without the assistant were (M = 0.66, SD = 0.34) and (M = 0.62, SD = 0.27) for the Precision and Recall, respectively. ***Time performance***: clinicians took 31% less diagnostic time with the assistant (M = 308 s, SD = 57.03 s) in comparison with no assistance (M = 377 s, SD = 44.56 s). **Additional Findings:**	It is unclear from the study the time periods the dataset were retrieved

Citation (Country)	Study Details	Participants & setting	Key findings	Observations/notes
	Inter-variability and intra-variability		***User expectations***: From the DOTS questionnaire, 98% of the 45 clinicians answered that they do understand what the system is thinking. Also, 93% of the clinicians trust the system capability. Finally, 91% accept and prefer the AI setup. ***Inter-variability and intra-variability***: On patients with Low severities, the Inter-Variability improved with the introduction of the AI assistant (CV inter = 46.69%) in comparison with no AI (CV inter = 57.69%). A total of 11% improvement. For classified patients with Medium severities, the improvement was of 3.28% with the introduction of AI. In terms of classified patients with High severities, the improvements were of 34.10%. For the Intra-Variability, the results showed that all groups improved their results with the introduction of AI. More precisely, Interns improved on the AI setup (CV inter = 29.28%) by a 6.65% in comparison with no AI (CV inter = 35.93%). From the group of Juniors, the improvements were even higher. With a 23.66% improvement, the variability of Juniors was reduced from a no AI setup (CV intra = 43.95%) to the AI setup (CV intra = 20.29%). On the same hand, Middles reduced their variability by a 14.58%. Finally, Seniors reduced the variability to a 19.64%.	
Fujioka et al (2021). Deep-learning approach with convolutional neural network for classification of maximum intensity projections of	**Study Design:** Retrospective observational study **Intervention:** CNN models constructed to calculate the probability of malignancy of an image using Xception, InceptionV3, InceptionResNetV2, DenseNet121, DenseNet161, and NASNetMobile (previously developed)	**Sample size:** 286 **Participants:** Patients who underwent DCE breast MRI at a hospital from January 2014 to December 2018 and were diagnosed as having normal, benign, or malignant lesions were eligible for enrolment in the study **Dataset details:** Dataset obtained from patients who underwent DCE breast MRI at a hospital from January 2014 to December	**Primary Findings:** The CNN models showed a mean AUC of 0.830 (range, 0.75–0.90). The best model was InceptionResNetV2. This model, Reader 1, and Reader 2 had sensitivities of 74.5%, 72.3%, and 78.7%; specificities of 96.0%, 88.0%, and 80.0%; and AUCs of 0.90, 0.82, and 0.85, respectively. No significant difference arose between the CNN models and human readers (p > 0.125).	Both readers 1 and 2 blindly evaluated images.

Citation (Country)	Study Details	Participants & setting	Key findings	Observations/notes
dynamic contrast-enhanced breast magnetic resonance imaging. Magnetic Resonance Imaging, 75, 1-8. (Japan)	**Comparator:** Human readers (a breast surgeon and a radiologist) **Study aim:** To assess the diagnostic performance of deep learning (DL) with convolutional neural networks (CNN) compared with that of human readers in differentiating between benign and malignant lesions on maximum intensity projection (MIP) images of dynamic contrast-enhanced (DCE) breast MRIs. **Data collection methods and dates:** Data retrieved from database of radiology reports and clinical records **Outcomes reported:** - Diagnostic performance (AUC, sensitivity, specificity)	2018 and were diagnosed as having normal, benign, or malignant lesions. For the training and validation phase, a total set of 286 images (31 normal, 75 benign, and 180 malignant cases) were used. For the test phase, a total of 72 images (12 normal, 13 benign, and 47 malignant cases) were used. **Cancer type:** Breast cancer **Imaging technique:** Dynamic contrast-enhanced breast magnetic resonance imaging (MRI)		
Goto et al (2023). Use of a deep learning algorithm for non-mass enhancement on breast MRI: comparison with radiologists' interpretations at various levels. Japanese Journal of Radiology, 1-10.	**Study Design:** Retrospective observational study **Intervention:** Deep learning algorithm using pretrained Residual Networks 50 (ResNet50) architecture (previously developed). **Comparator:** Human readers (three radiologists) **Study aim:** To evaluate the diagnostic performance of deep learning using the Residual Networks 50 (ResNet50) neural network constructed from different segmentations for distinguishing malignant and benign non-mass enhancement (NME) on breast	**Sample size:** 84 participants **Participants:** 84 women with 86 lesions (51 malignant and 35 benign) presenting NME on breast MRI **Dataset details:** Data were collected by reviewing the MRI reports in the electronic medical records at a university hospital between March 2010 and March 2013 **Cancer type:** Breast cancer **Imaging technique:** MRI	**Primary Findings:** The ResNet50 model from precise segmentation achieved diagnostic accuracy equivalent [area under the curve (AUC) = 0.91, 95% confidence interval (CI) 0.90, 0.93] to that of a highly experienced radiologist (AUC = 0.89, 95% CI 0.81, 0.96; p = 0.45). The model from rough segmentation showed diagnostic performance equivalent to a board-certified radiologist (AUC = 0.80, 95% CI 0.78, 0.82 vs. AUC = 0.79, 95% CI 0.70, 0.89, respectively). Both ResNet50 models from the precise and rough segmentation exceeded the diagnostic accuracy of a radiology resident (AUC = 0.64, 95% CI 0.52, 0.76)	All readers were blinded to the mammography and ultrasound findings, initial interpretation of NME, and final diagnosis. Readers were informed only of the lesion location and patient's age.

Citation (Country)	Study Details	Participants & setting	Key findings	Observations/notes
(Japan)	magnetic resonance imaging (MRI) and conduct a comparison with radiologists with various levels of experience **Data collection methods and dates:** Data were collected by reviewing the MRI reports in the electronic medical records at a university hospital between March 2010 and March 2013 **Outcomes reported:** - Diagnostic performance (sensitivity, specificity, accuracy, AUC)			
Heller et al (2021). Can an artificial intelligence decision aid decrease false-positive breast biopsies?. Ultrasound Quarterly, 37(1), 10-15. (USA)	**Study Design:** Retrospective observational study **Intervention:** The Koios DS for Breast Study Tool core engine, which uses a deep learning algorithm that characterises sonographically visualised breast lesions (commercially available) + human reader **Comparator:** Human readers (two radiologists) only **Study aim:** To evaluate the effect of an AI support system on breast ultrasound diagnostic accuracy **Data collection methods and dates:** Data were collected from institutional electronic medical records from June 2017 to January 2019	**Sample size:** 200 sonological lesions **Participants:** Not stated. 200 sonological lesions (155 benign and 45 malignant) were randomly selected. **Dataset details:** Data were collected from institutional electronic medical records for all breast biopsies performed in women from June 2017 to January 2019 **Cancer type:** Breast cancer **Imaging technique:** Ultrasound	**Primary Findings:** There was no significant difference in overall accuracy (73 vs 69.8%), NPV (100% vs 98.5%), PPV (45.5 vs 42.4%), sensitivity (100% vs 96.7%), and specificity (65.2 vs 61.9; P = 0.118–0.409) when comparing AI with pooled or individual reader assessment. Artificial intelligence was more accurate than readers for irregular shape (74.1% vs 57.4%, P = 0.002) and less accurate for round shape (26.5% vs 50.0%, P = 0.049). Artificial intelligence improved diagnostic accuracy for reader-rated low-confidence lesions with increased PPV (24.7% AI vs 19.3%, P = 0.004) and specificity (57.8% vs 44.6%, P = 0.008).	The two readers were blinded to clinical history and pathology results as well as to overall malignant versus benign lesion proportions in the study set.

Citation (Country)	Study Details	Participants & setting	Key findings	Observations/notes
	Outcomes reported: Diagnostic accuracy (accuracy, negative predictive value (NPV), positive predictive value (PPV), sensitivity, specificity)			
Jiang et al (2021). Artificial intelligence applied to breast MRI for improved diagnosis. Radiology, 298(1), 38-46. (USA)	**Study Design:** Retrospective observational study **Intervention:** QuantX (AI software) + human readers **Comparator:** Human readers (19 radiologists) alone **Study aim:** To evaluate whether the diagnostic performance of radiologists in the differentiation of cancer from noncancer at dynamic contrast material–enhanced (DCE) breast MRI is improved when using an AI system compared with conventionally available software **Data collection methods and dates:** Data were collected from an independent breast DCE MRI database and from three different medical institutions. Dates not stated **Outcomes reported:** - Reader diagnostic performance (AUC, sensitivity, specificity)	**Sample size:** 111 participants **Participants:** 111 women (54 malignant and 57 non-malignant lesions) **Dataset details:** Data were collected from an independent breast DCE MRI database and from three different medical institutions. Cases were accrued from patients presenting with the following clinical indications: high-risk screening (40%), diagnostic imaging work-up (21%), and evaluation of the extent of known disease (39%). **Cancer type:** Breast cancer **Imaging technique:** Dynamic contrast material–enhanced (DCE) MRI	**Primary Findings:** The average AUC of all readers improved from 0.71 to 0.76 (P = 0.04) when using the AI system. The average sensitivity improved when Breast Imaging Reporting and Data System (BI-RADS) category 3 was used as the cut point (from 90% to 94%; 95% CI for the change: 0.8%, 7.4%) but not when using BI-RADS category 4a (from 80% to 85%; 95% CI: 20.9%, 11%). The average specificity showed no difference when using either BI-RADS category 4a or category 3 as the cut point (52% and 52% [95% CI: 27.3%, 6.0%], and from 29% to 28% [95% CI: 26.4%, 4.3%], respectively).	
Lo Gullo et al (2020). Improved characterizatio	**Study Design:** Retrospective **Intervention:** Radiomics + Machine learning model (previously developed)	**Sample size:** 96 **Participants:** BRCA-positive patients who had an MRI from November 2013 to	**Primary Findings:** Consensus BI-RADS classification assessment by the radiologists achieved a diagnostic accuracy of 53.4%, sensitivity of 75% (30/40), specificity of 42.1%	Radiologists were blinded to the final histopathological diagnoses and prior or

Citation (Country)	Study Details	Participants & setting	Key findings	Observations/notes
n of sub-centimeter enhancing breast masses on MRI with radiomics and machine learning in BRCA mutation carriers. European radiology, 30, 6721-6731. (USA)	**Comparator:** Human readers (two radiologists) **Study aim:** To investigate whether radiomics features extracted from MRI of BRCA-positive patients with sub-centimeter breast masses can be coupled with machine learning to differentiate benign from malignant lesions using model-free parameter maps. **Data collection methods and dates:** Data on consecutive patients with genetic testing results available and who had an MRI from November 2013 to February 2019 that led to a biopsy or a short-term follow-up, were collected from the Department of Radiology database. **Outcomes reported:** - Diagnostic accuracy - Sensitivity - Specificity - PPV - NPV	February 2019 that led to a biopsy (BI-RADS 4) or imaging follow-up (BI-RADS 3) for sub-centimeter lesions **Dataset details:** Data on consecutive patients with genetic testing results available and who had an MRI from November 2013 to February 2019 that led to a biopsy or a short-term follow-up, were collected from the Department of Radiology database. **Cancer type:** Breast cancer **Imaging technique:** MRI	(32/76), PPV of 40.5% (30/74), and NPV of 76.2% (32/42). The machine learning model combining five parameters (age, lesion location, GLCM-based correlation from the pre-contrast phase, first-order coefficient of variation from the 1st post-contrast phase, and SZM-based gray level variance from the 1st post-contrast phase) achieved a diagnostic accuracy of 81.5%, sensitivity of 63.2% (24/38), specificity of 91.4% (64/70), PPV of 80.0% (24/30), and NPV of 82.1% (64/78).	subsequent conventional and MRI imaging
Mango et al (2020). Should we ignore, follow, or biopsy? Impact of artificial intelligence decision support on breast	**Study Design:** Retrospective observational study **Intervention:** AI decision support system - Koios DS for Breast system (previously developed) **Comparator:** Human readers (15 physicians)	**Sample size:** 900 **Participants:** 900 women (900 breast lesions – 470 benign and 430 malignant) with breast lesions on US images acquired between June 2004 and June 2016 **Dataset details:** Data were collected from 900 women (900 breast lesions – 470 benign and 430 malignant) with breast lesions on	**Primary Findings:** Mean reader AUC for cases reviewed with US only was 0.83 (95% CI, 0.78–0.89); for cases reviewed with US plus DS, mean AUC was 0.87 (95% CI, 0.84–0.90). PLR for the DS system was 1.98 (95% CI, 1.78–2.18) and was higher than the PLR for all readers but one. Fourteen readers had better AUC with US plus DS than with US only. Mean Kendall τ-b for US-only interreader variability was 0.54 (95% CI, 0.53–0.55); for US plus DS, it was 0.68 (95% CI, 0.67–0.69). Intrareader variability improved with DS;	All 900 cases were reviewed twice, in two sessions (900 cases per session) separated by a 4-week washout period.

Citation (Country)	Study Details	Participants & setting	Key findings	Observations/notes
ultrasound lesion assessment. AJR. American journal of roentgenology, 214(6), 1445. (USA)	**Study aim:** To assess the impact of AI-based decision support (DS) on breast US lesion assessment. **Data collection methods and dates:** Data were collected from screening mammography recalls and scheduled biopsies from over 20 U.S. institutions with identifying information, including institution, removed during anonymisation. Data were collected from images acquired between June 2004 and June 2016 **Outcomes reported:** - Sensitivity - Specificity - AUC	US images acquired between June 2004 and June 2016 from 20 institutions **Cancer type:** Breast cancer **Imaging technique:** Ultrasound	class switching (defined as crossing from BI-RADS category 3 to BI-RADS category 4A or above) occurred in 13.6% of cases with US only versus 10.8% of cases with US plus DS (p = 0.04).	
O'Connell et al (2022). Diagnostic performance of an artificial intelligence system in breast ultrasound. Journal of ultrasound in medicine, 41(1), 97-105. (USA/Italy)	**Study Design:** Prospective observational study **Intervention:** S-Detect for Breast AI program (previously developed) **Comparator:** Human readers (10 radiologists) **Study aim:** To study the performance of an AI programme designed to assist radiologists in the diagnosis of breast cancer, relative to measures obtained from conventional readings by radiologists **Data collection methods and dates:** Data were collected from subjects prospectively enrolled at both the University of Rochester and University Hospital Palermo during the timeframe 2018-2019.	**Sample size:** 299 **Participants:** 299 patients whose standard-of-care breast ultrasound revealed at least one suspicious lesion, and who were recommended to have either a biopsy or biannual ultrasound imaging follow-up (150 subjects were prospectively enrolled at the University of Rochester and 149 subjects were prospectively enrolled at the University Hospital Palermo, Italy during the timeframe 2018–2019). **Dataset details:** Dataset derived from a curated, anonymised group of 299 breast ultrasound images that contained at least one suspicious lesion and for which a final diagnosis was independently determined. **Cancer type:** Breast cancer **Imaging technique:** Ultrasound	**Primary Findings:** The concordance rate between S-Detect™ for Breast and the readers was significantly (P <0.05) non-inferior to the concordance rate among readers in shape, orientation, margin, and posterior classification. The sensitivity of S-Detect™ for Breast and the radiologists was 0.81 and 0.70, respectively. The specificity of S-Detect™ and the radiologists was 0.83 and 0.76, respectively. The accuracy of S-Detect™ for Breast and the radiologists was 0.82 and 0.73, respectively.	

Citation (Country)	Study Details	Participants & setting	Key findings	Observations/notes
	Outcomes reported: - Sensitivity - Specificity - Accuracy - Concordance rate			
Pacilè et al (2020). Improving breast cancer detection accuracy of mammography with the concurrent use of an artificial intelligence tool. Radiology: Artificial Intelligence, 2(6), e190208. (USA)	**Study Design:** Retrospective observational study (fully crossed/counterbalance design) **Intervention:** Human readers + AI (MammoScreen V1; Therapixel, Nice, France) – previously developed **Comparator:** Human readers (14 radiologists) **Study aim:** To evaluate the benefits of an AI–based tool for two-dimensional mammography in the breast cancer detection process. **Data collection methods and dates:** Data were retrospectively collected over a 3-year period (2013 and 2016) **Outcomes reported:** - AUC - Sensitivity - Specificity - Reading time	**Sample size:** 240 **Participants:** Only examinations from women presenting for screening without clinical symptoms were included. **Dataset details:** The final selected dataset included 240 patient cases (average age, 59 years; range, 37–85 years) with 80 true-positive, 40 false-negative, 80 true-negative, and 40 false-positive cases. **Cancer type:** Breast cancer **Imaging technique:** Mammography	**Primary Findings:** The average AUC across readers was 0.77 (95% CI: 0.72, 0.81) without AI and 0.80 (95% CI: 0.75, 0.84) with AI. The average difference in AUC was 0.03 (95% CI: 0.002, 0.06, P = 0.035). Average sensitivity was increased by 0.03 when using AI support (P = 0.021). Average specificity showed a lower level of improvement (P = 0.634). Reading time changed dependently to the AI-tool score. For low likelihood of malignancy (< 2.5%), the time was about the same in the first reading session and slightly decreased in the second reading session. For higher likelihood of malignancy, the reading time was on average increased with the use of AI. On the first reading session, the average reading time per case was 62.79 seconds for the unaided readings (95% CI: 60.77, 64.80) and 71.93 seconds for the readings with the AI support (95% CI: 69.52, 74.33). The difference was statistically significant (P< 0.001). For the second reading session, the average reading time per case was 57.22 seconds for the unaided readings (95% CI: 55.10, 59.33) and 62.16 seconds for the readings with AI (95% CI: 60.04, 64.29). The difference was statistically significant (P < 0.001).	Readers evaluated the cases independently, with an individually randomised order. They had no access to any information about the patient (e.g., previous mammography and other imaging examinations). There was a washout period of 4 weeks between the two reading sessions.
Pinto et al (2021). Impact of artificial intelligence decision	**Study Design:** Retrospective observational study **Intervention:** Human reader + AI CAD system (Transpara. version	**Sample size:** 190 **Participants:** 190 DBT examinations (from 190 women) consisting of 75 malignant lesions, 25 benign lesions, and 90 normal	**Primary Findings:** The examination-based reader-averaged AUC was higher when interpreting results with AI support than when reading unaided (0.88 [95% CI: 0.84, 0.92] vs 0.85 [95% CI: 0.80, 0.89], respectively; P = 0.01).	An enriched dataset (with malignant examinations) was used in this study.

Citation (Country)	Study Details	Participants & setting	Key findings	Observations/notes
support using deep learning on breast cancer screening interpretation with single-view wide-angle digital breast tomosynthesis. Radiology, 300(3), 529-536. (Netherlands)	1.6.0; ScreenPoint Medical) – previously developed **Comparator:** Human readers (14 radiologists) **Study aim:** To assess whether adding a deep learning–based AI system to single-view DBT image reading may allow for an improvement in the reading time and in the performance of radiologists for breast cancer detection. **Data collection methods and dates:** The dataset for this study was selected from all clinical DBT examinations performed at Radboud University Medical Center between June 2016 and February 2018. **Outcomes reported:** - AUC - Sensitivity - Specificity - Reading time	examinations. Patients 40 years of age or older who had undergone a bilateral imaging protocol because of recall from screening or clinical concerns were included. **Dataset details:** The dataset for this study was selected from all clinical DBT examinations performed at Radboud University Medical Center between June 2016 and February 2018, and contained a total of 4750 DBT studies from distinct women **Cancer type:** Breast cancer **Imaging technique:** Digital breast tomosynthesis (DBT)	The average sensitivity increased with AI support (64 of 74, 86% [95% CI: 80%, 92%] vs 60 of 74, 81% [95% CI: 74%, 88%]; P = 0.006), whereas no differences in the specificity (85 of 116, 73.3% [95% CI: 65%, 81%] vs 83 of 116, 71.6% [95% CI: 65%, 78%]; P = 0.48) or reading time (48 seconds vs 45 seconds; P = 0.35) were detected. The standalone per-examination AUC for the AI system was higher than that of the unaided reader-averaged AUC (0.90 [95% CI: 0.85, 0.94] vs 0.85 [95% CI: 0.80, 0.89], respectively; p = 0.03). When compared with each individual unaided reader, the AI system AUC was higher than that of all except two readers (reader 1 and reader 10), who had higher AUCs (0.90 and 0.93, respectively)	
Tsochatzidis et al (2019). Deep learning for breast cancer diagnosis from mammograms—a comparative study. Journal of Imaging, 5(3), 37. (USA)	**Study Design:** Retrospective observational (comparative) study **Intervention:** Deep convolutional neural networks (CNNs) – AlexNet, VGG, GoogLeNet/Inception, Residual Networks (ResNets) – previously developed **Comparator:** AI models above were compared amongst themselves **Study aim:** To investigate the performance of multiple deep	**Sample size:** Not stated **Participants:** Not stated. The dataset used contained 400 mass ROIs. The curated breast imaging subset of DDSM contained 10,239 mammographic images **Dataset details:** Two datasets were used. DDSM-400: This dataset consists of 400 mass ROIs extracted from the Digital Database for Screening Mammography (DDSM) that was developed and used in a previous project. The selected dataset was enriched due to a further processing of the	**Primary Findings:** CNNs trained under the fine-tuning scenario achieved better performance compared to the ones trained from scratch.	

Citation (Country)	Study Details	Participants & setting	Key findings	Observations/notes
	convolutional neural networks (CNNs) in the context of computer-aided diagnosis of breast cancer **Data collection methods and dates:** The dataset consists of 400 mass ROIs extracted from the Digital Database for Screening Mammography (DDSM) that was developed and used in a previous project. Dates not stated **Outcomes reported:** - AUC - Classification accuracy	ROIs, performed by expert radiologists, in order to acquire an accurate mass contour delineation using a semi-automatic segmentation method. CBIS-DDSM: This dataset is an updated and standardized version of DDSM. It contains 10,239 mammographic images. For this study, only cases concerning masses where extracted totaling 1319 and 378 ROIs for training and testing respectively. **Cancer type:** Breast cancer **Imaging technique:** Mammography	Table 2. Performance of deep neural networks using the from-scratch training scenario. | CNN | DDSM-400 | | CBIS-DDSM | | | | AUC | ACC | AUC | ACC | | AlexNet | 0.657 | 0.610 | 0.716 | 0.656 | | VGG-16 | 0.621 | 0.590 | 0.702 | 0.580 | | VGG-19 | 0.644 | 0.588 | 0.707 | 0.581 | | ResNet-50 | 0.595 | 0.548 | 0.637 | 0.627 | | ResNet-101 | 0.637 | 0.588 | 0.641 | 0.662 | | ResNet-152 | 0.596 | 0.543 | 0.609 | 0.647 | | GoogLeNet | 0.580 | 0.569 | 0.590 | 0.598 | | Inception-BN (v2) | 0.652 | 0.590 | 0.577 | 0.654 | Table 3. Performance of convolutional neural networks (CNNs) initialized on pre-trained weights (fine-tuning). | CNN | DDSM-400 | | CBIS-DDSM | | | | AUC | ACC | AUC | ACC | | AlexNet | 0.805 | 0.733 | 0.802 | 0.753 | | VGG-16 | 0.844 | 0.748 | 0.781 | 0.716 | | VGG-19 | 0.835 | 0.738 | 0.783 | 0.736 | | ResNet-50 | 0.856 | 0.743 | 0.804 | 0.749 | | ResNet-101 | 0.859 | 0.785 | 0.791 | 0.753 | | ResNet-152 | 0.786 | 0.630 | 0.793 | 0.755 | | GoogLeNet | 0.830 | 0.758 | 0.767 | 0.720 | | Inception-BN (v2) | 0.850 | 0.780 | 0.774 | 0.747 |	
Uhlig et al (2018). Novel breast imaging and machine learning: predicting breast lesion malignancy at cone-beam CT using machine learning techniques. American Journal of Roentgenology, 211(2), W123-W131. (Germany)	**Study Design:** Prospective observational study **Intervention:** Five machine learning techniques (random forests, back propagation neural networks (BPN), extreme learning machines, support vector machines, and K-nearest neighbors) – previously developed **Comparator:** Human readers **Study aim:** To evaluate the diagnostic performance of machine learning techniques for malignancy prediction at breast cone-beam CT (CBCT) and to compare them to human readers. **Data collection methods and dates:** Data were collected from an earlier project comparing breast CBCT to other breast imaging modalities	**Sample size:** 35 **Participants:** Study participants included female patients who underwent breast CBCT imaging because of suspicious breast lesions (BI-RADS category 4 or 5) identified at mammography or ultrasound, according to the BI-RADS 5th edition, who had American College of Radiology (ACR) breast density type C or D, and who were older than 40 years. This comprised 35 women (81 breast lesions: 45 malignant and 36 benign) **Dataset details:** The dataset for this study was selected from a subset of patients from an earlier project conducted from December 2015 to October 2017. **Cancer type:** Breast cancer **Imaging technique:** Breast cone-beam CT (CBCT)	**Primary Findings:** The diagnostic performance of the human readers was AUC of 0.84, sensitivity of 0.89, and specificity of 0.72 for reader 1 and AUC of 0.72, sensitivity of 0.71, and specificity of 0.67 for reader 2. Among the machine learning models, BPN provided superior AUC of 0.91 and specificity of 0.82, whereas sensitivity was highest for random forest (0.8955). The AUC was significantly higher for BPN than for either reader 1 ($p = 0.01$) or reader 2 ($p < 0.001$).	Both human readers were blinded to each other and to later diagnoses, and they assigned a BI-RADS score separately for each breast lesion

Citation (Country)	Study Details	Participants & setting	Key findings	Observations/notes
	conducted from December 2015 to October 2017 **Outcomes reported:** - Diagnostic performance (AUC, sensitivity, specificity)			
Vamvakas et al (2022). Breast Cancer Classification on Multiparametric MRI– Increased Performance of Boosting Ensemble Methods. Technology in Cancer Research & Treatment, 21, 15330338221087828. (Greece)	**Study Design:** Retrospective observational study **Intervention:** Four popular implementations of Decision Trees (DT) Boosting classifiers, namely Adaptive Boosting (AdaBoost), Gradient Boosting (GB), Extreme Gradient Boosting (XGBoost), and Light Gradient Boosting Machine (LightGBM) – previously developed **Comparator:** An SVM classifier was also trained and evaluated on the same feature subset to allow performance comparisons **Study aim:** To assess the utility of Boosting ensemble classification methods for increasing the diagnostic performance of multiparametric Magnetic Resonance Imaging (mpMRI) radiomic models, in differentiating benign and malignant breast lesions. **Data collection methods and dates:** Data were collected from a sample of breast MRI data obtained from a cohort of 293 female patients that had been consecutively examined at the	**Sample size:** 140 **Participants:** Female patients with mass-like lesions detected on mammography and/or ultrasonography **Dataset details:** The dataset included mpMR images of 140 female patients with mass-like breast lesions (70 benign and 70 malignant), consisting of Dynamic Contrast Enhanced (DCE) and T2-weighted sequences, and the Apparent Diffusion Coefficient (ADC) calculated from the Diffusion Weighted Imaging (DWI) sequence. **Cancer type:** Breast cancer **Imaging technique:** Multiparametric MRI (mpMRI)	**Primary Findings:** XGboost achieved the highest accuracy (Acc =0.88 [95% CI 0.84-0.92]) and overall performance (AUC =0.95 [95% CI 0.91-0.99]) followed by LGBM (Acc=0.87 [95% CI 0.83-0.91]/ AUC=0.94 [95% CI 0.90-0.98]), Adaboost (Acc=0.83 [95% CI 0.80-0.86] / AUC=0.90 [95% CI 0.87-0.93]), and GB (Acc=0.83 [95% CI 0.80-0.86] / AUC =0.89 [95% CI 0.86-0.92]). The observed interindividual differences in overall performances of XGBoost and LGBM were statistically significantly higher than AdaBoost and GB. The SVM classification model yielded statistically significantly lower performance (Acc=0.84 [95% CI 0.80-0.88] / AUC=0.88 [95% CI 0.84-0.92]) than XGBoost and LGBM, but this was found statistically comparable with the performances demonstrated by AdaBoost and GB. XGBoost has also achieved the highest sensitivity (Se=0.91 [95% CI 0.85-0.97]) and specificity (Sp=0.90 [95% CI 0.82-0.98]). Sensitivity and specificity metrics for the rest of the classification models were: LGBM Se=0.90 [95% CI 0.84–0.96] / Sp =0.89 [95% CI 0.81–0.97], AdaBoost Se=0.83 [95% CI 0.78–0.88] / Sp=0.82 [95% CI 0.75–0.89], GB Se =0.82 [95% CI 0.77–0.87] / Sp=0.80 [95% CI 0.73–0.87], SVM Se=0.80 [95% CI 0.77–0.88] / Sp =79 [95% CI 0.70–0.88].	Study authors noted that no power calculation for estimating the sample size selected for the study was done

Citation (Country)	Study Details	Participants & setting	Key findings	Observations/notes
	researcher's institution. No dates provided **Outcomes reported:** - Accuracy - Sensitivity - Specificity - AUC			
van Zelst et al (2020). Validation of radiologists' findings by computer-aided detection (CAD) software in breast cancer detection with automated 3D breast ultrasound: a concept study in implementation of artificial intelligence software. Acta Radiologica, 61(3), 312-320. (Netherlands)	**Study Design:** Retrospective observational study **Intervention:** AI model not stated. Computer-aided detection (CAD) software used, a commercially developed ABUS CAD software package (QVCAD, Qview Medical Inc., Los Altos, CA, USA) **Comparator:** Human readers (eight radiologists) **Study aim:** To investigate the effect of using computer-aided detection software to improve the performance of radiologists by validating findings reported by radiologists during screening with automated breast ultrasound. **Data collection methods and dates:** Data from a previously published multi-reader-multi-case (MRMC) observer study. Cases were extracted from a multi-institutional database containing ABUS examinations from 715 women. Dates not provided **Outcomes reported:** - AUC - Partial AUC (pAUC)	**Sample size:** 120 **Participants:** 120 women with dense breasts that included 60 randomly selected normal exams, 30 exams with benign lesions, and 30 malignant cases (20 mammography-negative). **Dataset details:** The final dataset consisted of 120 unilateral breast examinations (a total of 375 views) with 30 malignant cases, 30 cases containing benign lesions, and 60 normal cases with two years of negative follow-up **Cancer type:** Breast cancer **Imaging technique:** Automated three-dimensional breast ultrasound (ABUS)	**Primary Findings:** The overall difference in AUC was not statistically significant: 0.82 (95% CI=0.73–0.92) for unaided reading and 0.83 (95% CI=0.75–0.92) for reading after CAD validation (P=0.743). Validation by CAD improved the partial AUC for the interval within the specificity range of 80%–100%. Partial AUC improved significantly from 0.13 (95% CI=0.10–0.15) to 0.14 (95% CI=0.12–0.17) (P=0.037) after CAD rejected mostly benign lesions and normal tissue scored BI-RADS 3 or 4. **Additional Findings:** Four cancers detected by readers were completely missed by computer-aided detection and four other cancers were detected by both readers and computer-aided detection but falsely rejected due to technical limitations of our implementation of computer-aided detection validation. Validation of computer-aided detection discarded 42.6% of findings that were scored BI-RADS ≥ 3 by the radiologists, of which 85.5% were non-malignant findings.	The authors acknowledged that the prevalence of both benign and malignant breast disease was artificially enhanced to increase the power of the study. .

Citation (Country)	Study Details	Participants & setting	Key findings	Observations/notes
	Sensitivity Specificity			
Prostate Cancer				
Akatsuka et al (2019). Illuminating clues of cancer buried in prostate MR image: deep learning and expert approaches. Biomolecules, 9(11), p.673. (Japan)	**Study Design:** Retrospective (Not clearly stated) **Intervention:** Previously developed Deep convolutional neural network (dCNN)(Xception) **Comparator:** Human readers (radiologists) **Study aim:** to compare the deep learning-focused regions of magnetic resonance (MR) images with cancerous locations identified by radiologists and pathologists. **Data collection methods and dates:** MR imaging at the Nippon Medical School Hospital (NMSH) between January 2012 and May 2018 **Outcomes reported:** Classification accuracy Location comparison	**Sample size:** 105 patients, 307 MRI images **Participants:** patients who underwent prostate MR imaging. Patients with history of prior radiation, surgery, or androgen-deprivation therapies were excluded. **Dataset details:** Dataset obtained from a hospital in Japan **Cancer type:** Prostate cancer **Imaging technique:** MRI	**Primary Findings:** **Classification Using a Deep Neural Network** An ROC curve for classification accuracy using 10-fold cross validation yielded an average AUC of 0.90 (95% confidence interval (CI) 0.87–0.94). Result showed the case-level analysis for an average AUC of 0.93 (95% CI 0.87–0.99). In the case of the cancer images, 86.0% of the images were classified correctly, whereas 14.0% were misclassified. In the case of the non-cancer images, 78.3% were classified correctly, whereas 21.7% were misclassified. **Clinical Comparison of Cases Classified Using a Deep Neural Network** The clinicopathological features of the cancer and non-cancer cases classified by the deep convolutional neural network were compared. The Gleason score was higher in the misclassified cases than in the classified cases ($p = 0.03$). There were no significant differences between the classified and misclassified cases with respect to age, PSA, TPV, PSAD, clinical T stage, pathological T stage, and other blood test data **Additional Findings:** **Locational Comparison between Deep Learning-Focused Regions on MR Images and Expert-Identified Cancer Locations** The deep learning-focused regions overlapped the radiologist-identified targets in 70.5% of the MR images ($p < 0.001$), the deep learning-focused regions overlapped genuine cancer locations in 72.1% of the MR images ($p < 0.001$). In the remaining MR images, deep learning focused the following regions: transition zone (10.1%), peripheral zone (7.8%), and the others (region	The radiologists were blind to all clinicopathological information

Citation (Country)	Study Details	Participants & setting	Key findings	Observations/notes
			outside of prostate gland). Pathologists evaluated the deep leaning-focused regions in the non-overlapping images and found that deep learning focused on following regions: dilated prostatic ducts, lymphocyte aggregation, and others (normal stroma and adipose tissue).	
Arslan et al (2023). Does deep learning software improve the consistency and performance of radiologists with various levels of experience in assessing bi-parametric prostate MRI?. Insights into Imaging, 14(1), pp.1-10. (Turkey)	**Study Design:** Retrospective (Not clearly stated) **Intervention:** Human + Commercially available DL software (Prostate AI, Version Syngo.Via VB60, Siemens Healthcare) **Comparator:** Human (four radiologists) alone **Study aim:** The aims of the study were twofold: First, to investigate whether the commercially available DL software increases the PI-RADS scoring consistency on bi-parametric MRI among radiologists with various experience levels; Second, to assess whether the DL software improves the performance of radiologists in identifying clinically significant prostate cancer (csPCa). **Data collection methods and dates:** Authors reviewed consecutive patients who underwent a prostate MRI scan due to suspicion of PCa or active surveillance between January 2019 and December 2020. **Outcomes reported:** - Inter-rater agreement - Performance identifying csPCa,	**Sample size:** 153 men, 153 MRI's **Participants:** patients having whole-mount pathology or biopsy for patients with a PI-RADS ≥ 3 score assigned during routine clinical reading; having a prostate MRI scan obtained at 3 T without an endorectal coil following PI-RADS version 2; and ≥ 18 months of follow-up without any clinical, laboratory, or imaging evidence of PCa for patients with a PI-RADS score ≤ 2. **Dataset details:** Data obtained from consecutive patients who underwent a prostate MRI scan due to suspicion of PCa (i.e., increased prostate-specific antigen or suspicious digital rectal examination) or active surveillance between January 2019 and December 2020. **Cancer type:** Prostate cancer **Imaging technique:** MRI	**Primary Findings:** **The inter-rater agreement among the radiologist with and without the DL software** Radiologists changed their initial PI-RADS scores in 1/153 (0.65%), 2/153 (1.3%), 0/153 (0%), and 3/153 (1.9%) of the patients with the DL software. Fleiss' kappa Score among the radiologists without the DL software was 0.39, equating to a fair agreement. Fleiss' kappa Score among the radiologists increased from 0.39 to 0.40 with the DL software, not representing a signifcant diference (p=0.56). **The performance of the radiologists in identifying csPCa with and without DL software** The AUROCs of the experienced radiologist, less experienced radiologist 1 2, and less-experienced radiologist 3 without the DL software were 0.92 (95% CI 0.88–0.96), 0.85 (95% CI 0.79–0.91), 0.81 (95% CI 0.73–0.88), 0.78 (95% CI 0.70–0.86). The AUROC of the standalone DL software was 0.76 (95% CI 0.67–0.84). The AUROCs of the experienced radiologist, less-experienced radiologist 1, less-experienced radiologist 2, and less-experienced radiologist 3 with the DL software were 0.92 (95% CI 0.88–0.96), 0.86 (95% CI 0.81–0.92), 0.81 (95% CI 0.73–0.88), and 0.79 (95% CI 0.71–0.87). The AUROCs of the experienced radiologist and less-experienced radiologist 1 were significantly	

Citation (Country)	Study Details	Participants & setting	Key findings	Observations/notes
			higher than that of the DL software (p < 0.0001 and p = 0.04). In contrast, the AUROCs of the remaining less-experienced radiologists 2 and 3 did not significantly differ from that of the DL software (p = 0.63 and p = 0.23). The AUROCs of radiologists in identifying csPCa with and without the DL software did not differ for radiologists (p > 0.05).	
Faiella et al (2022). Quantib prostate compared to an expert radiologist for the diagnosis of prostate cancer on mpMRI: a single-center preliminary study. Tomography, 8(4), pp.2010-2019. (Italy)	**Study Design:** Retrospective (Not clearly stated) **Intervention:** Human (inexperienced radiologist) + Previously developed AI software Quantib Prostate (Quantib B.V., Rotterdam, The Netherlands) **Comparator:** Human (expert radiologist) **Study aim:** To evaluate the clinical utility of an AI radiology solution, Quantib Prostate, for prostate cancer (PCa) lesions detection on multiparametric Magnetic Resonance Images (mpMRI). **Data collection methods and dates:** mpMRI exams collected from 2019 to 2020 and seen by the same expert radiologist **Outcomes reported:** - Lesions identified - Sensitivity (number of true positives/(number of true positives + number of false positives)) - PPV (number of true negatives/(number of true	**Sample size:** 108 patients with 108 mpMRI exams **Participants:** Three groups of patients were assessed: patients with positive mpMRI, positive target biopsy, and/or at least one positive random biopsy (group A, 73 patients); patients with positive mpMRI and a negative biopsy (group B, 14 patients), and patients with negative mpMRI who did not undergo biopsy (group-C, 21 patients). **Dataset details:** Not stated **Cancer type:** Prostate cancer **Imaging technique:** Multi-parametric Magnetic Resonance Imaging (mpMRI)	**Primary Findings:** **Lesions found** In group A, the expert radiologist found 96 lesions in 73 mpMRI exams; of them, 17.7% were PIRADS 3, 56.3% were PIRADS 4, and 26% were PIRADS 5. The AI-assisted radiologist found 121 lesions; of them, 0.8% were PIRADS 3, 53.7% were PIRADS 4, and 45.5% were PIRADS 5. At biopsy, 33.9% of the lesions were ISUP 1, 31.4% were ISUP 2, 22% were ISUP 3, 10.2% were ISUP 4, and 2.5% were ISUP 5. Evaluating group A, the expert radiologist reached a sensitivity of 71.7 and a PPV of 84.4%, while the AI-assisted radiologist reached a sensitivity of 92.3% and a PPV of 90.1%. Analyzing the cases which resulted in false negatives from expert radiologist evaluation and true positives from AI-assisted radiologist analysis (23 ROIs), 12 were ISUP 1, 7 were ISUP 2, 3 were ISUP 3, and only 1 was ISUP 4. In group A, nine cases were false negatives for both the expert radiologist and AI-assisted radiologist (four ISUP 1 and five ISUP 2). In group B, the expert radiologist found 17 lesions in 14 mpMRI exams (47.1% PIRADS 3 and 52.9% PIRADS 4). The AI-assisted radiologist found 14 lesions in the same 14 mpMRI exams (71.4% PIRADS 3 and 28.6% PIRADS 4). Moreover, 21.4% were in the PZ and 78.6% in the TZ.	Radiologists were blinded to biopsy results

Citation (Country)	Study Details	Participants & setting	Key findings	Observations/notes
	negatives + number of false positives)).		In group C, the expert radiologist did not find any lesions. The AI-assisted radiologist found 37 lesions in 21 patients; of them, 86.5% were PIRADS 3, and the rest were PIRADS 4; moreover, 32.4% were in the PZ and 67.6% in the TZ.	
Forookhi et al (2023). Bridging the experience gap in prostate multiparametric magnetic resonance imaging using artificial intelligence: A prospective multi-reader comparison study on inter-reader agreement in PI-RADS v2.1, image quality and reporting time between novice and expert readers. European Journal of Radiology, 161, p.110749. (Italy)	**Study Design:** A prospective observational study **Intervention:** Human + commercially available AI-assisted software (Quantib® Prostate) **Comparator:** Human (four novice readers) alone **Study aim:** To determine the impact of using a semi-automatic commercially available AI-assisted software (Quantib® Prostate) on inter-reader agreement in PI-RADS scoring at different PI-QUAL ratings and grades of reader confidence and on reporting times among novice readers in multiparametric prostate MRI. **Data collection methods and dates:** consecutive patients were enrolled at a tertiary referral center between October 2021 and February 2022. **Outcomes reported:** - Inter-reader agreement - Receiver Operating Curve analysis - Reporting time, and Image quality and grade of confidence among readers	**Sample size:** 200 patients, 200 scans **Participants:** The cohort underwent MRI examination for clinical suspicion for PCa due to either an increase from baseline PSA levels or positive DRE findings, as per clinical practice. 56 patients were excluded according to the following criteria: (a) patients in active surveillance (n = 34); (b) patients who had previously undergone radical prostatectomy or radiation therapy (n = 9); (c) prior diagnosis of PCa (n = 5); (d) incompatibility between imaging data and AI-assisted software resulting from incorrect processing or loss of data during transfer from the local PACS server (n = 8). **Dataset details:** Dataset obtained from a tertiary referral Centre in Italy **Cancer type:** Prostate cancer **Imaging technique:** Multiparametric magnetic resonance imaging	**Primary Findings:** **Inter-reader agreement in PI-RADS scoring** Novice readers with more experience (readers 2 and 3) had lower kappa scores when using the AI-assisted software, except for batch 4 for Reader 3 where inter-reader kappa agreement improved from 0.29 to 0.46. On the contrary, less experienced novice readers (readers 1 and 4) showed statistically significant improvement ($p < 0.001$) in inter-reader agreement with the software. Kappa scores for Reader 1 were higher in all batches, with an overall increase from 0.67 to 0.74. Reader 4 showed improvements in batches 2 and 3, with kappa scores increasing from 0.55 to 0.62 and 0.54 to 0.59, respectively. In the re-evaluation of the 1st batch, a comparable trend was noted with agreement consistently higher in Readers 2 and 3 without the software, on the other hand, improvement with the software was noted in Readers 1 and 4. Overall, kappa scores ranged from 0.29 to 0.81 without Quantib® and from 0.27 to 0.77 with Quantib®. Subgroup analysis revealed a similar increase in overall inter-reader agreement with AI-assisted reading among less experienced novice readers. In the peripheral zone, kappa coefficient values rose from 0.53 to 0.60 and from 0.37 to 0.42 for Readers 1 and 4, respectively. In the transition zone, the scores similarly improved from 0.28 to 0.43 and from 0.48 to 0.49 for the two readers. **Receiver Operating Curve analysis** Among less experienced readers, Quantib® resulted in improved diagnostic accuracy in all	Readers were blinded to expert and individual reports.

Citation (Country)	Study Details	Participants & setting	Key findings	Observations/notes
			batches with Reader 1 and in batches 1, 3, 5 and overall, in Reader 4; AUC ranges rose from 0.73 to 0.81, without the software, to 0.75 to 0.86, with the software. More experienced readers achieved a higher diagnostic accuracy without Quantib®. Overall sensitivity findings were in line with the pattern observed with AUCs, rising from 51.8 % to 65.8 % and from 59.6 % to 61.4 % in readers 1 and 4, respectively. Overall specificity decreased in all instances of software use, ranging from 94.3 % to 98.7 %, without the software, to 86.8 to 98.4 %, with the software. In the peripheral zone, when using the software, AUCs improved from 0.76 to 0.82 in Reader 1 and from 0.77 to 0.78 in Reader 4. In the transition zone, with the software, AUCs increased from 0.68 to 0.79 for Reader 1 but stayed constant at 0.86 for Reader 4. The AUCs for Readers 2 and 3 decreased both in the transition zone and in peripheral zones with the software. **Reporting time** The results showed statistically significant differences ($p < 0.001$) between reporting times. Evaluation times were longer amongst all readers when reporting with Quantib®. Total mean reader times ranged from a minimum of 123.81 +/- 51.25 sec to a maximum of 189.14 +/- 67.08 sec without Quantib®, and from 697.44 +/- 98.88 sec to 792.47 +/- 122.37 sec with Quantib®. The uploading time (tUp) was evidently shown to be the most time-consuming step in the workflow followed by time for segmentation (tSeg) and time for lesion identification (tID). **Image quality and grade of confidence among readers** In all four readers, overall inter-reader agreement was higher with greater PI-QUAL scores and grades of confidence. Kappa coefficient values were higher with Quantib® at all PI-QUAL scores	

Citation (Country)	Study Details	Participants & setting	Key findings	Observations/notes
			in Readers 1 and 4, as well as at PI-QUAL 3 in Reader 2. Quantib® had the same effect on these three readers at lower levels of confidence, especially at grade 3. Inter-reader agreements on PI-QUAL scores were 0.15 (slight) for Reader 1 vs Reader 2; 0.13 (slight) for Reader 1 vs Reader 3; 0.02 (slight) for Reader 1 vs Reader 4; 0.59 for Reader 2 vs Reader 3 (moderate); 0.09 (slight) for Reader 2 vs Reader 4; 0.11 (slight) for Reader 3 vs Reader 4.	
Patsanis et al (2023). A comparison of Generative Adversarial Networks for automated prostate cancer detection on T2-weighted MRI. Informatics in Medicine Unlocked, 39, p.101234. (Norway)	**Study Design:** Retrospective (Not clearly stated) **Intervention:** Six previously developed relevant 2D GANs were selected for investigation: f-AnoGAN, HealthyGAN, StarGAN, StarGAN-v2, FP-GAN and DeScarGAN. For each model, the code was publicly available. **Comparator:** AI models were compared amongst themselves **Study aim:** To assess the potential of several Generative Adversarial Networks (GAN) models for the task of PCa detection on T2W MRI. **Data collection methods and dates:** Transverse T2W MR images from two datasets (N = 1160) were used in this study: an in-house collected dataset (N = 961) and the publicly available PROSTATEx Challenge training dataset (N = 199). The in-house dataset consisted of diagnostic MR images from men enrolled in the standardized prostate cancer pathway at St. Olavs Hospital, Trondheim	**Sample size:** 1,160 patients, 1,160 MRI images **Participants:** Men enrolled in the standardized prostate cancer pathway due to suspicion of prostate cancer **Dataset details:** One publicly available dataset (from the Netherlands) and an in-house dataset obtained from a hospital in Norway. **Cancer type:** Prostate cancer **Imaging technique:** MRI	**Primary Findings:** All models except f-AnoGAN and StarGAN-v2 performed best when trained on input images with a pixel spacing of 0.4 × 0.4 mm. FP-GAN performed best, with an AUC of 0.76 (95% CI: 0.65–0.84). This was significantly better than the performance of f-AnoGAN and StarGAN-v2, but not HealthyGAN, StarGAN, and DeScarGAN. FP-GAN and StarGAN are the only models that convincingly visualize the tumor on the PCa detection map. The performance of FP-GAN was further evaluation on the test sets. The AUC was 0.72 on both the internal and external test sets using the initial model. Stable performance with a standard deviation of 1%–4% was observed across the five randomly initialized models. All model initializations successfully detected the malignant area in a patient with a histopathologically confirmed GGG 2 tumor. The anomaly scores corresponding to all model initializations are consistently higher (p < 0.001) for positive than negative patients in the test sets.	

Citation (Country)	Study Details	Participants & setting	Key findings	Observations/notes
	University Hospital, Trondheim, Norway, from January 2013 to December 2020. **Outcomes reported:** - Classification performance (AUC)			
Tong et al (2023). Comparison of a Deep Learning-Accelerated vs. Conventional T2-Weighted Sequence in Biparametric MRI of the Prostate. Journal of Magnetic Resonance Imaging. (USA)	**Study Design:** Retrospective **Intervention:** A commercially developed proprietary deep learning-based prototypical computer-aided detection algorithm (DL-CAD) (MR Prostate AI, version 1.3.2, build July 07, 2021, front end build November 06, 2019, Siemens Healthcare) **Comparator:** Human (three abdominal fellowship trained radiologists) **Study aim:** To compare the diagnostic ability of a prototype deep learning-accelerated T2-weighted image (DL-T2) against the conventional clinical T2-weighted image (CL-T2) in both a reader study and a study utilizing a commercially developed prototype deep learning-based computer-assisted detection (DL-CAD). **Data collection methods and dates:** The picture archiving and communication system (PACS) was searched for consecutive patients who had an MRI of the prostate from December 28, 2020 to April 28, 2021	**Sample size:** 160 scans from 80 patients **Participants:** Patients were included with indications of suspected prostate cancer or a diagnosed low-risk prostate cancer on active surveillance. Patients were included if their imaging protocol had both the conventional axial T2-weighted image (CL-T2) and the deep learning-accelerated axial T2 (DL-T2). DL-T2 sequence was routinely included in clinical scans as a backup T2-weighted image in case of artifact. Other exclusion criteria included the presence of a hip arthroplasty, prior treatment of prostate cancer, or no adequate follow-up. **Dataset details:** Dataset obtained from the institutional clinical picture archiving and communication system (PACS) (Visage Imaging, Berlin, Germany). **Cancer type:** Prostate cancer **Imaging technique:** Biparametric MRI	**Primary Findings:** **Radiology Reader Results** There was no significant difference in overall image quality for readers 1 (axial CL-T2: 3.72 ± 0.53, axial DL-T2: 3.89 ± 0.39, P = 0.99; coronal CL-T2: 3.86 ± 0.35, coronal DL-T2: 3.94 ± 0.25, P = 0.99) and 2 (axial CL-T2: 3.33 ± 0.82, axial DL-T2: 3.31 ± 0.74, P = 0.49; coronal CL-T2: 3.39 ± 0.71, coronal DL-T2: 3.31 ± 0.71, P = 0.20). Reader 3 rated CL-T2 with significantly higher overall image quality, though the difference was small (axial CL-T2: 3.67 ± 0.63, axial DL-T2: 3.51 ± 0.62; coronal CL-T2: 3.73 ± 0.52, coronal DL-T2: 3.48 ± 0.62). There was no significant difference in AUC of the ROC curve between CL-bpMRI and DL-bpMRI in all readers in patient-based analysis: (CL-bpMRI, DL-bpMRI) – reader 1 (0.77, 0.78, P = 0.98); reader 2 (0.65, 0.66, P = 0.95); reader 3 (0.57, 0.60, P = 0.52); lesion-based (CL-bpMRI, DL-bpMRI) – reader 1 (0.71, 0.70, P = 0.92); reader 2 (0.58, 0.62, P = 0.70); reader 3 (0.57, 0.60, P = 0.70). In patient-based analysis, there was no significant ence in AUC of ROC between CL-bpMRI and DL-bpMRI: (CL-bpMRI, DL-bpMRI) – reader 1 (0.71, 0.70, P = 0.92); reader 2 (0.58, 0.62, P = 0.70); reader 3 (0.57, 0.60, P = 0.70). Light's kappa was fair, measuring 0.35 for inter reader variation. In lesion-based analysis results, reader 1 identified a total of 34 lesions on CL-bpMRI (29 Peripheral Zone (PZ), 5 Transition	Radiologists blinded to acquisition method.

Citation (Country)	Study Details	Participants & setting	Key findings	Observations/notes
	Outcomes reported: - Image quality - Diagnostic performance		Zone (TZ)) and 27 lesions on DL-bpMRI (21 PZ, 6 TZ). Reader 2 identified a total of 44 lesions on CL-bpMRI (33 PZ, 11 TZ) and 51 lesions on DL-bpMRI (32 PZ, 19 TZ). Reader 3 identified a total of 17 lesions on CL-bpMRI (16 PZ, 1 TZ) and 15 lesions on DL-bpMRI (12 PZ, 3 TZ) **DL-CAD results** DL-CAD did not have significantly different sensitivity in patient-based evaluation or lesion-based evaluation when assessing CL-bpMRI compared to DL-bpMRI but had significantly lower specificity when evaluating DL-bpMRI. On lesion-based analysis, DL-CAD identified 22 PZ lesions on CL-bpMRI and 24 PZ lesions on DL-bpMRI and 30 TZ lesions on CL-bpMRI and 41 TZ lesions on DL-bpMRI. Two csPCa were missed on the CL-bpMRI but detected on DL-bpMRI and both were located in the TZ.	
Zhang, et al (2022). Pseudoprospective paraclinical interaction of radiology residents with a deep learning system for prostate cancer detection: experience, performance, and identification of the need for intermittent recalibration. I	**Study Design:** Retrospective, pseudoprospective, paraclinical analysis was performed in a cohort **Intervention:** A previously established and validated DL algorithm, convolutional neural network (CNN) **Comparator:** Human (radiologists-in-training) **Study aim:** To estimate the prospective utility of a previously retrospectively validated convolutional neural network (CNN) for prostate cancer (PC) detection on prostate magnetic resonance imaging **Data collection methods and dates:** Consecutive patients were examined	**Sample size:** 201 examinations from 201 patients **Participants:** All men had suspicion for prostate cancer based on prostate-specific antigen elevation, clinical examination, or participation in the active surveillance program. Included patients had mpMRI performed on one of the institutional MRI systems and MRI/TRUS-fusion biopsy performed at the institutions. **Dataset details:** Dataset obtained from an active surveillance programme in Germany. **Cancer type:** Prostate cancer **Imaging technique:** MRI	**Primary Findings:** **Time to Finalization of Paraclinical Image Interpretation** Median time between image acquisition and end of research interpretation was 30 hours (IQR, 8.6–139.2 hours). Median time from research interpretation to availability of final pathology reports was of 5.7 days (IQR, 1.7–10.6 days). **Patient-Level Comparison of Pre- and Post-CNN Research and Clinical PI-RADS Assessment** The CNN achieved an ROC area under the curve of 0.77 on a patient basis. Using PI-RADS ≥3-emulating probability threshold (c3), CNN had a patient-based sensitivity of 81.8% and specificity of 54.8%, not statistically different from the current clinical routine PI-RADS ≥4 assessment at 90.9% and 54.8%, respectively (P = 0.30/P = 1.0). In general, residents achieved similar sensitivity and specificity before and after CNN review.	

Citation (Country)	Study Details	Participants & setting	Key findings	Observations/notes
nvestigative Radiology, 57(9), pp.601-612. (Germany)	between November 2019 and September 2020 **Outcomes reported:** - Time to image interpretation - Clinical performance		**Sextant-Level Comparison of Pre- and Post-CNN Research and Clinical PI-RADS Assessment** On a prostate sextant basis, clinical assessment possessed the highest ROC area under the curve of 0.82, higher than CNN (AUC = 0.76, P = 0.21) and significantly higher than resident performance before and after CNN review (AUC = 0.76 / 0.76, P ≤ 0.03). **Additional Findings:** **Residents' Subjective Survey Results** The resident survey indicated CNN to be helpful and clinically useful. In the survey, radiologists-in-training stated that they "completely" or "qualitatively" agreed with the CNN prediction in most cases (59%). In 9%, the CNN identified lesions that the residents chose to add in their second assessment. Cases were felt to be undercalled in 34%.	
Lung cancer				
Baldwin et al (2020). External validation of a convolutional neural network artificial intelligence tool to predict malignancy in pulmonary nodules. Thorax, 75(4), pp.306-312. (UK)	**Study Design:** Retrospective (Not clearly stated) **Intervention:** Previously developed AI model (Lung Cancer Prediction CNN (LCP-CNN) **Comparator:** Brock model **Study aim:** To compare the performance of an AI algorithm, the lung cancer prediction convolutional neural network (LCP-CNN), with that of the Brock University model, recommended in UK guidelines.	**Sample size:** There were 1,397 nodules in 1,187 patients, **Participants:** Adult patients reported as having one or more solid pulmonary nodules of 5–15 mm in maximal axial diameter detected on thoracic CT scan. With CT slice thickness of 3mm or less. **Dataset details:** Dataset obtained from three hospitals in the UK **Cancer type:** Lung cancer **Imaging technique:** CT scan	**Primary Findings:** The area under the curve for LCP-CNN was 89.6% (95% CI 87.6 to 91.5), compared with 86.8% (95% CI 84.3 to 89.1) for the Brock model (p≤0.005). Using the LCP-CNN, 24.5% of nodules scored below the lowest cancer nodule score, compared with 10.9% using the Brock score. Using the predefined thresholds, the LCP-CNN gave one false negative (0.4% of cancers), whereas the Brock model gave six (2.5%), while specificity statistics were similar between the two models. The LCP-CNN had a sensitivity of 99.57 (95% CI 98.62 to 100.00) and a specificity of 28.03 (95% CI 25.51 to 30.62), compared with Brock's sensitivity of 97.44 (95% CI 95.26 to 99.18) and specificity of 29.23 (95% CI 26.69 to 31.88).	Data were enriched to contain at least a 10% cancer prevalence

Citation (Country)	Study Details	Participants & setting	Key findings	Observations/notes
	Data collection methods and dates: Retrospective data collection ran from January 2018 to August 2019. **Outcomes reported:** - Performance efficacy		When typical perifissural nodules and intra-pulmonary lymph nodes, which would not usually warrant follow-up, were excluded from the validation cohort the discriminatory ability of both models reduced. The LCP-CNN still outperformed the Brock model (AUC 86.4% (95% CI 82.2 to 90.3) compared with Brock AUC of 81.1% (95% CI 76.3 to 85.6); p=0.0113). Rule-out rates were also lower for this cohort, but the LCP-CNN still ruled out 16.7% of nodules with only one false negative, and Brock model ruled out 19.3% with six false negatives.	
Jacobs et al (2021). Deep learning for lung cancer detection on screening CT scans: results of a large-scale public competition and an observer study with 11 radiologists. Radiology: Artificial Intelligence, 3(6), p.e210027. (USA/Canada/Netherlands/Belgium)	**Study Design:** Retrospective (No clearly stated) **Intervention:** Three top-performing algorithms from the Kaggle Data Science Bowl 2017 public competition: grt123, Julian de Wit and Daniel Hammack (JWDH), and Aidence (all previously developed deep learning algorithms) **Comparator:** Human (11 radiologists) **Study aim:** To determine whether deep learning algorithms developed in a public competition could identify lung cancer on low-dose CT scans with a performance similar to that of radiologists. **Data collection methods and dates:** 300 patient scans were used for model assessment; 150 patient scans were from the competition set and 150 were from an independent	**Sample size:** 300 patient CT scans **Participants:** For the cancer-positive scans, the screening CT scan obtained before the lung cancer diagnosis was included. Only scans in patients for whom the diagnosis followed within 1 year of the CT scan were included. Non cancer scans were selected from individuals who did not have a lung cancer diagnosis during the course of the screening program and for whom the minimum follow-up period was 2 years. **Dataset details:** The scans originated from the National Lung Screening Trial, The Danish Lung Cancer Screening Trial and The screening program at the Lahey Hospital and Medical Center (Burlington, Mass). **Cancer type:** Lung cancer **Imaging technique:** Low dose CT scans	**Primary Findings:** **DSB2017 Competition Results** The AUC values of the top 10 algorithms were high and ranged between 0.85 and 0.88. **Observer Experiment** For the top three solutions (grt123, JWDH, and Aidence), software packages that can process unseen CT scans were compiled, and the correlation scores between the recomputed and the submitted scores of the algorithms were all above 0.99. All readers completed the full set of 300 scans of the observer experiment, and the average reading time per scan ranged from 96 seconds to 275 seconds. The AUC values were 0.88 (95% CI: 0.84, 0.91) for grt123, 0.90 (95% CI: 0.87, 0.93) for Aidence, and 0.90 (95% CI: 0.87, 0.93) for JWDH when the models were assessed on all 300 scans. For the radiologists, the AUCs ranged from 0.84 (95% CI: 0.80, 0.88) to 0.94 (95% CI: 0.92, 0.96), with an average AUC of 0.92 (95% CI: 0.89, 0.95). The top three algorithms showed good performance, and no performance drop was seen on the independent validation data. The statistical analysis showed that the average AUC among the	It is unclear from the study the time periods the dataset were retrieved. The radiologists were informed that about one-third of the scans were cancer positive, but they were blinded to clinical information and the results of the algorithms.

Citation (Country)	Study Details	Participants & setting	Key findings	Observations/notes
	dataset (data collection dates not stated) **Outcomes reported:** - Diagnostic performance (AUC)		11 radiologists was higher than that of the grt123 algorithm (P = .02); whereas the AUCs from the other two models were not significantly worse compared with those of the radiologists (JWDH, P = .29; and Aidence, P = .26).	
Maldonado et al (2021). Validation of the BRODERS classifier (Benign versus aggRessive nODule Evaluation using Radiomic Stratification), a novel HRCT-based radiomic classifier for indeterminate pulmonary nodules. European Respiratory Journal, 57(4). (USA)	**Study Design:** Retrospective (Not clearly stated) **Intervention:** BRODERS classifier used by CANARY AI software **Comparator:** Brock model **Study aim:** To reports the independent external validation of the Mayo Clinic BRODERS (Benign versus aggRessive nODule Evaluation using Radiomic Stratification) classifier, radiomics model, for the classification into benign and malignant lung nodules. **Data collection methods and dates:** Dates not provided, images taken from the NLST and the Vanderbilt databases **Outcomes reported:** - Diagnostic performance	**Sample size:** 685 images for the training set and 170 patients/ images for the validation set **Participants:** Patients with screen-detected IPNs with largest diameter ranging from 7 to 30 mm **Dataset details:** The validation dataset included consecutive patients with incidentally identified IPNs enrolled into the Vanderbilt University pulmonary nodule registry. Training set was obtained from the National Lung Screening Trial **Cancer type:** Lung cancer **Imaging technique:** CT	**Primary Findings:** For the entire Vanderbilt validation set (n=170, 54% malignant), the AUC was 0.87 (95% CI 0.81–0.92) for the Brock model and 0.90 (95% CI 0.85–0.94) for the BRODERS model. Using the optimal cut-off determined by Youden's index, the sensitivity was 92.3%, the specificity was 62.0%, the positive (PPV) and negative predictive values (NPV) were 73.7% and 87.5%, respectively. For nodules with intermediate pre-test probability of malignancy, Brock score of 5–65% (n=97), the sensitivity and specificity were 94% and 46%, respectively, the PPV was 78.4% and the NPV was 79.2%. Conclusions: The BRODERS radiomic predictive model performs well on an independent dataset and may facilitate the management of indeterminate pulmonary nodules.	It is unclear from the study the time periods the dataset were retrieved
Tam et al (2021). Augmenting lung cancer diagnosis on chest radiographs:	**Study Design:** Retrospective (Not clearly stated) **Intervention:** a commercially available AI algorithm (Red Dot, Behold.ai, London, UK) +/- radiologists	**Sample size:** 396 examinations from 296 patients **Participants:** 1, 2 or 3 cm both central and peripheral lung tumors were collected. No tumor was included that was >3.5 cm	**Primary Findings:** **Radiologist performance** The mean accuracy of cancer detection is 87% (84-90%) and overall mean sensitivity to cancer is 78% (69-86%). This corresponds to between 136 and 171 patients being diagnosed correctly for tumors and between 62 and 27 patients with	It is unclear from the study the time periods the dataset were retrieved It appears that some of the study authors are

Citation (Country)	Study Details	Participants & setting	Key findings	Observations/notes
Positioning artificial intelligence to improve radiologist performance. Clinical Radiology, 76(8), pp.607-614. (UK)	**Comparator:** Human (radiologists) **Study aim:** To evaluate the role that AI could play in assisting radiologists as the first reader of chest radiographs (CXRs), to increase the accuracy and efficiency of lung cancer diagnosis by flagging positive cases before passing the remaining examinations to standard reporting **Data collection methods and dates:** Dataset obtained from the NHS Cancer Registry database to yield a list of 7 years' worth of lung cancers from the hospital site. **Outcomes reported:** - Diagnostic performance	**Dataset details:** Dataset obtained from the NHS Cancer Registry database, UK **Cancer type:** Lung cancer **Imaging technique:** X-rays	missed cancer pathologies. All radiologists had a low rate of false positives, between one and nine examinations (average precision 95.67%). The correlation between the radiologists' reports shows an average agreement of 86.7% and corresponding average Cohen's kappa score of 0.72, denoting good overall agreement. Agreement between all radiologists occurs in 80% of cases. Predictions made by radiologist 1 and radiologist 3 are statistically different ($p<0.05$). **AI performance** The AI algorithm achieved an overall accuracy of 87% on this tumor dataset, equivalent to the mean performance of the radiologists. The algorithm sensitivity was superior to two of three radiologists at 80% whilst specificity was marginally lower than radiologists at 93%. There was an increase in false-positive examinations, with an overall precision of 92%. **Radiologist plus AI** Overall accuracy and sensitivity were increased with AI, improving average scores by +3.67% and +13.33% respectively. False-negative cases, were reduced by 15-40 cases. Combined performance showed an increase in false-positive examinations, with an average precision change of -5.33% and specificity change of -6%. For radiologists, improvements were statistically significant when compared to their standalone performance ($p<0.05$). Agreement between radiologists improved with AI, with radiologist + AI labels agreeing in 92% of cases (+12%). Average proportional agreement increased to 94.33% (+7.63%) and the average Cohen's Kappa score was 0.89 (+0.17), suggesting very good agreement. Radiologist + AI predictions were statistically similar ($p>0.05$). On average, missed tumors were reduced by 60% by a single radiologist with AI. Combining the predictions of all	employed by the company that created the AI model

Citation (Country)	Study Details	Participants & setting	Key findings	Observations/notes
			radiologists and taking any positive prediction of a tumor as the given label, reduced missed tumors by 65.4%. **Algorithm performance on radiologist misses** The algorithm detected eight of these cases, which would have been otherwise missed. In total, the algorithm detected 70.2% of all tumors, which were missed by at least one radiologist. **Distracting findings** Radiologist performance was significantly reduced on these examinations, with accuracy and sensitivity decreasing by 18% and 30%, respectively, when compared to examinations without distracting findings. The algorithm's performance on tumors was also decreased, but to a lesser extent, with accuracy and sensitivity decreasing by 12% and 10%, respectively. Combined radiologist + AI approach improves accuracy and sensitivity overall; improvements are significantly larger when distracting findings are present. Accuracy increases by 9% compared to a 1% increase without. **Additional Findings:** Overall sensitivity for tumors increased with tumor size for both radiologists and the algorithm; however, combined sensitivity showed performance improvements on cancers of all sizes, with the greatest sensitivity increase (+0.17) coming in tumors 1-2 cm in size.	
Toğaçar et al (2020). Detection of lung cancer on chest CT images using minimum redundancy	**Study Design:** Retrospective (Not clearly stated) **Intervention:** Previously developed AI models LeNet, AlexNet and VGG-16 CNNs.	**Sample size:** The dataset consists of CT images collected from 69 different patients, 100 images (50 cancerous and 50 non-cancerous). **Participants:** images were acquired as part of routine care and not as part of a controlled research study or clinical trial.	**Primary Findings:** The LeNet with RMSprop optimizer and LeNet with ADAM optimizer achieved 81.20 % and 73.82 % classification accuracy. As for AlexNet with SGD and SGD-Drop approaches, the models yielded 85.12 % and 89.14 % classification accuracy, respectively. Lastly, 78.09 % classification accuracy was provided by VGG-16.	It is unclear from the study the time periods the dataset were retrieved

Citation (Country)	Study Details	Participants & setting	Key findings	Observations/notes
maximum relevance feature selection method with convolutional neural networks. Biocybernetics and Biomedical Engineering, 40(1), pp.23-39. (Turkey)	**Comparator:** AI models above were compared amongst themselves **Study aim:** The study consists of five experiments. The aim of the first two experiments was to measure the success of CNNs and the machine learning classifiers without image augmentation techniques. The path followed in the third and fourth experiments was the same as in the first two experiments. The only difference was to learn whether the image augmentation techniques can contribute to the success rates of the models. **Data collection methods and dates:** The images were randomly selected from the dataset (No dates given) **Outcomes reported:** - Classification accuracy	**Dataset details:** Dataset obtained from the Cancer Imaging Archive (USA) **Cancer type:** Lung cancer **Imaging technique:** CT scans	The best achievement was obtained via AlexNet with SGD-Drop architecture with an accuracy of 89.14 %. In the second experiment, the specified AlexNet model was utilized as a feature extractor. 1000 features describing the dataset were extracted from the last fully-connected layer of the model so as to apply as the input to machine learning classifiers. For all classifiers, 10-fold cross-validation method was used. The softmax classifier achieved the best success rate as 83.33 %. The deep models were superior to conventional machine learning models. In the third experiment, the image augmentation techniques were utilized during the training of the models. The number of the epoch was set to 150. The best success rate was provided by AlexNet with an accuracy of 83.04 %. In the fourth experiment, AlexNet model was reused with image augmentation techniques during the training. In this setup, the AlexNet was used as a feature extractor. The deep features were applied as the input to the classifiers. For all classifiers, 10-fold cross-validation method was used. The best success rate was provided by k NN classifier as the accuracy of 98.74 %. In the last experiment, the dimension of the feature set obtained using image augmentation techniques was reduced using the PCA before the classification task. Then, k NN classifier was fed with the reduced feature set. As a result, the accuracy of 97.92 % was achieved. Then, using the mRMR algorithm with the 1000 features obtained from the fc8 layer of AlexNet architecture. 33, 50, 100, 150 and 200 most efficient features were determined and ranked, respectively. The extracted features were re-classified with the k NN classifier. It is seen that PCA decreases the classification accuracy from 98.74%–97.92 %. The PCA method obtained this success with only 33 features. However, the PCA	

Citation (Country)	Study Details	Participants & setting	Key findings	Observations/notes
			method consumed less time for the training of the model using fewer features. In addition, the performance results of the k NN classifier with and without PCA method were found as rather close. Then, the most efficient features were selected by the mRMR method of 1000 features obtained from the last layer of AlexNet without using the PCA method. The best success of rate was obtained as 99.51% with 200 features provided by mRMR. It is seen that the 100, 150 and 200 features obtained from the mRMR algorithm were more successful than the 1000 features obtained from the fc8 layer of AlexNet. After this point, the experiment was extended by focusing on the k NN classifier. The model achieved an accuracy of 99.51 %, sensitivity of 99.32 %, specificity of 99.71 % and F-score of 99.51 %. In summary, the combination of data augmentation techniques, the deep features provided by AlexNet, the mRMR feature selection method and the k NN classifier ensure a robust and high sensitivity diagnosis model for lung cancer detection using chest CT images. The overall model accuracy was improved from 89.14%–99.51 %.	
Ueda et al (2021). Artificial intelligence-supported lung cancer detection by multi-institutional readers with multi-vendor chest radiographs: a retrospective clinical	**Study Design:** Retrospective clinical validation study **Intervention:** The AI-based CAD used in this study is EIRL Chest X-ray Lung nodule (LPIXEL Inc.), commercially available in Japan as of August 2020 **Comparator:** Human readers (Eighteen readers - nine general physicians and nine radiologists) **Study aim:** To investigate the performance improvement of	**Sample size:** A total of 312 radiographs (59 malignant radiographs from 59 patients and 253 non-malignant radiographs from 253 patients) **Participants:** The eligibility criteria for the radiographs were Mass lesions larger than 30 mm in size were excluded. **Dataset details:** Dataset obtained from at Osaka City University Hospital **Cancer type:** Lung cancer **Imaging technique:** X-ray	**Primary Findings:** **The deep learning-based computer-assisted detection model performance** The standalone CAD sensitivity, specificity, accuracy, PPV, and NPV were 0.66 (0.53–0.78), 0.96 (0.92–0.98), 0.90 (0.86–0.93), 0.78 (0.64–0.88), and 0.92 (0.88–0.95) with mFPI of 0.05, respectively. **Reader performance test** All readers improved their overall performance by referring to the CAD output. The overall increases due to using the CAD for sensitivity, specificity, accuracy, PPV, and NPV were 1.22 (1.14–1.30), 1.00 (1.00–1.01), 1.03 (1.02–1.04), 1.07 (1.03–	The readers were double blinded (did not know the ratio of malignant to normal cases, and clinical information regarding the radiographs was not made available to them)

Citation (Country)	Study Details	Participants & setting	Key findings	Observations/notes
validation study. BMC cancer, 21, pp.1-8. (Japan)	physicians with varying levels of chest radiology experience when using a commercially available AI-based computer-assisted detection (CAD) software to detect lung cancer nodules on chest radiographs from multiple vendors **Data collection methods and dates:** Chest radiographs with lung cancers were consecutively collected from patients who had been subsequently surgically diagnosed with lung cancer between July 2017 and June 2018 **Outcomes reported:** - Diagnostic performance		1.11), and 1.02 (1.01–1.03), respectively. General physicians benefited more from the use of the CAD than radiologists did. The performance of general physicians was improved from 0.47 to 0.60 for sensitivity, from 0.96 to 0.97 for specificity, from 0.87 to 0.90 for accuracy, from 0.75 to 0.82 for PPV, and from 0.89 to 0.91 for NPV while the performance of radiologists was improved from 0.51 to 0.60 for sensitivity, from 0.96 to 0.96 for specificity, from 0.87 to 0.90 for accuracy, from 0.76 to 0.80 for PPV, and from 0.89 to 0.91 for NPV. The rate of improvement was particularly high for general physicians. General physicians were more likely to change their assessment from FN to TP by referencing correct positive CAD output (68 times (0.59) in general physicians, 49 (0.49) in radiologists) and from FP to TN by correct negative CAD output (29 times (0.36) in general physicians, 24 times (0.29) in radiologists). The less experienced the reader was, the higher the rate of sensitivity improvement. Conversely, the more experienced the readers were, the more limited the support capabilities of the CAD were. Radiologists were less likely to change their opinion than general physicians, and it was more difficult for radiologists to change their decisions from FP to TN (24 times) than from FN to TP (49 times). Results show an instance in which a physician mistakenly changed their decision from TP to FN due to the FN output of the CAD.	
Wataya et al (2023). Radiologists with and without deep learning–based computer-	**Study Design:** Retrospective **Intervention:** Human + Previously developed AI model pulmonary nodule CAD system attached to SYNAPSE SAI Viewer V1.4 (FUJIFILM Corporation).	**Sample size:** 101 patients with 101 nodules/masses **Participants:** nodules/masses with the following characteristics were included: undistorted by other pulmonary conditions, 6–70 mm in size, absence of other abnormalities in the slices around the	**Primary Findings:** **Performance of the radiologists in characterizing and diagnosing the nodules/masses with and without CAD** The AUCs for ill-defined boundary, irregular margin, irregular shape, calcification, pleural contact, and malignancy in all 15 radiologists,	The readers were blinded to the patients' clinical backgrounds, age, and sex The authors of this manuscript declare relationships with the

Citation (Country)	Study Details	Participants & setting	Key findings	Observations/notes
aided diagnosis: comparison of performance and interobserver agreement for characterizing and diagnosing pulmonary nodules/masses. European Radiology, 33(1), pp.348-359. (Japan)	**Comparator:** Human (15 radiologists) **Study aim:** To compare the performance of radiologists in characterizing and diagnosing pulmonary nodules/masses with and without deep learning (DL)–based computer-aided diagnosis (CAD). **Data collection methods and dates:** CT performed between January and March 2018 **Outcomes reported:** - Diagnostic performance - Median assessment time	nodules/masses that may facilitate the diagnosis, and clinically or pathologically determined to be benign or malignant. **Dataset details:** Dataset obtained from Osaka University Hospital **Cancer type:** Lung cancer **Imaging technique:** CT scans	irregular margin and irregular shape in L and ill-defined boundary and irregular margin in M improved significantly ($p < 0.05$); no significant improvements were found in H. L showed the greatest increase in the AUC for malignancy (not significant). **Interobserver agreement on the characterization and diagnosis with and without CAD** Intraclass correlation coefficients (ICC) improved with CAD for all items, except for lobular shape in M and malignancy in H. In L&M&H, the ICC improved from a moderate correlation to a good correlation with CAD in three items: irregular margin [from 0.68 to 0.74 with CAD], irregular shape [from 0.61 to 0.71], and calcification [from 0.69 to 0.76]), whereas it showed a good correlation both with and without CAD in ground-glass opacity (from 0.82 to 0.87) and pleural contact (from 0.74 to 0.79). A poor correlation was found both with and without CAD in lobular shape (from 0.42 to 0.47) and pleural indentation (from 0.47 to 0.58). In L, when focused on the items with significant increases in the AUC, the ICC for ill-defined boundary achieved a good correlation with CAD (from 0.65 to 0.72), and the correlation of irregular shape with CAD improved from poor to moderate (from 0.49 to 0.62). Similarly, in M, the ICC for ill-defined boundary achieved a good correlation with CAD (from 0.61 to 0.73) and irregular margin (from 0.71 to 0.75) maintained a good correlation with CAD. **Comparison of reading time** The median assessment time among the 15 radiologists significantly decreased from 83.6 ± 21.9s to 69.9 ± 29.1s with CAD ($p= 0.01$), although decreases in the individual groups were not statistically significant (L: from 79.5 ± 8.2s to 64.8 ± 19.8s, $p =0.31$, M: from 91.8 ± 30.2s to	following company: FUJIFILM Corporation (who developed the AI model)

Citation (Country)	Study Details	Participants & setting	Key findings	Observations/notes
			78.6 ± 34.9s, p =0.13, and H: from 79.4 ± 19.0s to 66.2 ± 28.4s, p= 0.31). No statistical significance was observed in the range of the decrease among groups (L vs. M: p = 0.84; M vs. H: p = 1.00; L vs. H: p= 1.00). Regarding the assessment time for each radiologist, it was prolonged by CAD only for three of the 15 radiologists, and the maximum rate of prolongation was limited to 18.1% (from 83 s without CAD to 98 s with CAD). Among the 12 radiologists with shortened assessment time, the maximum rate of shortening was 50.0% (from 80 to 40s).	

7.3 Quality appraisal

Table 7. Quality appraisal results

Study	Test	Risk of bias (QUADAS-2)				Applicability concerns (QUADAS-2)			Risk of bias (QUADAS-C)			
		P	I	R	FT	P	I	R	P	I	R	FT
Akatsuka, 2019	Human	?	✓	✓	✓	✓	✓	✓	?	?	✓	✓
	AI	?	✓	✓	✓	✓	✓	✓				
Baldwin, 2020	Brock	?	✓	✓	✓	✓	✓	✓	?	?	✓	✓
	AI	?	✓	✓	✓	✓	✓	✓				
Faiella, 2022	Expert	?	?	✓	✓	✓	✓	✓	?	?	✓	✓
	Human with AI	?	?	✓	✓	✓	✓	✓				
Fujioka, 2021	Human	✓	✗	✓	✓	✓	?	✓	✓	✗	✓	✓
	AI	✓	✗	✓	✓	✓	?	✓				
Goto, 2023	Human	✓	?	✓	✓	✓	✓	✓	✓	?	✓	✓
	AI	✓	✓	✓	✓	✓	✓	✓				
Jacobs, 2021	Human	✗	?	✓	✓	✓	✓	✓	✗	?	✓	✓
	AI	✗	?	✓	✓	✓	✓	✓				
Lo Gullo 2020	Human	✓	✓	✓	✓	✓	✓	✓	✓	✓	✓	✓
	AI	✓	✓	✓	✓	✓	✓	✓				
Maldonado, 2021	Brock	✓	✓	✓	✓	✓	✓	✓	✓	✓	✓	✓
	AI	✓	✓	✓	✓	✓	✓	✓				
O'Connell, 2022	Human	?	?	✓	✗	✓	✓	✓	?	✗	✓	✗
	AI	?	?	✓	✗	✓	✓	✓				
Tong, 2023	Human	✓	✓	✓	✓	✓	✓	✓	✓	✓	✓	✓
	AI	✓	✓	✓	✓	✓	✓	✓				
Uhlig, 2018	Human	?	✓	✓	✓	✓	✓	✓	?	?	✓	✓
	AI	?	✓	✓	✓	✓	✓	✓				
Arslan, 2023	Human	✓	?	✓	✓	✓	✓	✓	✓	?	✓	✓
	Human with AI	✓	?	✓	✓	✓	✓	✓				
Calisto, 2022	Human	?	?	✓	✓	✓	✓	✓	?	?	✓	✓
	Human with AI	?	?	✓	✓	✓	✓	✓				
Forookhi, 2023	Human	✓	✓	✓	✓	✓	✓	✓	✓	✓	✓	?
	Human with AI	✓	✓	✓	✓	✓	✓	✓				
Heller, 2021	Human	✓	✓	✓	✓	✓	✓	✓	✓	?	✓	✓
	Human with AI	✓	✓	✓	✓	✓	✓	✓				
Jiang, 2021	Human with CAE	✗	?	✓	✓	✓	✓	✓	✗	✗	✓	?
	Human with AI	✗	?	✓	✓	✓	✓	✓				
Mango, 2020	Human	?	?	✓	✓	✓	✓	✓	?	✗	✓	✓
	Human with AI	?	?	✓	✓	✓	✓	✓				
Pacilè , 2020	Human	✗	✗	✓	✓	✓	✓	✓	✗	✗	✓	✓
	Human with AI	✗	✗	✓	✓	✓	✓	✓				
Pinto, 2021	Human	✗	✗	✓	✓	✓	✓	✓	✗	✗	✓	✓
	Human with AI	✗	✗	✓	✓	✓	✓	✓				
Tam, 2021	Human	✗	✓	✓	✓	✓	✓	✓	✗	?	✓	✓
	Human with AI	✗	✓	✓	✓	✓	✓	✓				
Ueda, 2021	Human	?	✓	✓	✓	✓	✓	✓	?	?	✓	✓
	Human with AI	?	✓	✓	✓	✓	✓	✓				
Van Zelst, 2020	Human	✗	?	✓	✓	✓	✓	✓	✗	?	✓	✓
	Human with AI	✗	?	✓	✓	✓	✓	✓				
Wataya, 2023	Human	✗	?	✓	✓	✓	✓	✓	✗	✗	✓	✓
	Human with AI	✗	?	✓	✓	✓	✓	✓				
Zhang, 2022	Human	✓	✓	✓	✓	✓	✓	✓	✓	?	✓	✓
	Human with AI	✓	✓	✓	✓	✓	✓	✓				
Patsanis, 2023	AI	?	?	✓	✓	✓	✓	✓	?	?	✓	✓
	AI	?	?	✓	✓	✓	✓	✓				
Toğaçar, 2020	AI	?	?	✓	✓	✓	✓	✓	?	?	✓	✓
	AI	?	?	✓	✓	✓	✓	✓				
Tsochatzidis, 2019	AI	?	?	?	?	?	✓	?	?	✗	?	?
	AI	?	?	?	?	?	✓	?				
Vamvakas, 2022	AI	?	?	✓	✓	✓	✓	✓	?	?	✓	✓
	AI	?	?	✓	✓	✓	✓	✓				

P = patient selection; I = index test; R = reference standard; FT = flow and timing.
✓ indicates low risk; ✗ indicates high risk; ? indicates unclear risk.

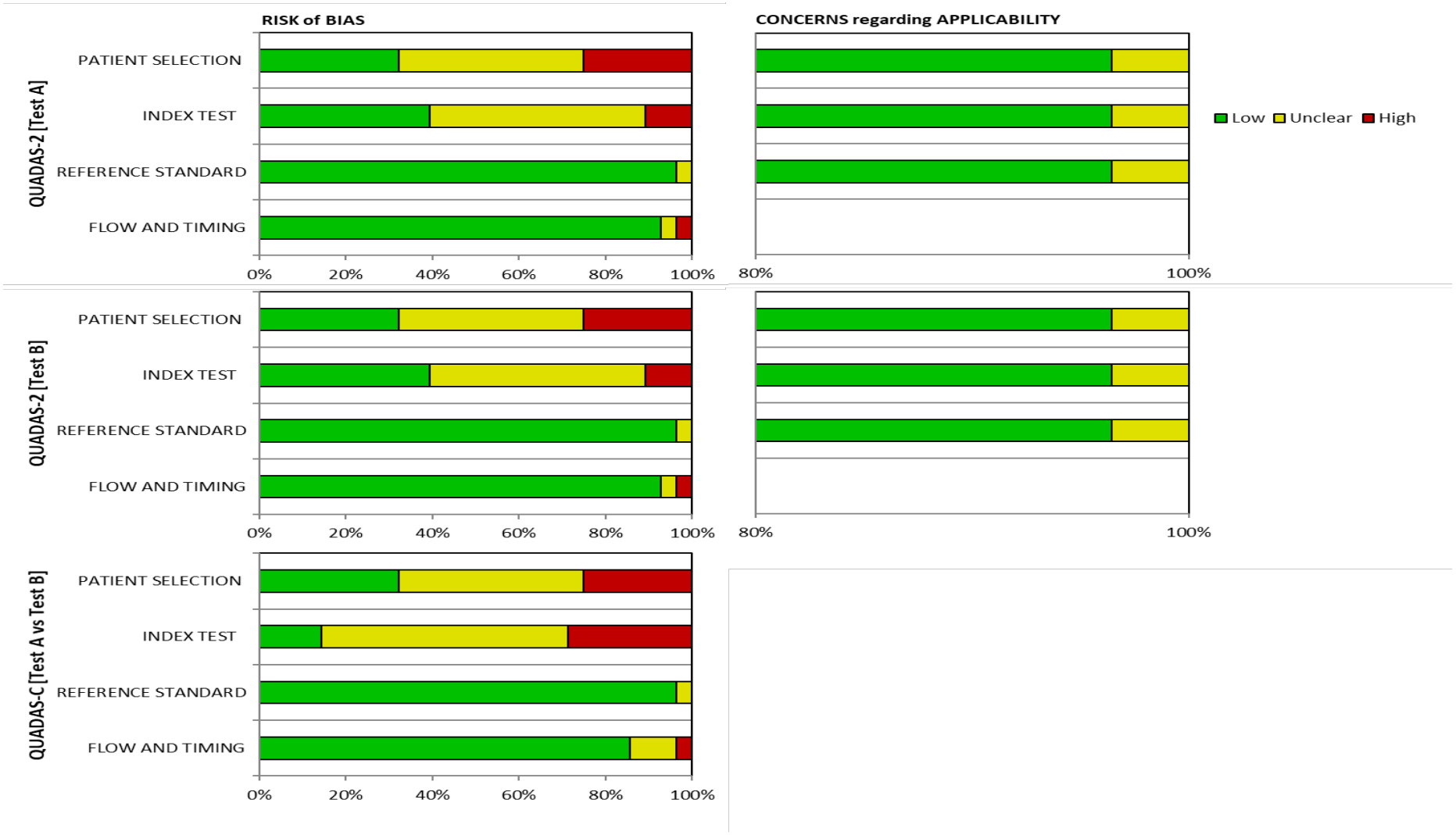

Figure 1. Graphical display of quality appraisal results for studies included in the synthesis of the rapid review

7.4 Information available on request

The following are available on request: protocol; search strategies for Embase, CENTRAL and ScanMedicine.

8. ADDITIONAL INFORMATION

8.1 Conflicts of interest

The review team declares no conflicts of interest.

8.2 Acknowledgements

The Public Health Wales team would like to thank James Triscott, Gareth Ashman, Delyth James, Josie Jackson, Rebecca Andrews, Christopher Rolls, David Jarrom, Anthony Cope, and Robert Hall for their time, expertise and contributions during stakeholder meetings in guiding the focus of the review and interpretation of findings.

9. APPENDIX

APPENDIX 1: Reference list for studies included in the map

Breast

1. Adachi, M., Fujioka, T., Mori, M., Kubota, K., Kikuchi, Y., Xiaotong, W., Oyama, J., Kimura, K., Oda, G., Nakagawa, T., Uetake, H. and Tateishi, U. (2020) 'Detection and Diagnosis of Breast Cancer Using Artificial Intelligence Based assessment of Maximum Intensity Projection Dynamic Contrast-Enhanced Magnetic Resonance Images', Diagnostics, 10(5), pp. 20.
2. Barinov, L., Jairaj, A., Becker, M., Seymour, S., Lee, E., Schram, A., Lane, E., Goldszal, A., Quigley, D. and Paster, L. (2019) 'Impact of Data Presentation on Physician Performance Utilizing Artificial Intelligence-Based Computer-Aided Diagnosis and Decision Support Systems', Journal of Digital Imaging, 32(3), pp. 408-416.
3. Bhowmik, A., Monga, N., Belen, K., Varela, K., Sevilimedu, V., Thakur, S. B., Martinez, D. F., Sutton, E. J., Pinker, K. and Eskreis-Winkler, S. (2023) 'Automated Triage of Screening Breast MRI Examinations in High-Risk Women Using an Ensemble Deep Learning Model', Investigative radiology., 12.
4. Caballo, M., Hernandez, A. M., Lyu, S. H., Teuwen, J., Mann, R. M., van Ginneken, B., Boone, J. M. and Sechopoulos, I. (2021) 'Computer-aided diagnosis of masses in breast computed tomography imaging: deep learning model with combined handcrafted and convolutional radiomic features', Journal of Medical Imaging, 8(2), pp. 024501.
5. Calisto, F. M., Santiago, C., Nunes, N. and Nascimento, J. C. (2022) 'BreastScreening-AI: Evaluating medical intelligent agents for human-AI interactions', Artificial Intelligence in Medicine, 127.
6. Fujioka, T., Katsuta, L., Kubota, K., Mori, M., Kikuchi, Y., Kato, A., Oda, G., Nakagawa, T., Kitazume, Y. and Tateishi, U. (2020) 'Classification of Breast Masses on Ultrasound Shear Wave Elastography using Convolutional Neural Networks', Ultrasonic Imaging, 42(4), pp. 213-220.
7. Fujioka, T., Kubota, K., Mori, M., Kikuchi, Y., Katsuta, L., Kasahara, M., Oda, G., Ishiba, T., Nakagawa, T. and Tateishi, U. (2019) 'Distinction between benign and malignant breast masses at breast ultrasound using deep learning method with convolutional neural network', Japanese Journal of Radiology, 37(6), pp. 466-472.
8. Fujioka, T., Yashima, Y., Oyama, J., Mori, M., Kubota, K., Katsuta, L., Kimura, K., Yamaga, E., Oda, G., Nakagawa, T., Kitazume, Y. and Tateishi, U. (2021) 'Deep-learning approach with convolutional neural network for classification of maximum intensity projections of dynamic contrast-enhanced breast magnetic resonance imaging', Magnetic Resonance Imaging, 75, pp. 1-8.
9. Gheflati, B. and Rivaz, H. (2022) 'Vision Transformers for Classification of Breast Ultrasound Images', Annual International Conference Of The IEEE Engineering In Medicine And Biology Society, 2022, pp. 480-483.
10. Goto, M., Sakai, K., Toyama, Y., Nakai, Y. and Yamada, K. (2023) 'Use of a deep learning algorithm for non-mass enhancement on breast MRI: comparison with radiologists' interpretations at various levels', Japanese Journal of Radiology, 18, pp. 18.

11. Hayashida, T., Odani, E., Kikuchi, M., Nagayama, A., Seki, T., Takahashi, M., Futatsugi, N., Matsumoto, A., Murata, T., Watanuki, R., Yokoe, T., Nakashoji, A., Maeda, H., Onishi, T., Asaga, S., Hojo, T., Jinno, H., Sotome, K., Matsui, A., Suto, A., Imoto, S. and Kitagawa, Y. (2022) 'Establishment of a deep-learning system to diagnose BI-RADS4a or higher using breast ultrasound for clinical application', Cancer Science, 113(10), pp. 3528-3534.
12. Hejduk, P., Marcon, M., Unkelbach, J., Ciritsis, A., Rossi, C., Borkowski, K. and Boss, A. (2022) 'Fully automatic classification of automated breast ultrasound (ABUS) imaging according to BI-RADS using a deep convolutional neural network', European Radiology, 32(7), pp. 4868-4878.
13. Heller, S. L., Wegener, M., Babb, J. S. and Gao, Y. (2020) 'Can an Artificial Intelligence Decision Aid Decrease False-Positive Breast Biopsies?', Ultrasound Quarterly, 37(1), pp. 10-15.
14. Hoffmann, R., Reich, C. and Skerl, K. (2022) 'Evaluating different combination methods to analyse ultrasound and shear wave elastography images automatically through discriminative convolutional neural network in breast cancer imaging', International Journal of Computer Assisted Radiology & Surgery, 17(12), pp. 2231-2237.
15. Interlenghi, M., Salvatore, C., Magni, V., Caldara, G., Schiavon, E., Cozzi, A., Schiaffino, S., Carbonaro, L. A., Castiglioni, I. and Sardanelli, F. (2022) 'A Machine Learning Ensemble Based on Radiomics to Predict BI-RADS Category and Reduce the Biopsy Rate of Ultrasound-Detected Suspicious Breast Masses', Diagnostics, 12.
16. Jiang, Y., Edwards, A. V. and Newstead, G. M. (2021) 'Artificial Intelligence Applied to Breast MRI for Improved Diagnosis', Radiology, 298(1), pp. 38-46.
17. Jing, X., Dorrius, M. D., Wielema, M., Sijens, P. E., Oudkerk, M. and van Ooijen, P. (2022) 'Breast Tumor Identification in Ultrafast MRI Using Temporal and Spatial Information', Cancers, 14.
18. Lo Gullo, R., Daimiel, I., Rossi Saccarelli, C., Bitencourt, A., Gibbs, P., Fox, M. J., Thakur, S. B., Martinez, D. F., Jochelson, M. S., Morris, E. A. and Pinker, K. (2020) 'Improved characterization of sub-centimeter enhancing breast masses on MRI with radiomics and machine learning in BRCA mutation carriers', European Radiology, 30(12), pp. 6721-6731.
19. Makrogiannis, S., Zheng, K. and Harris, C. (2021) 'Discriminative Localized Sparse Approximations for Mass Characterization in Mammograms', Frontiers in Oncology, 11, pp. 725320.
20. Mango, V. L., Sun, M., Wynn, R. T. and Ha, R. (2020) 'Should We Ignore, Follow, or Biopsy? Impact of Artificial Intelligence Decision Support on Breast Ultrasound Lesion Assessment', AJR. American Journal of Roentgenology, 214(6), pp. 1445-1452.
21. Naranjo, I. D., Gibbs, P., Reiner, J. S., Gullo, R. L., Thakur, S. B., Jochelson, M. S., Thakur, N., Baltzer, P. A. T., Helbich, T. H. and Pinker, K. (2022) 'Breast Lesion Classification with Multiparametric Breast MRI Using Radiomics and Machine Learning: A Comparison with Radiologists' Performance', Cancers, 14.
22. O'Connell, A. M., Bartolotta, T. V., Orlando, A., Jung, S. H., Baek, J. and Parker, K. J. (2022) 'Diagnostic Performance of an Artificial Intelligence System in Breast Ultrasound', Journal of Ultrasound in Medicine, 41(1), pp. 97-105.

23. Pacile, S., Lopez, J., Chone, P., Bertinotti, T., Grouin, J. M. and Fillard, P. (2020) 'Improving Breast Cancer Detection Accuracy of Mammography with the Concurrent Use of an Artificial Intelligence Tool', Radiology Artificial intelligence, 2(6), pp. e190208.
24. Patel, B. K., Ranjbar, S., Wu, T., Pockaj, B. A., Li, J., Zhang, N., Lobbes, M., Zhang, B. and Mitchell, J. R. (2018) 'Computer-aided diagnosis of contrast-enhanced spectral mammography: A feasibility study', European Journal of Radiology, 98, pp. 207-213.
25. Pfob, A., Sidey-Gibbons, C., Barr, R. G., Duda, V., Alwafai, Z., Balleyguier, C., Clevert, D. A., Fastner, S., Gomez, C., Goncalo, M., Gruber, I., Hahn, M., Hennigs, A., Kapetas, P., Lu, S. C., Nees, J., Ohlinger, R., Riedel, F., Rutten, M., Schaefgen, B., Schuessler, M., Stieber, A., Togawa, R., Tozaki, M., Wojcinski, S., Xu, C., Rauch, G., Heil, J. and Golatta, M. (2022) 'The importance of multi-modal imaging and clinical information for humans and AI-based algorithms to classify breast masses (INSPiRED 003): an international, multicenter analysis', European Radiology, 32(6), pp. 4101-4115.
26. Pinto, M. C., Rodriguez-Ruiz, A., Pedersen, K., Hofvind, S., Wicklein, J., Kappler, S., Mann, R. M. and Sechopoulos, I. (2021) 'Impact of Artificial Intelligence Decision Support Using Deep Learning on Breast Cancer Screening Interpretation with Single-View Wide-Angle Digital Breast Tomosynthesis', Radiology, 300(3), pp. 529-536.
27. Romeo, V., Clauser, P., Rasul, S., Kapetas, P., Gibbs, P., Baltzer, P. A. T., Hacker, M., Woitek, R., Helbich, T. H. and Pinker, K. (2022) 'AI-enhanced simultaneous multiparametric 18F-FDG PET/MRI for accurate breast cancer diagnosis', European Journal of Nuclear Medicine & Molecular Imaging, 49(2), pp. 596-608.
28. Romeo, V., Cuocolo, R., Apolito, R., Stanzione, A., Ventimiglia, A., Vitale, A., Verde, F., Accurso, A., Amitrano, M., Insabato, L., Gencarelli, A., Buonocore, R., Argenzio, M. R., Cascone, A. M., Imbriaco, M., Maurea, S. and Brunetti, A. (2021) 'Clinical value of radiomics and machine learning in breast ultrasound: a multicenter study for differential diagnosis of benign and malignant lesions', European Radiology, 31(12), pp. 9511-9519.
29. Sabani, A., Landsmann, A., Hejduk, P., Schmidt, C., Marcon, M., Borkowski, K., Rossi, C., Ciritsis, A. and Boss, A. (2022) 'BI-RADS-Based Classification of Mammographic Soft Tissue Opacities Using a Deep Convolutional Neural Network', Diagnostics, 12(7), pp. 28.
30. Takahashi, K., Fujioka, T., Oyama, J., Mori, M., Yamaga, E., Yashima, Y., Imokawa, T., Hayashi, A., Kujiraoka, Y., Tsuchiya, J., Oda, G., Nakagawa, T. and Tateishi, U. (2022) 'Deep Learning Using Multiple Degrees of Maximum-Intensity Projection for PET/CT Image Classification in Breast Cancer', Tomography, 8(1), pp. 131-141.
31. Tanaka, H., Chiu, S. W., Watanabe, T., Kaoku, S. and Yamaguchi, T. (2019) 'Computer-aided diagnosis system for breast ultrasound images using deep learning', Physics in Medicine & Biology, 64(23), pp. 235013.
32. Toprak, A. (2018) 'Extreme Learning Machine (ELM)-Based Classification of Benign and Malignant Cells in Breast Cancer', Medical Science Monitor, 24, pp. 6537-6543.
33. Truhn, D., Schrading, S., Haarburger, C., Schneider, H., Merhof, D. and Kuhl, C. (2019) 'Radiomic versus Convolutional Neural Networks Analysis for

Classification of Contrast-enhancing Lesions at Multiparametric Breast MRI', Radiology, 290(2), pp. 290-297.
34. Tsochatzidis, L., Costaridou, L. and Pratikakis, I. (2019) 'Deep Learning for Breast Cancer Diagnosis from Mammograms-A Comparative Study', Journal of Imaging, 5(3), pp. 13.
35. Uhlig, J., Uhlig, A., Kunze, M., Beissbarth, T., Fischer, U., Lotz, J. and Wienbeck, S. (2018) 'Novel Breast Imaging and Machine Learning: Predicting Breast Lesion Malignancy at Cone-Beam CT Using Machine Learning Techniques', AJR. American Journal of Roentgenology, 211(2), pp. W123-W131.
36. Vamvakas, A., Tsivaka, D., Logothetis, A., Vassiou, K. and Tsougos, I. (2022) 'Breast Cancer Classification on Multiparametric MRI - Increased Performance of Boosting Ensemble Methods', Technology in Cancer Research & Treatment, 21, pp. 15330338221087828.
37. van Zelst, J. C., Tan, T., Mann, R. M. and Karssemeijer, N. (2020) 'Validation of radiologists' findings by computer-aided detection (CAD) software in breast cancer detection with automated 3D breast ultrasound: a concept study in implementation of artificial intelligence software', Acta Radiologica, 61(3), pp. 312-320.
38. Wang, K., Patel, B. K., Wang, L., Wu, T., Zheng, B. and Li, J. (2019) 'A dual-mode deep transfer learning (D2TL) system for breast cancer detection using contrast enhanced digital mammograms', IISE Transactions on Healthcare Systems Engineering, 9, pp. 357-370.
39. Wu, N., Phang, J., Park, J., Shen, Y., Huang, Z., Zorin, M., Jastrzebski, S., Fevry, T., Katsnelson, J., Kim, E., Wolfson, S., Parikh, U., Gaddam, S., Lin, L. L. Y., Ho, K., Weinstein, J. D., Reig, B., Gao, Y., Toth, H., Pysarenko, K., Lewin, A., Lee, J., Airola, K., Mema, E., Chung, S., Hwang, E., Samreen, N., Kim, S. G., Heacock, L., Moy, L., Cho, K. and Geras, K. J. (2020) 'Deep Neural Networks Improve Radiologists' Performance in Breast Cancer Screening', IEEE Transactions on Medical Imaging, 39(4), pp. 1184-1194.
40. Yang, K., Suzuki, A., Ye, J., Nosato, H., Izumori, A. and Sakanashi, H. (2022) 'CTG-Net: Cross-task guided network for breast ultrasound diagnosis', PLoS ONE [Electronic Resource], 17(8), pp. e0271106.

Gynaecological

1. Christiansen, F., Epstein, E. L., Smedberg, E., Akerlund, M., Smith, K. and Epstein, E. (2021) 'Ultrasound image analysis using deep neural networks for discriminating between benign and malignant ovarian tumors: comparison with expert subjective assessment', *Ultrasound in Obstetrics & Gynecology,* 57(1), pp. 155-163.
2. Nakagawa, M., Nakaura, T., Namimoto, T., Iyama, Y., Kidoh, M., Hirata, K., Nagayama, Y., Oda, S., Sakamoto, F., Shiraishi, S. and Yamashita, Y. (2019) 'A multiparametric MRI-based machine learning to distinguish between uterine sarcoma and benign leiomyoma: comparison with 18F-FDG PET/CT', *Clinical Radiology,* 74(2), pp. 167.e1-167.e7.
3. Nakagawa, M., Nakaura, T., Namimoto, T., Iyama, Y., Kidoh, M., Hirata, K., Nagayama, Y., Yuki, H., Oda, S., Utsunomiya, D. and Yamashita, Y. (2019) 'Machine Learning to Differentiate T2-Weighted Hyperintense Uterine Leiomyomas from Uterine Sarcomas by Utilizing Multiparametric Magnetic

Resonance Quantitative Imaging Features', *Academic Radiology,* 26(10), pp. 1390-1399.
4. Saida, T., Mori, K., Hoshiai, S., Sakai, M., Urushibara, A., Ishiguro, T., Minami, M., Satoh, T. and Nakajima, T. (2022) 'Diagnosing Ovarian Cancer on MRI: A Preliminary Study Comparing Deep Learning and Radiologist Assessments', *Cancers,* 14(4), pp. 16.
5. Toyohara, Y., Sone, K., Noda, K., Yoshida, K., Kurokawa, R., Tanishima, T., Kato, S., Inui, S., Nakai, Y., Ishida, M., Gonoi, W., Tanimoto, S., Takahashi, Y., Inoue, F., Kukita, A., Kawata, Y., Taguchi, A., Furusawa, A., Miyamoto, Y., Tsukazaki, T., Tanikawa, M., Iriyama, T., Mori-Uchino, M., Tsuruga, T., Oda, K., Yasugi, T., Takechi, K., Abe, O. and Osuga, Y. (2022) 'Development of a deep learning method for improving diagnostic accuracy for uterine sarcoma cases', *Scientific Reports,* 12(1), pp. 19612.
6. Urushibara, A., Saida, T., Mori, K., Ishiguro, T., Inoue, K., Masumoto, T., Satoh, T. and Nakajima, T. (2022) 'The efficacy of deep learning models in the diagnosis of endometrial cancer using MRI: a comparison with radiologists', *BMC Medical Imaging,* 22(1), pp. 80.
7. Urushibara, A., Saida, T., Mori, K., Ishiguro, T., Sakai, M., Masuoka, S., Satoh, T. and Masumoto, T. (2021) 'Diagnosing uterine cervical cancer on a single T2-weighted image: Comparison between deep learning versus radiologists', *European Journal of Radiology,* 135.

Lung

1. Astaraki, M., Yang, G., Zakko, Y., Toma-Dasu, I., Smedby, O. and Wang, C. (2021) 'A Comparative Study of Radiomics and Deep-Learning Based Methods for Pulmonary Nodule Malignancy Prediction in Low Dose CT Images', Frontiers in Oncology, 11.
2. Baldwin, D. R., Gustafson, J., Pickup, L., Arteta, C., Novotny, P., Declerck, J., Kadir, T., Figueiras, C., Sterba, A., Exell, A., Potesil, V., Holland, P., Spence, H., Clubley, A., O'Dowd, E., Clark, M., Ashford-Turner, V., Callister, M. E. and Gleeson, F. V. (2020) 'External validation of a convolutional neural network artificial intelligence tool to predict malignancy in pulmonary nodules', Thorax., 5.
3. Gursoy Coruh, A., Yenigun, B., Uzun, C., Kahya, Y., Buyukceran, E. U., Elhan, A., Orhan, K. and Kayi Cangir, A. (2021) 'A comparison of the fusion model of deep learning neural networks with human observation for lung nodule detection and classification', British Journal of Radiology, 94(1123), pp. 20210222.
4. Hunter, B., Chen, M., Ratnakumar, P., Alemu, E., Logan, A., Linton-Reid, K., Tong, D., Senthivel, N., Bhamani, A., Bloch, S., Kemp, S. V., Boddy, L., Jain, S., Gareeboo, S., Rawal, B., Doran, S., Navani, N., Nair, A., Bunce, C., Kaye, S., Blackledge, M., Aboagye, E. O., Devaraj, A. and Lee, R. W. (2022) 'A radiomics-based decision support tool improves lung cancer diagnosis in combination with the Herder score in large lung nodules', EBioMedicine, 86, pp. 104344.
5. Jacobs, C., Setio, A. A. A., Scholten, E. T., Gerke, P. K., Bhattacharya, H., Hoesein, F. A. M., Brink, M., Ranschaert, E., de Jong, P. A., Silva, M., Geurts, B., Chung, K., Schalekamp, S., Meersschaert, J., Devaraj, A., Pinsky, P. F., Lam, S. C., van Ginneken, B. and Farahani, K. (2021) 'Deep learning for lung cancer detection on screening ct scans: Results of a large-scale public

competition and an observer study with 11 radiologists', Radiology: Artificial Intelligence, 3.
6. Kitajima, K., Matsuo, H., Kono, A., Kuribayashi, K., Kijima, T., Hashimoto, M., Hasegawa, S., Murakami, T. and Yamakado, K. (2021) 'Deep learning with deep convolutional neural network using FDG-PET/CT for malignant pleural mesothelioma diagnosis', Oncotarget, 12(12), pp. 1187-1196.
7. Maldonado, F., Varghese, C., Rajagopalan, S., Duan, F., Balar, A. B., Lakhani, D. A., Antic, S. L., Massion, P. P., Johnson, T. F., Karwoski, R. A., Robb, R. A., Bartholmai, B. J. and Peikert, T. (2021) 'Validation of the BRODERS classifier (Benign versus aggRessive nODule Evaluation using Radiomic Stratification), a novel HRCT-based radiomic classifier for indeterminate pulmonary nodules', European Respiratory Journal, 57(4), pp. 04.
8. Nishio, M., Nishizawa, M., Sugiyama, O., Kojima, R., Yakami, M., Kuroda, T. and Togashi, K. (2018) 'Computer-aided diagnosis of lung nodule using gradient tree boosting and Bayesian optimization', PLoS ONE [Electronic Resource], 13(4), pp. e0195875.
9. Sollini, M., Kirienko, M., Gozzi, N., Bruno, A., Torrisi, C., Balzarini, L., Voulaz, E., Alloisio, M. and Chiti, A. (2023) 'The Development of an Intelligent Agent to Detect and Non-Invasively Characterize Lung Lesions on CT Scans: Ready for the "Real World"?', Cancers, 15(2), pp. 05.
10. Tam, M., Dyer, T., Dissez, G., Morgan, T. N., Hughes, M., Illes, J., Rasalingham, R. and Rasalingham, S. (2021) 'Augmenting lung cancer diagnosis on chest radiographs: positioning artificial intelligence to improve radiologist performance', Clinical Radiology, 76(8), pp. 607-614.
11. Togacar, M., Ergen, B. and Comert, Z. (2020) 'Detection of lung cancer on chest CT images using minimum redundancy maximum relevance feature selection method with convolutional neural networks', Biocybernetics and Biomedical Engineering, 40, pp. 23-39.
12. Ueda, D., Yamamoto, A., Shimazaki, A., Walston, S. L., Matsumoto, T., Izumi, N., Tsukioka, T., Komatsu, H., Inoue, H., Kabata, D., Nishiyama, N. and Miki, Y. (2021) 'Artificial intelligence-supported lung cancer detection by multi-institutional readers with multi-vendor chest radiographs: a retrospective clinical validation study', BMC Cancer, 21(1), pp. 1120.
13. Wataya, T., Yanagawa, M., Tsubamoto, M., Sato, T., Nishigaki, D., Kita, K., Yamagata, K., Suzuki, Y., Hata, A., Kido, S. and Tomiyama, N. (2023) 'Radiologists with and without deep learning-based computer-aided diagnosis: comparison of performance and interobserver agreement for characterizing and diagnosing pulmonary nodules/masses', European Radiology, 33, pp. 348-359.
14. Zhang, Q. and Yoon, S. (2022) 'A novel self-adaptive convolutional neural network model using spatial pyramid pooling for 3D lung nodule computer-aided diagnosis', IISE Transactions on Healthcare Systems Engineering, 12, pp. 75-88.

Prostate

1. Akatsuka, J., Yamamoto, Y., Sekine, T., Numata, Y., Morikawa, H., Tsutsumi, K., Yanagi, M., Endo, Y., Takeda, H., Hayashi, T., Ueki, M., Tamiya, G., Maeda, I., Fukumoto, M., Shimizu, A., Tsuzuki, T., Kimura, G. and Kondo, Y.

(2019) 'Illuminating Clues of Cancer Buried in Prostate MR Image: Deep Learning and Expert Approaches', *Biomolecules,* 9(11), pp. 30.
2. Arslan, A., Alis, D., Erdemli, S., Seker, M. E., Zeybel, G., Sirolu, S., Kurtcan, S. and Karaarslan, E. (2023) 'Does deep learning software improve the consistency and performance of radiologists with various levels of experience in assessing bi-parametric prostate MRI?', *Insights into Imaging,* 14.
3. Bhattacharya, I., Seetharaman, A., Kunder, C., Shao, W., Chen, L. C., Soerensen, S. J. C., Wang, J. B., Teslovich, N. C., Fan, R. E., Ghanouni, P., Brooks, J. D., Sonn, G. A. and Rusu, M. (2022) 'Selective identification and localization of indolent and aggressive prostate cancers via CorrSigNIA: an MRI-pathology correlation and deep learning framework', *Medical Image Analysis,* 75, pp. 102288.
4. Bonekamp, D., Kohl, S., Wiesenfarth, M., Schelb, P., Radtke, J. P., Gotz, M., Kickingereder, P., Yaqubi, K., Hitthaler, B., Gahlert, N., Kuder, T. A., Deister, F., Freitag, M., Hohenfellner, M., Hadaschik, B. A., Schlemmer, H. P. and Maier-Hein, K. H. (2018) 'Radiomic Machine Learning for Characterization of Prostate Lesions with MRI: Comparison to ADC Values', *Radiology,* 289(1), pp. 128-137.
5. Faiella, E., Vertulli, D., Esperto, F., Cordelli, E., Soda, P., Muraca, R. M., Moramarco, L. P., Grasso, R. F., Beomonte Zobel, B. and Santucci, D. (2022) 'Quantib Prostate Compared to an Expert Radiologist for the Diagnosis of Prostate Cancer on mpMRI: A Single-Center Preliminary Study', *Tomography,* 8(4), pp. 2010-2019.
6. Forookhi, A., Laschena, L., Pecoraro, M., Borrelli, A., Massaro, M., Dehghanpour, A., Cipollari, S., Catalano, C. and Panebianco, V. (2023) 'Bridging the experience gap in prostate multiparametric magnetic resonance imaging using artificial intelligence: A prospective multi-reader comparison study on inter-reader agreement in PI-RADS v2.1, image quality and reporting time between novice and expert readers', *European Journal of Radiology,* 161, pp. 110749.
7. Gresser, E., Schachtner, B., Stuber, A. T., Solyanik, O., Schreier, A., Huber, T., Froelich, M. F., Magistro, G., Kretschmer, A., Stief, C., Ricke, J., Ingrisch, M. and Norenberg, D. (2022) 'Performance variability of radiomics machine learning models for the detection of clinically significant prostate cancer in heterogeneous MRI datasets', *Quantitative Imaging in Medicine and Surgery,* 12, pp. 4990-5003.
8. Hamm, C. A., Baumgartner, G. L., Biessmann, F., Beetz, N. L., Hartenstein, A., Savic, L. J., Frobose, K., Drager, F., Schallenberg, S., Rudolph, M., Baur, A. D. J., Hamm, B., Haas, M., Hofbauer, S., Cash, H. and Penzkofer, T. (2023) 'Interactive Explainable Deep Learning Model Informs Prostate Cancer Diagnosis at MRI', *Radiology,* 307(4), pp. e222276.
9. Hosseinzadeh, M., Saha, A., Brand, P., Slootweg, I., de Rooij, M. and Huisman, H. (2022) 'Deep learning-assisted prostate cancer detection on bi-parametric MRI: minimum training data size requirements and effect of prior knowledge', *European Radiology,* 32(4), pp. 2224-2234.
10. Patsanis, A., Sunoqrot, M. R. S., Langorgen, S., Wang, H., Selnaes, K. M., Bertilsson, H., Bathen, T. F. and Elcho, M. (2023) 'A comparison of Generative Adversarial Networks for automated prostate cancer detection on T2-weighted MRI', *Informatics in Medicine Unlocked,* 39.

11. Tong, A., Bagger, B., Patricelli, R., Amerika, P., VI, A., Qian, K., Grimm, R., Kaman, A., Keerthivasan, M. B., Nickel, M. D., von Busch, H. and Chandarana, H. (2023) 'Comparison of a Deep Learning-Accelerated vs. Conventional T2-Weighted Sequence in Biparametric MRI of the Prostate', *Journal of Magnetic Resonance Imaging.*
12. Zhang, K. S., Schelb, P., Netzer, N., Tavakoli, A. A., Keymling, M., Wehrse, E., Hog, R., Rotkopf, L. T., Wennmann, M., Glemser, P. A., Thierjung, H., von Knebel Doeberitz, N., Kleesiek, J., Gortz, M., Schutz, V., Hielscher, T., Stenzinger, A., Hohenfellner, M., Schlemmer, H. P., Maier-Hein, K. and Bonekamp, D. (2022) 'Pseudoprospective Paraclinical Interaction of Radiology Residents With a Deep Learning System for Prostate Cancer Detection: Experience, Performance, and Identification of the Need for Intermittent Recalibration', *Investigative Radiology,* 57(9), pp. 601-612.

Other cancer types

1. Ammari, S., Bone, A., Balleyguier, C., Moulton, E., Chouzenoux, E., Volk, A., Menu, Y., Bidault, F., Nicolas, F., Robert, P., Rohe, M. M. and Lassau, N. (2022) 'Can Deep Learning Replace Gadolinium in Neuro-Oncology?: A Reader Study', *Investigative Radiology,* 57(2), pp. 99-107.
2. Anai, K., Hayashida, Y., Ueda, I., Hozuki, E., Yoshimatsu, Y., Tsukamoto, J., Hamamura, T., Onari, N., Aoki, T. and Korogi, Y. (2022) 'The effect of CT texture-based analysis using machine learning approaches on radiologists' performance in differentiating focal-type autoimmune pancreatitis and pancreatic duct carcinoma', *Japanese Journal of Radiology,* 40(11), pp. 1156-1165.
3. Erdim, C., Yardimci, A. H., Bektas, C. T., Kocak, B., Koca, S. B., Demir, H. and Kilickesmez, O. (2020) 'Prediction of Benign and Malignant Solid Renal Masses: Machine Learning-Based CT Texture Analysis', *Academic Radiology,* 27(10), pp. 1422-1429.
4. Malinauskaite, I., Hofmeister, J., Burgermeister, S., Neroladaki, A., Hamard, M., Montet, X. and Boudabbous, S. (2020) 'Radiomics and Machine Learning Differentiate Soft-Tissue Lipoma and Liposarcoma Better than Musculoskeletal Radiologists', *Sarcoma,* 2020, pp. 7163453.
5. Massa'a, R. N., Stoeckl, E. M., Lubner, M. G., Smith, D., Mao, L., Shapiro, D. D., Abel, E. J. and Wentland, A. L. (2022) 'Differentiation of benign from malignant solid renal lesions with MRI-based radiomics and machine learning', *Abdominal Radiology,* 47(8), pp. 2896-2904.
6. Matsuo, H., Nishio, M., Kanda, T., Kojita, Y., Kono, A. K., Hori, M., Teshima, M., Otsuki, N., Nibu, K. I. and Murakami, T. (2020) 'Diagnostic accuracy of deep-learning with anomaly detection for a small amount of imbalanced data: discriminating malignant parotid tumors in MRI', *Scientific Reports,* 10(1), pp. 19388.
7. Nakagawa, M., Nakaura, T., Yoshida, N., Azuma, M., Uetani, H., Nagayama, Y., Kidoh, M., Miyamoto, T., Yamashita, Y. and Hirai, T. (2023) 'Performance of Machine Learning Methods Based on Multi-Sequence Textural Parameters Using Magnetic Resonance Imaging and Clinical Information to Differentiate Malignant and Benign Soft Tissue Tumors', *Academic Radiology,* 30(1), pp. 83-92.
8. Okimoto, N., Yasaka, K., Kaiume, M., Kanemaru, N., Suzuki, Y. and Abe, O. (2023) 'Improving detection performance of hepatocellular carcinoma and

interobserver agreement for liver imaging reporting and data system on CT using deep learning reconstruction', *Abdominal Radiology,* 48(4), pp. 1280-1289.
9. Shin, S. Y., Shen, T. C., Wank, S. A. and Summers, R. M. (2023) 'Fully-automated detection of small bowel carcinoid tumors in CT scans using deep learning', *Medical Physics,* 29, pp. 29.
10. Takeuchi, M., Seto, T., Hashimoto, M., Ichihara, N., Morimoto, Y., Kawakubo, H., Suzuki, T., Jinzaki, M., Kitagawa, Y., Miyata, H. and Sakakibara, Y. (2021) 'Performance of a deep learning-based identification system for esophageal cancer from CT images', *Esophagus,* 18(3), pp. 612-620.
11. Uhlig, J., Biggemann, L., Nietert, M. M., Beisbarth, T., Lotz, J., Kim, H. S., Trojan, L. and Uhlig, A. (2020) 'Discriminating malignant and benign clinical T1 renal masses on computed tomography: A pragmatic radiomics and machine learning approach', *Medicine,* 99(16), pp. e19725.
12. von Schacky, C. E., Wilhelm, N. J., Schafer, V. S., Leonhardt, Y., Gassert, F. G., Foreman, S. C., Gassert, F. T., Jung, M., Jungmann, P. M., Russe, M. F., Mogler, C., Knebel, C., von Eisenhart-Rothe, R., Makowski, M. R., Woertler, K., Burgkart, R. and Gersing, A. S. (2021) 'Multitask Deep Learning for Segmentation and Classification of Primary Bone Tumors on Radiographs', *Radiology,* 301(2), pp. 398-406.
13. von Schacky, C. E., Wilhelm, N. J., Schafer, V. S., Leonhardt, Y., Jung, M., Jungmann, P. M., Russe, M. F., Foreman, S. C., Gassert, F. G., Gassert, F. T., Schwaiger, B. J., Mogler, C., Knebel, C., von Eisenhart-Rothe, R., Makowski, M. R., Woertler, K., Burgkart, R. and Gersing, A. S. (2022) 'Development and evaluation of machine learning models based on X-ray radiomics for the classification and differentiation of malignant and benign bone tumors', *European Radiology,* 32(9), pp. 6247-6257.
14. Vos, M., Starmans, M. P. A., Timbergen, M. J. M., van der Voort, S. R., Padmos, G. A., Kessels, W., Niessen, W. J., van Leenders, G., Grunhagen, D. J., Sleijfer, S., Verhoef, C., Klein, S. and Visser, J. J. (2019) 'Radiomics approach to distinguish between well differentiated liposarcomas and lipomas on MRI', *British Journal of Surgery,* 106(13), pp. 1800-1809.
15. Weng, J., Wildman-Tobriner, B., Buda, M., Yang, J., Ho, L. M., Allen, B. C., Ehieli, W. L., Miller, C. M., Zhang, J. and Mazurowski, M. A. (2023) 'Deep learning for classification of thyroid nodules on ultrasound: validation on an independent dataset', *Clinical Imaging,* 99, pp. 60-66.
16. Wentland, A. L., Yamashita, R., Kino, A., Pandit, P., Shen, L., Brooke Jeffrey, R., Rubin, D. and Kamaya, A. (2023) 'Differentiation of benign from malignant solid renal lesions using CT-based radiomics and machine learning: comparison with radiologist interpretation', *Abdominal Radiology,* 48(2), pp. 642-648.
17. Zhang, M., Tong, E., Hamrick, F., Lee, E. H., Tam, L. T., Pendleton, C., Smith, B. W., Hug, N. F., Biswal, S., Seekins, J., Mattonen, S. A., Napel, S., Campen, C. J., Spinner, R. J., Yeom, K. W., Wilson, T. J. and Mahan, M. A. (2021) 'Machine-Learning Approach to Differentiation of Benign and Malignant Peripheral Nerve Sheath Tumors: A Multicenter Study', *Neurosurgery,* 89(3), pp. 509-517.
18. Zhuge, Y., Ning, H., Mathen, P., Cheng, J. Y., Krauze, A. V., Camphausen, K. and Miller, R. W. (2020) 'Automated glioma grading on conventional MRI

images using deep convolutional neural networks', *Medical Physics,* 47(7), pp. 3044-3053.
19. Ziegelmayer, S., Reischl, S., Havrda, H., Gawlitza, J., Graf, M., Lenhart, N., Nehls, N., Lemke, T., Wilhelm, D., Lohofer, F., Burian, E., Neumann, P. A., Makowski, M. and Braren, R. (2023) 'Development and Validation of a Deep Learning Algorithm to Differentiate Colon Carcinoma From Acute Diverticulitis in Computed Tomography Images', *JAMA Network Open,* 6(1), pp. e2253370**.**

APPENDIX 2: Titles and weblinks for ongoing or recently completed trials

1. An AI Platform Integrating Imaging Data and Models, Supporting Precision Care Through Prostate Cancer's Continuum (ProCAncer-I). Available at: https://clinicaltrials.gov/ct2/show/record/NCT05380518
2. Does triage of chest X-rays with artificial intelligence shorten the time to lung cancer diagnosis: a randomised controlled trial. Available at: https://www.cochranelibrary.com/central/doi/10.1002/central/CN-02538677/full
3. Jager et al (2023). Clinical Trial Protocol: Developing an Image Classification Algorithm for Prostate Cancer Diagnosis on Three-dimensional Multiparametric Transrectal Ultrasound. Available at: https://www.ncbi.nlm.nih.gov/pmc/articles/PMC9975006/
4. Mammography Screening With Artificial Intelligence (MASAI) (MASAI). Available at: https://clinicaltrials.gov/study/NCT04838756
5. Diagnostic Performance of Breast Cancer Screening Second Reading Process Assisted by AI (IMA-L2). Available at: https://clinicaltrials.gov/ct2/show/record/NCT05800132
6. A Retrospective Analysis of Magnetic Resonance Imaging Data for Breast Cancer Screening in the Open Consortium for Decentralized Medical Artificial Intelligence (ODELIA). Available at: https://clinicaltrials.gov/ct2/show/record/NCT05698056
7. Detection of ISUP≥2 Prostate Cancers Using Multiparametric MRI: Prospective Multicenter Comparison of the PI-RADS Score and an Artificial Intelligence System. Available at: https://clinicaltrials.gov/ct2/show/record/NCT04732156
8. DOLCE: Determining the Impact of Optellum's Lung Cancer Prediction (LCP) Artificial Intelligence Solution on Service Utilisation, Health Economics and Patient Outcomes. Available at: https://clinicaltrials.gov/ct2/show/record/NCT05389774
9. Artificial intelligence in mammography study. Available at: https://www.isrctn.com/ISRCTN60839016
10. Evaluating the Performance of AI in Evaluating Breast MRI Performed With Dose Reduction. Available at: https://clinicaltrials.gov/ct2/show/record/NCT04340180
11. Artificial Intelligence in Large-scale Breast Cancer Screening (ScreenTrustCAD). Available at: https://clinicaltrials.gov/ct2/show/record/NCT04778670
12. Development and validation of the AI-based diagnosis system for pathological findings in invasive front of colorectal cancer. Available at: https://upload.umin.ac.jp/cgi-open-bin/ctr_e/ctr_view.cgi?recptno=R000044488
13. Can ovarian cancer detection be improved using AI-driven diagnostic support applied to ultrasound images? Available at: https://www.isrctn.com/ISRCTN88222986
14. Automatic Detection in MRI of Prostate Cancer: DAICAP (DAICAP). Available at: https://clinicaltrials.gov/ct2/show/record/NCT05513820
15. A prospective clinical study for a rectal CRM automatic detection system based on Faster-RCNN. Available at: https://www.cochranelibrary.com/central/doi/10.1002/central/CN-02434527/full
16. Diagnostic Efficiency and Impact on Physicians' Learning Process of an Artificial Intelligence Ultrasound Diagnosis System for Thyroid Nodules: a Multicentre

Randomized Controlled Trial. Available at: https://www.cochranelibrary.com/central/doi/10.1002/central/CN-01975026/full
17. 17. Clinical Research on a Novel Deep-learning Based System in Pancreatic Mass Diagnosis. Available at: https://www.cochranelibrary.com/central/doi/10.1002/central/CN-02183990/full
18. 18. Development and validation of artificial intelligence-based rapid on-site cytologic evaluation during endoscopic ultrasound guided fine needle aspiration for pancreatic mass. Available at: https://www.clinicalkey.com/#!/content/playContent/1-s2.0-S0016510723015626?returnurl=https:%2F%2Flinkinghub.elsevier.com%2Fretrieve%2Fpii%2FS0016510723015626%3Fshowall%3Dtrue&referrer=https:%2F%2Fwww.giejournal.org%2F
19. IDEAL: Artificial Intelligence and Big Data for Early Lung Cancer Diagnosis Prospective Study (Phase 2). Available at: https://clinicaltrials.gov/ct2/show/record/NCT03753724
20. New Strategies Based on Artificial Intelligence in Breast Cancer Screening Programs in Córdoba With Digital Mammography and Digital Breast Tomosynthesis. A Prospective Evaluation. Available at: https://clinicaltrials.gov/ct2/show/record/NCT04949776
21. Clinical Utility of Artificial Intelligence Augmented Endobronchial Ultrasound Elastography in Lymph Node Staging for Lung Cancer https://clinicaltrials.gov/ct2/show/record/NCT04816981

APPENDIX 3: Summary of Artificial intelligence (AI) models investigated as interventions

Citation (Dataset country)	Name and type of intervention/control	AI model description	Reference standard
Breast cancer			
Calisto et al (2022) **Portugal**	**Intervention:** BreastScreening-AI. A DenseNet model (Deep neural network) (previously developed) + clinician **Control:** Clinician only	The DenseNet was developed using PyTorch - a deep learning library that is widely used by the machine learning community. The DenseNet architecture used in BreastScreening-AI was DenseNet-161. The DenseNet was initially pretrained on ImageNet, a large dataset of 1.2 million images from 1000 classes. Training was performed using the Adam optimizer, with the default parameters (learning rate of 10^{-3} and weight decay of 10^{-4}).	Set by the head of radiology using BI-RADS
Fujioka et al (2021) **Japan**[3]	**Intervention:** CNN models constructed to calculate the probability of malignancy of an image using Xception, InceptionV3, InceptionResNetV2, DenseNet121, DenseNet161, and NASNetMobile (previously developed) **Control:** Human readers (a breast surgeon and a radiologist)	The CNNs were performed on DEEPstation (UEI, Tokyo, Japan) containing the graphics processing unit GeForce GTX 1080 (NVIDIA, Santa Clara, CA, USA), central processing unit Core i7–8700 (Intel, CA, USA), and graphical user interface-based DL tool Deep Analyzer (GHELIA, Tokyo, Japan). The CNNs were initialized by the ImageNet (http://www.image-net.org/) pretraining model and fine-tuned to yield better performance. The parameters of optimisation were as follows: optimiser algorithm = Adam (lr = 0.0001, β1 = 0.9, β2 = 0.999, eps = le-8, decay = 0, amsgrad = False). The image sets for training and validation phase were randomly split into training data and validation data in the ratio of 9:1 per epoch, and supervised learning with 500 epochs was performed	Histopathological examination/ follow-up
Goto et al (2023) **Japan**	**Intervention:** Deep learning algorithm using pretrained Residual Networks 50 (ResNet50) architecture (previously developed). **Control:** Human readers (three radiologists)	The training was implemented using the Adam optimizer fixed to 0.001. The diagnostic model was trained with a random selection of 70% of the data set. Tenfold cross-validation was performed to create the trained model. The classification performance was evaluated using 30% of the test data set.	Histopathological examination

[3] If the country the dataset was obtained from was not stated within the study, the country the study was conducted in is provided

Heller et al (2021) **USA**	**Intervention:** A commercially available FDA-approved AI software (Koios DS; Koios Medical, New York, New York) + human reader **Control:** Human readers (two radiologists) only	The Koios DS for Breast Study Tool core engine, which uses a deep learning algorithm that characterises sonographically visualised breast lesions by generating a probability of malignancy, which is in turn equated to BI-RADS categories. The software is vendor-neutral and is the first and currently only FDA-approved decision support tool based on proprietary algorithms. The algorithms are stated to be derived from both pathology proven cases or imaging follow-up obtained from more than 400,000 cases, more than 25 institutions, and multiple ultrasound machine types and vendors.	Histopathological examination
Jiang et al (2021) **USA**[2]	**Intervention:** QuantX (AI software) + human readers **Control:** Human readers (19 radiologists) alone	QuantX is a computer-assisted diagnostic MRI software aid for use in the interpretation of breast images. This system was developed at the University of Chicago and then translated and produced as QuantX at Quantitative Insights, now Qlarity Imaging (Chicago, Ill). Training and validation steps were performed on patient cases independent from the test set.	Ground truth based on final pathology reports for biopsied cancers and biopsied noncancers. Ground truth for the nonbiopsied noncancers was obtained from clinical and radiology reports and a negative follow-up MRI examination at a minimum of 12 months after the considered MRI examination
Lo Gullo et al (2020) **USA**	**Intervention:** Radiomics + Machine learning model (previously developed) **Control:** Human readers (two radiologists)	An in-house code written in MATLAB (The MathWorks, Inc.) was used to input the ROIs into the open-source CERR software environment (freely available through GitHub) which calculated the radiomics features. No details on training or validation provided.	Histopathology established by either image-guided needle biopsy or surgery

Mango et al (2020) **USA**	**Intervention:** AI decision support system - Koios DS for Breast system (previously developed) **Control:** Human readers (15 physicians)	The training data (over 400,000 clinical examples) were gathered from over 25 machines and 25 different healthcare systems and sites. The 900 cases used in this validation study were completely excluded from the testing and development of the AI system.	Pathology or imaging follow-up
O'Connell et al (2022) **USA/Italy**	**Intervention:** S-Detect for Breast AI program (previously developed) **Control:** Human readers (10 radiologists)	S-Detect™ for Breast is a software based on a convolutional neural network (Samsung Medison Co., Ltd., South Korea) that has been trained to classify lesions using over 10,000 breast scans against "gold standard" biopsy assessments.	Ground truth generated from biopsy or a 24-month follow-up
Pacilè et al (2020) **USA**	**Intervention:** Human readers + AI (MammoScreen V1; Therapixel, Nice, France) – previously developed **Control:** Human readers (14 radiologists)	The AI system used (MammoScreen V1; Therapixel, Nice, France) uses two groups of deep convolutional neural networks (CNN) combined together with an aggregation module. The (symmetric) dream-nets were trained directly from images and their status (negative or positive). The detection CNN was trained from images and their annotations regardless of the statuses, while the (symmetric) characterization CNN were trained from image annotations and their status.	Histopathological examination
Pinto et al (2021) **Netherlands**	**Intervention:** Human reader + AI CAD system (Transpara. version 1.6.0; ScreenPoint Medical) – previously developed **Control:** Human readers (14 radiologists)	The AI system identifies suspicious regions and assigns to them a score between 1 and 100 representing the level of suspicion (LoS) of cancer present (100 indicates the highest suspicion). Information about the AI training and validation not provided.	One-year normal follow-up or histopathologic assessment
Tsochatzidis et al (2019) **USA**	**Intervention:** Deep convolutional neural networks (CNNs) – AlexNet, VGG, GoogLeNet/Inception, Residual Networks (ResNets) – previously developed **Control:** AI models above were compared amongst themselves	For the training process the Adam optimization method was employed.	Not stated
Uhlig et al (2018) **Germany**	**Intervention:** Five machine learning techniques (random forests, back propagation neural networks (BPN), extreme learning machines, support	Implementation of machine learning techniques comprises two steps: an initial training step, using the clinical dataset with an input-output pair to train the model, followed by a testing step, where the performance of the prediction model is tested on new data not used for training and therefore unknown to the model.	Core needle biopsy with subsequent histopathologic evaluation for

	vector machines, and K-nearest neighbors) – previously developed **Control:** Human readers (two readers)		breast lesions rated as BI-RADS category 4 or 5 by at least one reader or no evidence of size progression on imaging follow-up for at least 12 months for breast lesions rated as BI-RADS categories 1–3 by both readers
Vamvakas et al (2022) **Greece**	**Intervention:** Four popular implementations of Decision Trees (DT) Boosting classifiers, namely Adaptive Boosting (AdaBoost), Gradient Boosting (GB), Extreme Gradient Boosting (XGBoost), and Light Gradient Boosting Machine (LightGBM) – previously developed **Control:** An SVM classifier	Python implementations for XGBoost and LightGBM were obtained from their original sources [https://github.com/dmlc/ xgboost], [https://github.com/microsoft/LightGBM] and used through the scikit-learn Application Programming Interface (API), which is a common framework for ML applications. The final feature subset was used to train the GB, AdaBoost, XGBoost, LightGBM and SVM classifiers in differentiating benign from malignant breast lesions.	Histological verification from core needle biopsy or surgical excision
van Zelst et al (2020) **Netherlands[2]**	**Intervention:** AI model not stated. Computer-aided detection (CAD) software used, a commercially developed ABUS CAD software package (QVCAD, Qview Medical Inc., Los Altos, CA, USA) **Control:** Human readers (eight radiologists)	Information about the AI training not provided.	Histopathologic examination
Prostate cancer			
Akatsuka et al (2019) **Japan**	**Intervention:** Previously developed Deep convolutional neural network (dCNN)(Xception)	Three deep convolutional neural network models, Xception, inceptionV3 and VGG16, were pre-trained on ImageNet with classification layers	Histopathological diagnosis

	Control: Human readers (radiologists)	adapted to the study's labels. Xception was selected in this study because it showed the most precise performance for MR image classification. 10-fold cross-validation was used to test the prediction models, randomly dividing the whole cases in a 1:9 ratio, using one part for testing and the other nine parts for training	
Arslan et al (2023) **Turkey**	**Intervention:** Human + Commercially available DL software (Prostate AI, Version Syngo.Via VB60, Siemens Healthcare) **Control:** Human readers (four radiologists)	The DL software used in this study has three modules: (i) preprocessing module, (ii) DL-based lesion detection module, and (iii) DL-based lesion classification module. No model training or fine-tuning was performed in this study. The model was only used for performance testing.	Whole-mount pathology or MRI/ultrasound fusion-guided biopsy
Faiella et al (2022) **Italy**	**Intervention:** Previously developed AI software Quantib Prostate (Quantib B.V., Rotterdam, The Netherlands) + human (inexperienced radiologist) **Control:** Human reader (expert radiologist)	Quantib Prostate offers features for the reading of prostate MRI in one workflow. The semi-automated combination of bi-parametric data provided supports Region of Interest (ROI) determination and enables prostate lesion evaluation. No information about AI training and validation provided.	Biopsy results and radiology reports
Forookhi et al (2023) **Italy**	**Intervention:** Human + commercially available AI-assisted software (Quantib® Prostate) **Control:** Human readers (four novice readers)	No information about AI training and validation provided.	Reports from the expert radiologist
Patsanis et al (2023) **Norway**	**Intervention:** Six previously developed relevant 2D GANs were selected for investigation: f-AnoGAN, HealhtyGAN, StarGAN, StarGAN-v2, FP-GAN and DeScarGAN. For each model, the code was publicly available. **Control:** AI models above were compared amongst themselves	For each model, the code was publicly available. All input annotations for training were on the image level, i.e., each input image was labeled as negative or positive. All models were trained to generate 2D images representing a negative patient.	Manual delineations of PI-RADS ≥3 lesions by imaging experts /radiologists based on targeted biopsy
Tong et al (2023) **USA[2]**	**Intervention:** A commercially developed proprietary deep learning-based prototypical computer-aided detection algorithm (DL-CAD) (MR	The deep learning-based reconstruction algorithm was trained in a supervised manner using more than 10,000 slices of fully sampled T2 TSE acquisitions obtained from volunteers using 1.5 T and 3 T MR scanning systems (MAGNETOM scanners, Siemens Healthcare) of various regions	Adequate follow up was defined as a prostate biopsy within 1

	Prostate AI, version 1.3.2, build July 07, 2021, front end build November 06, 2019, Siemens Healthcare) **Control:** Human readers (three abdominal fellowship trained radiologists)	of the body, including head, pelvis, and knee. The training was implemented in PyTorch and performed using a commercially available GPU cluster with 32 GB of memory.	year of the MRI or stability of PSA of at least 1 year if mpMRI was prospectively determined to be PI-RADS 1 or 2.
Zhang et al (2022) **Germany**	**Intervention:** A previously established and validated DL algorithm, convolutional neural network (CNN) **Control:** Human readers (radiologists-in-training)	The utilized deep learning (DL) system is based on a task-specific CNN U-Net architecture and was previously retrospectively trained and validated using single-scanner biparametric data (T2-weighted and diffusion-weighted images), demonstrating similar performance to clinical PI-RADS assessment.	Combined extended systematic and targeted MRI/TRUS-fusion biopsy.
Lung cancer			
Baldwin et al (2020) **UK**	**Intervention:** Previously developed AI model (Lung Cancer Prediction CNN (LCP-CNN) **Control:** Brock model	The LCP-CNN is an AI model that analyses parts of a CT scan around a nodule of interest and provides a score from 0 to 100 for that nodule. In the first phase of training, the LCP-CNN was primed using hundreds of thousands of images selected and curated carefully to teach the network the kinds of visual discrimination tasks that may form the building blocks for a nodule discrimination task. The second phase comprised full supervised training on a version of the NLST data. This was performed on CT images of all solid and semi-solid nodules of at least 6mm in diameter from the NLST dataset that were not reported as pure ground glass opacities (GGO); all GGOs were excluded because there were too few examples of malignant GGOs to train the system reliably. The derivation and internal validation of the LCP-CNN was performed using eight-fold cross-validation, where all images and nodules for a given patient were assigned to the same fold, and in each of the eight training operations, one eighth of the data were reserved as an auxiliary set for convergence testing and parameter/threshold setting, and one final eighth was kept for internal validation. Because the NLST contains many more benign nodules than cancers, class balancing was used during training, since otherwise the resulting network would be tuned always to predict “benign”, since that would be the dominant class.	Ground truth (based on histology (required for any cancer), resolution, stability or (for pulmonary lymph nodes only) expert opinion

Jacobs et al (2021) **USA/Canada/Netherlands/ Belgium**	**Intervention:** Three top-performing algorithms from the Kaggle Data Science Bowl 2017 public competition: grt123, Julian de Wit and Daniel Hammack (JWDH), and Aidence (all pPreviously developed deep learning algorithms) **Control:** Human readers (11 radiologists)	No information about AI training and validation provided.	Set by histopathologic examination for cancer-positive scans and imaging follow-up for at least 2 years for cancer-negative scans
Maldonado et al (2021) **USA**	**Intervention:** BRODERS classifier used by CANARY AI software **Control:** Brock model	The BRODERS classifier (Benign versus aggRessive nODule Evaluation using Radiomic Stratification) is a conventional predictive radiomic model based on eight imaging features capturing nodule location, shape, size, texture and surface characteristics. A training set of 726 incidentally detected indeterminate pulmonary nodules (IPNs) from the NLST database was used to internally validate the BRODERS classifier	Final diagnosis
Tam et al (2021) **UK**	**Intervention:** A commercially available AI algorithm (Red Dot, Behold.ai, London, UK) +/- radiologists **Control:** Human readers (radiologists)	No information about AI training and validation provided.	The ground-truth of each examination was established by a combination of the cancer registry database records, the electronic clinical record, and review of both subsequent and prior imaging.
Toğaçar et al (2020) **Turkey**[2]	**Intervention:** Previously developed AI models LeNet, AlexNet and VGG-16 CNNs. **Control:** AI models above were compared amongst themselves	In training of the deep models, RMSprop, ADAM and Stochastic Gradient Descent (SGD) optimization methods were examined.	Each sample in the dataset was examined and labeled by experienced specialists.

Ueda et al (2021) **Japan**	**Intervention:** The AI-based CAD used in this study is EIRL Chest X-ray Lung nodule (LPIXEL Inc.), commercially available in Japan as of August 2020 **Control:** Human readers (Eighteen readers - nine general physicians and nine radiologists)	The CAD was developed based on an encoder-decoder network categorizing segmentation technique in DL. No information about AI training and validation provided.	Set by two author radiologists
Wataya et al (2023) **Japan**	**Intervention:** Human + Previously developed AI model pulmonary nodule CAD system attached to SYNAPSE SAI Viewer V1.4 (FUJIFILM Corporation). **Control:** Human readers (15 radiologists)	No information about AI training and validation provided.	Established through the agreement between two board-certificated chest radiologists with 17 and 25 years of diagnostic experience.
Abbreviations: Artificial intelligence (AI), Breast Imaging Reporting and Data System (BI-RADS), Back Propagation Neural Networks (BPN), Convolutional Neural Network (CNN), Computer Aided Diagnosis (CAD), DT (Decision Trees), Deep convolutional neural network (DCNN), Deep Learning (DL), Deep Learning Computer Aided Diagnosis (DLCAD), The United States Food and Drug Administration (FDA), Gradient Boosting (GB), Lung Cancer Prediction Convolutional Neural Network (LCP-CNN), Region of Interest (ROI), Level of suspicion (LOS), Stochastic Gradient Descent (SGD), Support Vector Machine (SVM), Prostate Imaging Reporting and Data System (PI-RADS).			

APPENDIX 4: MEDLINE search strategy

Ovid MEDLINE(R) ALL <1946 to June 19, 2023>

1 ("artificial intelligence" or AI).tw. 61802
2 (radiomic* or "machine learning" or "deep learning" or "neural network*").tw. 182269
3 artificial intelligence/ or machine learning/ 68965
4 or/1-3 250797
5 (diagnos* adj3 imag*).tw. 54007
6 "diagnostic aid*".tw. 3847
7 exp Diagnostic imaging/ 2912910
8 ("medical imaging" adj3 diagnos*).tw. 504
9 ((X-ray or CT or MRI or PET or CBCT or MRCP or MIBG or MRS or ultrasound) adj5 diagnos*).tw. 95951
10 mammogra*.tw. 36225
11 (("positron emission tomography" or "computed tomography") adj5 diagnos*).tw. 19194
12 ("Metaiodobenzylguanidine scan" adj5 diagnos*).tw. 3
13 ("Magnetic resonance" adj (spectroscopy or imaging or angiogram*) adj5 diagnos*).tw. 13135
14 ((cerebral or brain) adj angiogram* adj5 diagnos*).tw. 144
15 or/5-14 2977628
16 (neoplas* or tumo?r* or malignan* or cancer* or carcinoma* or adenocarcinoma* or melanoma* or lymphoma* or myeloma* or sarcoma*).tw. 4122728
17 exp Neoplasms/ 3844620
18 16 or 17 5092487
19 4 and 15 and 18 11866
20 (case reports or comment or editorial or letter or review or systematic review or meta analysis).pt. 7437910
21 ("systematic review" or meta-analysis or meta-analyses).ti. 301263
22 20 or 21 7474118
23 19 not 22 10317
24 limit 23 to (english language and yr="2018 -Current") 7881
25 afghanistan/ or africa/ or africa, northern/ or africa, central/ or africa, eastern/ or "africa south of the sahara"/ or africa, southern/ or africa, western/ or albania/ or algeria/ or andorra/ or angola/ or "antigua and barbuda"/ or argentina/ or armenia/ or azerbaijan/ or bahamas/ or bahrain/ or bangladesh/ or barbados/ or belize/ or benin/ or bhutan/ or bolivia/ or borneo/ or "bosnia and herzegovina"/ or botswana/ or brazil/ or brunei/ or bulgaria/ or burkina faso/ or burundi/ or cabo verde/ or cambodia/ or cameroon/ or central african republic/ or chad/ or exp china/ or comoros/ or congo/ or cote d'ivoire/ or croatia/ or cuba/ or "democratic republic of the congo"/ or cyprus/ or djibouti/ or dominica/ or dominican republic/ or ecuador/ or egypt/ or el salvador/ or equatorial guinea/ or eritrea/ or eswatini/ or ethiopia/ or fiji/ or gabon/ or gambia/ or "georgia (republic)"/ or ghana/ or grenada/ or guatemala/ or guinea/ or guinea-bissau/ or guyana/ or haiti/ or honduras/ or independent state of samoa/ or exp india/ or indian ocean islands/ or indochina/ or indonesia/ or iran/ or iraq/ or jamaica/ or jordan/ or kazakhstan/ or kenya/ or kosovo/ or kuwait/ or kyrgyzstan/ or laos/ or lebanon/ or liechtenstein/ or lesotho/ or liberia/ or libya/ or madagascar/ or malaysia/ or malawi/ or mali/ or malta/ or mauritania/ or mauritius/ or mekong valley/ or melanesia/ or micronesia/ or monaco/ or mongolia/ or montenegro/ or morocco/ or mozambique/ or myanmar/ or namibia/ or nepal/ or nicaragua/ or

niger/ or nigeria/ or oman/ or pakistan/ or palau/ or exp panama/ or papua new guinea/ or paraguay/ or peru/ or philippines/ or qatar/ or "republic of belarus"/ or "republic of north macedonia"/ or romania/ or exp russia/ or rwanda/ or "saint kitts and nevis"/ or saint lucia/ or "saint vincent and the grenadines"/ or "sao tome and principe"/ or saudi arabia/ or serbia/ or sierra leone/ or senegal/ or seychelles/ or singapore/ or somalia/ or south africa/ or south sudan/ or sri lanka/ or sudan/ or suriname/ or syria/ or taiwan/ or tajikistan/ or tanzania/ or thailand/ or timor-leste/ or togo/ or tonga/ or "trinidad and tobago"/ or tunisia/ or turkmenistan/ or uganda/ or ukraine/ or united arab emirates/ or uruguay/ or uzbekistan/ or vanuatu/ or venezuela/ or vietnam/ or west indies/ or yemen/ or zambia/ or zimbabwe/ 1291789

26 "Organisation for Economic Co-Operation and Development"/ 539

27 australasia/ or exp australia/ or austria/ or baltic states/ or belgium/ or exp canada/ or chile/ or colombia/ or costa rica/ or czech republic/ or exp denmark/ or estonia/ or europe/ or finland/ or exp france/ or exp germany/ or greece/ or hungary/ or iceland/ or ireland/ or israel/ or exp italy/ or exp japan/ or korea/ or latvia/ or lithuania/ or luxembourg/ or mexico/ or netherlands/ or new zealand/ or north america/ or exp norway/ or poland/ or portugal/ or exp "republic of korea"/ or "scandinavian and nordic countries"/ or slovakia/ or slovenia/ or spain/ or sweden/ or switzerland/ or turkey/ or exp united kingdom/ or exp united states/ 3490253

28 European Union/ 17665

29 Developed Countries/ 21362

30 or/26-29 3506177

31 25 not 30 1202341

32 24 not 31 7813

Health and Care
Research Wales
Evidence Centre
Canolfan Dystiolaeth
Ymchwil Iechyd a
Gofal Cymru

The Health and Care Research Wales Evidence Centre

Our dedicated team works together with Welsh Government, the NHS, social care, research institutions and the public to deliver vital research to tackle health and social care challenges facing Wales.

Funded by Welsh Government, through Health and Care Research Wales, the Evidence Centre answers key questions to improve health and social care policy and provision across Wales.

Along with our collaborating partners, we conduct reviews of existing evidence and new research, to inform policy and practice needs, with a focus on ensuring real-world impact and public benefit that reaches everyone.

Director: Professor Adrian Edwards

Associate Directors: Dr Alison Cooper, Dr Natalie Joseph-Williams, Dr Ruth Lewis

@EvidenceWales

healthandcareevidence@cardiff.ac.uk

www.researchwalesevidencecentre.co.uk